

University of Kentucky

UKnowledge

Theses and Dissertations--Pharmacology and
Nutritional Sciences

Pharmacology and Nutritional Sciences

2021

Robust RNA Integrity-to-Neuronal Gene Expression Association in Autopsy Brain Tissue Not Explained by Post-Mortem Variables; and Acute Behavioral Stress Does Not Alter RNA Quality, While Progesterone Protects Against Effects of Stress Exposure

Eleanor S. Johnson

University of Kentucky, esjohnson93@gmail.com

Author ORCID Identifier:

 <https://orcid.org/0000-0001-9356-4339>

Digital Object Identifier: <https://doi.org/10.13023/etd.2021.384>

[Right click to open a feedback form in a new tab to let us know how this document benefits you.](#)

Recommended Citation

Johnson, Eleanor S., "Robust RNA Integrity-to-Neuronal Gene Expression Association in Autopsy Brain Tissue Not Explained by Post-Mortem Variables; and Acute Behavioral Stress Does Not Alter RNA Quality, While Progesterone Protects Against Effects of Stress Exposure" (2021). *Theses and Dissertations--Pharmacology and Nutritional Sciences*. 40.

https://uknowledge.uky.edu/pharmacol_etds/40

This Doctoral Dissertation is brought to you for free and open access by the Pharmacology and Nutritional Sciences at UKnowledge. It has been accepted for inclusion in Theses and Dissertations--Pharmacology and Nutritional Sciences by an authorized administrator of UKnowledge. For more information, please contact UKnowledge@lsv.uky.edu.

STUDENT AGREEMENT:

I represent that my thesis or dissertation and abstract are my original work. Proper attribution has been given to all outside sources. I understand that I am solely responsible for obtaining any needed copyright permissions. I have obtained needed written permission statement(s) from the owner(s) of each third-party copyrighted matter to be included in my work, allowing electronic distribution (if such use is not permitted by the fair use doctrine) which will be submitted to UKnowledge as Additional File.

I hereby grant to The University of Kentucky and its agents the irrevocable, non-exclusive, and royalty-free license to archive and make accessible my work in whole or in part in all forms of media, now or hereafter known. I agree that the document mentioned above may be made available immediately for worldwide access unless an embargo applies.

I retain all other ownership rights to the copyright of my work. I also retain the right to use in future works (such as articles or books) all or part of my work. I understand that I am free to register the copyright to my work.

REVIEW, APPROVAL AND ACCEPTANCE

The document mentioned above has been reviewed and accepted by the student's advisor, on behalf of the advisory committee, and by the Director of Graduate Studies (DGS), on behalf of the program; we verify that this is the final, approved version of the student's thesis including all changes required by the advisory committee. The undersigned agree to abide by the statements above.

Eleanor S. Johnson, Student

Dr. Eric Blalock, Major Professor

Dr. Rolf Craven, Director of Graduate Studies

ROBUST RNA INTEGRITY-TO-NEURONAL GENE EXPRESSION ASSOCIATION
IN AUTOPSY BRAIN TISSUE NOT EXPLAINED BY POST-MORTEM
VARIABLES; AND ACUTE BEHAVIORAL STRESS DOES NOT ALTER RNA
QUALITY, WHILE PROGESTERONE PROTECTS AGAINST EFFECTS OF STRESS
EXPOSURE

DISSERTATION

A dissertation submitted in partial fulfillment of the
requirements for the degree of Doctor of Philosophy in the
College of Medicine
at the University of Kentucky

By
Eleanor Stiles Johnson
Lexington, Kentucky
Director: Dr. Eric Blalock, Associate Professor of Pharmacology and Nutritional
Sciences
Lexington, Kentucky
2021

Copyright © Eleanor Stiles Johnson 2021
<https://orcid.org/0000-0001-9356-4339>

ABSTRACT OF DISSERTATION

ROBUST RNA INTEGRITY-TO-NEURONAL GENE EXPRESSION ASSOCIATION IN AUTOPSY BRAIN TISSUE NOT EXPLAINED BY POST-MORTEM VARIABLES; AND ACUTE BEHAVIORAL STRESS DOES NOT ALTER RNA QUALITY, WHILE PROGESTERONE PROTECTS AGAINST EFFECTS OF STRESS EXPOSURE

Transcriptional profiling (TP) is a common tool to determine RNA expression levels. It allows for thousands of genes to be analyzed simultaneously, and determines differences in gene expression levels due to various pathologies. RNA quality also impacts the reported expression level. One of the most common approaches for assessing RNA quality is Agilent Technology's RNA integrity number (RIN). The use of RINs allowed scientists to standardize the assessment and reporting of RNA quality by predominantly using rRNA traits to assign a quantitative value. Recent work provided evidence that RINs are associated with transcriptional profiles, and possibly has a stronger connection to some pathologies. Because of the effect RIN has on gene expression, many have tried to correct for its influence using techniques such as multiple regression. Despite this, there has been relatively little work done on determining 1) how RNA quality impacts TP results, 2) when RNA degradation begins to impact gene expression, and 3) the relationship between RINs and gene expression. To investigate this, individual profiles from human, control, brain tissue with disambiguated RINs were analyzed. A robust set of mRNA species, particularly related to neurons, were significantly correlated with RINs, indicating that neurons are more susceptible to the effects of RNA degradation in brain tissue. Most of the decline in mRNA expression occurs within a narrow RIN range of 7.2 to 8.6, with values greater than 8.6 not needing RIN-correction and values less than 7.2 being too degraded to give accurate readings. This non-linear relationship between RINs and mRNA expression may be important to consider for RIN-correction procedures. Also, it was confirmed that RINs appear to be confounded with certain pathologies. RNA quality is possibly influenced by ante-mortem factors that occur during life and may exacerbate post-mortem effects.

Post-mortem variables are a key focus for RNA quality, while ante-mortem factors such as stress and neuropathology are less understood. During stress, glucocorticoids (GCs) released from the adrenal glands are associated with neurotoxic and RNA degrading effects in brain that may contribute to ante-mortem influences on RNA quality. Recent evidence has shown that progesterone (P4) may counter GC's effects during stress. To determine if acute psychosocial stress impacts RNA quality and

whether P4 protects against the effects of this stress, male and female rats were administered a vehicle or P4 daily during water maze training, and then underwent an acute stress (restraint) before the probe trial. Female, P4-stressed animals had improved probe trial performance compared to their vehicle-stressed counterparts, and neither stress nor P4 influenced RNA quality. Stressed animals had higher blood plasma GC levels, as expected. In the hippocampus, acute stress and P4 did not alter Sgk1 protein levels between sexes, but Sgk1 mRNA was significantly increased in male vehicle-stressed subjects, and this stress effect was blocked by P4. Based on prior work showing both age and stress sensitivity, we also assessed microglial-myelin fragment co-labeling, and found that this was increased in males, particularly the progesterone groups. Taken together, this indicates that acute behavioral stress does not appreciably impact RNA quality from brain tissue, and that the behavioral and molecular effects of acute stress are partially disrupted by P4.

KEYWORDS: RNA Integrity Numbers, Microarrays, Alzheimer's disease, Acute Psychosocial Stress, Glucocorticoids, Progesterone

Eleanor Stiles Johnson
(Name of Student)

09/17/2021
Date

ROBUST RNA INTEGRITY-TO-NEURONAL GENE EXPRESSION ASSOCIATION
IN AUTOPSY BRAIN TISSUE NOT EXPLAINED BY POST-MORTEM
VARIABLES; AND ACUTE BEHAVIORAL STRESS DOES NOT ALTER RNA
QUALITY, WHILE PROGESTERONE PROTECTS AGAINST EFFECTS OF STRESS
EXPOSURE

By
Eleanor Stiles Johnson

Dr. Eric Blalock
Director of Dissertation

Dr. Rolf Craven
Director of Graduate Studies

09/17/2021
Date

DEDICATION

To my parents, Dave and Janinne Johnson, thank you so much for all of the opportunities you have given me. I would not be here without your love and support.

To Erin and Michael Mitchell, my sister and brother-in-law, thank you for being there for me through everything. You all have been my sanity throughout my academic career.

To Sophia, Lucas, and Hayley Mitchell, my wonderful nieces and nephew, who have brought so much love and so many smiles to my life. I hope nothing but the best for you all.

ACKNOWLEDGMENTS

The following dissertation and the work associated with it were completed under the guidance of Dr. Eric Blalock. You have been a fantastic mentor, and I am truly lucky to have you as my boss and friend. You have helped to provide me with opportunities to grow, not only as a scientist but as a person. Your depth in knowledge, not only in science but a variety of topics, and genuine kindness are traits to aspire to in addition to your storytelling and tangents.

Not only have I had Dr. Blalock's mentorship, but that of my committee: Dr. Nada Porter, Dr. Donna Wilcock, and Dr. Liz Head. No matter how busy your schedules were, you were always willing to help and meet with me when needed. I have seen all of you place students as a top priority, despite the growing responsibilities you all have taken on over the years.

I also would not be where I am today without Dr. Kendra Stenzel. Kendra, you taught me the ins and outs of the lab and that determination and a positive attitude can make all the difference. You showed me that while it takes a little more work, you can use the knowledge gained earning a doctorate to find a place in non-traditional fields.

There are so many people that have been a part of my graduate experience. First, the people who started this experience with me in the department, Dr. Adam Ghoweri and Dr. Brittany Rice, and of course the good friends I made along the way in NSPS, Dr. Courtney Turpin and Lucy Yanckello, along with so many others, thank you. And of course, NSPS would not be the organization it is without the phenomenal guidance of Dr. Sarah Police. Also, I have to thank those who have helped me along the way as I sometimes fumbled through the science, Katie Anderson, Danny Craig, Dr. Chris Gant,

Dr. Hilaree Frazier, and Dr. Susan Kraner. And of course, this department would not run without Mrs. Kelley Secrest, who has answered probably as many of my questions over the years as Eric.

I also would be remiss if I did not thank my friends from the Graduate School Congress. Not only did the organization give me a chance to meet other graduate students I probably never would have, but it also opened my eyes to how individuals can make a difference in our communities. The friends I have made through GSC have made me a more thoughtful and determined person.

I also cannot forget my friends from before I started graduate school. Alex Laine, you have known me longer than anyone outside of my family. You have been there for me, whether I was trying to explain my project to you or just talk about our lives and history. You'll always be my sister. Dr. Kristyn van der Meulen, you were my first lab partner at Wittenberg, and ten years later, you are one of my dearest friends. You've been there for me through every step of this crazy process and have helped me remember that there is life outside of the lab.

And finally, I have to thank my family. Mom and Dad, you have always been there for me and supported me in whatever I tried. I would not be here without you all. Erin and Michael Mitchell, you are my siblings. You've helped me remember that life continues on and that there is more to life than school. And finally, Sophia, Lucas, and Hayley Mitchell, my favorite nieces and nephew, you all always bring a smile to my face and remind me of the important things in life.

TABLE OF CONTENTS

LIST OF TABLES	vi
LIST OF FIGURES	vii
LIST OF ADDITIONAL FILES	viii
CHAPTER 1. Transcriptional Profiling	1
<i>1.1 Types of transcriptional profiling and its common techniques</i>	<i>1</i>
1.1.1 Microarrays	1
1.1.1.1 History of microarrays	1
1.1.1.2 Oligonucleotide microarray mechanism	3
1.1.1.3 RNA isolation and processing.....	5
1.1.2 RNA-Seq	6
<i>1.2 RNA integrity numbers.....</i>	<i>11</i>
1.2.1 Role in transcriptional profiling	11
1.2.2 Determining RNA integrity number values.....	12
CHAPTER 2. Declining RNA integrity in control autopsy brain tissue is robustly and asymmetrical association with selective neuronal with selective neuronal signal loss: a meta-analysis.....	16
2.1 Summary	16
2.2 Introductions	16
2.3 Methods.....	20
2.3.1 Identifying datasets and preparing cel files	20
2.3.2 Differences in brain RNA quality across species	20
2.3.3 Pre-statistical processing and individual study analysis	20
2.3.4 Separate dataset approaches	21
2.3.4.1 Defining significant metavariable-correlated genes.....	21
2.3.4.2 Comparing across separate datasets.	21
2.3.5 Unified dataset analysis	22
2.3.5.1 Approaches for unifying independent datasets/ removing batch effects.	22
2.3.5.2 Template analysis.....	22
2.3.6 Alzheimer’s disease gene relationship.....	23
2.4 Results.....	23
2.4.1 Overview of dataset	23

2.4.2	Differences in RNA quality across species.....	28
2.4.3	Metadata correlation analysis of individual datasets	28
2.4.4	Cross-Dataset analysis using individual datasets.....	31
2.4.5	Merged datasets analysis	33
2.4.5.1	Approaches for merging multiple datasets.....	35
2.4.5.2	Template Analysis	37
2.4.6	Relationship between Alzheimer’s disease and RIN-sensitive genes.....	40
2.5	<i>Discussion</i>	46
CHAPTER 3. RNA Degradation, Glucocorticoid, and Glucocorticoid Receptors		53
3.1	<i>mRNA degradation pathways</i>	53
3.1.1	Non-sense mediated decay	54
3.1.2	Glucocorticoid receptor mediated mRNA decay.....	55
3.2	<i>Glucocorticoid receptors</i>	58
3.2.1.1	Structure.....	58
3.2.1.2	Mechanisms of action	59
3.3	<i>Glucocorticoids</i>	62
3.3.1	Interactions with progesterone and allopregnanolone	64
3.3.2	Role in stress and Hypothalamus-Pituitary-Adrenal-Axis.....	66
3.3.2.1	Mechanism.....	66
3.3.2.2	Stress Response.....	68
3.3.2.2.1	Relationship between stress and aging.....	68
3.3.2.2.2	Chronic stress.....	69
3.3.2.2.3	Acute stress	71
CHAPTER 4. Progesterone pretreatment attenuates acute stress action on hippocampus without the apparent disruption of the hypothalamic-pituitary-adrenal axis in young adult male and female rats		73
4.1	<i>Summary</i>	73
4.2	<i>Introduction</i>	74
4.3	<i>Methods</i>	77
4.3.1	Animals	77
4.3.2	Oral progesterone	78
4.3.3	Water Maze	78
4.3.3.1	Visual Cue.....	78
4.3.3.2	Spatial Cue.....	79
4.3.3.3	Restraint stress and probe trial	79

4.3.3.4	Blood and tissue collection	80
4.3.4	Immunohistochemistry	80
4.3.5	Plasma Analysis.....	81
4.3.6	Western blot	82
4.3.7	Real Time- qPCR: RIPA Extract and cDNA Synthesis.....	84
4.3.8	Statistical analysis	85
4.4	<i>Results</i>	85
4.4.1	Morris Water Maze.....	85
4.4.1.1	Spatial Cue	85
4.4.1.2	Struggles during restraint stress	86
4.4.1.3	Probe trials	86
4.4.2	Trunk Plasma Hormones Levels.....	90
4.4.3	Immunohistochemistry	93
4.4.4	Western Blot.....	98
4.4.5	Real Time-PCR	98
4.5	<i>Discussion</i>	101
CHAPTER 5.	Dissertation Discussions.....	109
5.1	<i>Introduction</i>	109
5.2	<i>Declining RNA integrity in control autopsy brain tissue is robustly and asymmetrical association with selective neuronal mRNA signal loss: a meta-analysis</i>	110
5.2.1	Implications	110
5.2.2	Future Directions	113
5.3	<i>Progesterone pretreatment attenuates acute stress action on hippocampus without the apparent disruption of the hypothalamic-pituitary-adrenal axis in young adult male and female rats</i>	115
5.3.1	Implications	115
5.3.2	Future Directions	117
5.4	<i>Concluding remarks</i>	119
	References	121
	VITA	142

LIST OF TABLES

Table 2.1. Data-subset information	24
Table 2.2. RIN comparisons across species.	29
Table 2.3. RIN-sensitive pathways.	36
Table 2.4. Templates to which gene expression most commonly fit.....	41
Table 4.1. ANOVA values for IHC Analysis	96
Table 4.2. RIN values by sex and group	100

LIST OF FIGURES

Figure 1.1. Chemical synthesis cycle of oligonucleotide microarray.	4
Figure 1.2. Microarray experimental steps.	7
Figure 1.3. Parts of the RIN electropherogram.	13
Figure 1.4. Representative electropherograms for each RIN integer.	14
Figure 2.1. Presence cut-offs established in a dataset- dependent fashion.	26
Figure 2.2 PCA plots and monovalent inorganic cation transmembrane transport pathway expression.	27
Figure 2.3. Metadata correlations to RIN.....	30
Figure 2.4. Sex effect on RNA degradation.	32
Figure 2.5. Overlapping significant genes between 3 datasets, and direction of significant genes.	34
Figure 2.6. Number of significant genes associated with cumulative RIN.	38
Figure 2.7. Flow chart of template analysis.....	39
Figure 2.8. Representative gene expression templates.	43
Figure 2.9. Relationship between RIN-sensitive genes and AD-associated genes.....	45
Figure 3.1. Glucocorticoid receptor mediated mRNA decay.....	57
Figure 3.2. Hypothalamus-pituitary-adrenal-axis.	67
Figure 4.1. Spatial Cue.	87
Figure 4.2. Number of struggles during restraint stress.	88
Figure 4.3. Normalized velocity during probe trial.	89
Figure 4.4. Distance during probe trial.....	91
Figure 4.5. Hormone concentrations from trunk plasma.	92
Figure 4.6. Example of hippocampal section used for IHC.	94
Figure 4.7. Iba1 expression changes in stratum oriens.	95
Figure 4.8. Mean signal for overlapping Iba1 and Mbp.	97
Figure 4.9. Western blot analysis.	99
Figure 4.10. Sgk1 mRNA expression.....	102

LIST OF ADDITIONAL FILES

Supplemental Data 2.1. Common significant RIN-sensitive genes from GSE25219, GSE45878, and GSE71620.....[XML 79 KB]

Supplemental Data 2.2. Independent validation of correlation direction in RIN-sensitive genes[XML 43 KB]

Supplemental Data 2.3. RNA degradation templates and associated genes[XML 49 KB]

Supplemental Data 2.4. Genes common to Miller et al. and significant genes from individual study analysis.....[XML 2,080 KB]

Supplemental Data 2.5. Genes common to Hargis & Blalock and significant genes from individual study analysis.....[XML 3,112 KB]

Supplemental Data 2.6. RMA data for GSE22521.....[XML 5,217 KB]

Supplemental Data 2.7. RMA data for GSE25219.....[XML 4,749 KB]

Supplemental Data 2.8. RMA data for GSE45878.....[XML 6,068 KB]

Supplemental Data 2.9. RMA data for GSE46706.....[XML 28,304 KB]

Supplemental Data 2.10. RMA data for GSE53987.....[XML 7,537 KB]

Supplemental Data 2.11. RMA data for GSE71620.....[XML 53,710 KB]

Supplemental Data 4.1. Information for individual subjects.....[XML 12 KB]

CHAPTER 1. TRANSCRIPTIONAL PROFILING

1.1 Types of transcriptional profiling and its common techniques

In the most basic sense, transcriptional profiling is a group of techniques that simultaneously measure multiple genes' RNA expression. Often, these techniques can analyze thousands of genes from the sample, allowing for a more encompassing picture of what is occurring within tissues or cells. In the past 25 years, transcriptional profiling has been done using microarrays (the first transcriptional profiling technique of the modern era) or RNA-sequencing (RNA-seq; which has grown in popularity in the last decade) and have been cited over 272,000 times on PubMed. This rise indicates how the field and its unbiased approach to findings have become more impactful to the scientific community. Transcriptional profiling has allowed for gene expression, microRNA, long non-coding RNA, transcriptional factor binding assays, and genotyping analysis (Bumgarner, 2013; Hrdlickova, Toloue, & Tian, 2017; Jaksik, Iwanaszko, Rzeszowska-Wolny, & Kimmel, 2015) in a variety of conditions and diseases across tissues and species (Jaksik et al., 2015).

1.1.1 Microarrays

1.1.1.1 History of microarrays

Today's microarray technology's early predecessors first appeared in 1975 using colony hybridization (Grunstein & Hogness, 1975). They cloned DNA into *E. coli* plasmids on agar plates and covered with nitrocellulose filter, and then the *E. coli* on the filters were lysed, and the DNA was denatured and fixed to the filter. This process created randomly distributed spots of cloned fragments from the DNA on the filter, which could then be hybridized with a radiolabeled probe for DNA or RNA of interest ((Grunstein & Hogness, 1975) reviewed in (Bumgarner, 2013)). Gergen et al. adapted Grunstein and Hogness' approach to creating an ordered array, using a microtiter plate for the medium, and creating a machine to copy the pattern into the agar (Gergen, Stern, & Wensink, 1979). This approach and those adapted from it continued to be the closest thing to the modern microarrays through the 1980s. The early 1990s saw this procedure automated, and with the addition of the growing libraries of cDNA references, set the stage for the more modern microarrays (Bumgarner, 2013).

Fodor et al. introduced a method that would become instrumental in the development of microarrays, a light-directed chemical synthesis ((Fodor et al., 1991); reviewed in (Lenoir & Giannella, 2006)). This process synthesized up to 1024 unique peptides simultaneously. Amino acids were attached to a photoremovable protecting group using photolithographic techniques. These protecting groups were then either protected from a laser using a mask or the protective group removed. A light-directed peptide synthesis occurred with another protecting group (Fodor et al., 1991). The masks would change between each round of removing the photolabile to create different peptide sequences. Once the sequences were synthesized, the peptide chains were flooded with fluorescent markers to determine the composition of the peptides (Fodor et al., 1991; Lenoir & Giannella, 2006). They also developed a scanner for reading the output of this process, similar to that used in fluorescent-activated cell sorting (Lenoir & Giannella, 2006). This development would become crucial for the development of oligonucleotide microarrays.

In 1995, the first publication involving cDNA hybridization spotting microarrays was published (Schena, Shalon, Davis, & Brown, 1995). Using the aspects of techniques already standardized (e.g., fluorescent in situ hybridization, dot blot) (Lenoir & Giannella, 2006), they analyzed the *Arabidopsis thaliana*'s cDNA. They found that using florescent probes made from *A. thaliana*'s RNA saturated the high-sensitivity detector, while the negative controls did not; the moderate-sensitivity provided quantifiable results (Schena et al., 1995).

The following year, oligonucleotide microarrays were published for the first time, building off the work of Fodor et al. (Lockhart et al., 1996). The significant difference between oligonucleotide and spotting microarrays is that instead of hybridizing onto a surface (e.g., glass), oligonucleotide microarrays covalently bind their chemically synthesized oligonucleotides detectors to the glass surfaces (Lockhart et al., 1996). Affymetrix, which Thermo Fisher Scientific later acquired, uses this approach in their microarrays (Bumgarner, 2013).

Another technique for oligonucleotide microarrays was also introduced in 1996. Blanchard et al. also used oligonucleotide synthesis. Instead of masks as Lockhart et al. (1996) and Fodor et al. (1991), however, they used microfabricated ink-jet pumps, which

are similar to those found in some ink-jet printers of the time. These pumps added four different synthetic nucleotides to a glass slide with hydrophilic and hydrophobic areas. (Blanchard, Kaiser, & Hood, 1996). The nucleotides were then able to bond within the hydrophilic areas but were constrained by the hydrophobic regions (Blanchard et al., 1996; Bumgarner, 2013). Agilent Technologies, another well-known microarray company, licensed this technology (Bumgarner, 2013).

A group also developed a third type of microarray at Tufts University, the bead-based fiber-optic arrays. This method synthesizes a DNA probe on polystyrene beads at the end of the fiber optic array (Bumgarner, 2013; Walt, 2000). The DNA hybridizes to a fluorescent marker and is excited by laser light. The emitted fluorescent light is then captured and sent to the opposite end of the fiber for detection and analysis (Walt, 2000). Illumina, Inc. licensed this technology (Bumgarner, 2013).

Affymetrix, Agilent Technologies, and Illumina, Inc. are three of the largest microarray companies in the last 25 years. This work will focus primarily on Affymetrix and the oligonucleotide microarrays since they are used in Chapter 2.

1.1.1.2 Oligonucleotide microarray mechanism

Oligonucleotide microarrays require two forms of preparation: creating the microarray probes and RNA isolation and processing. Using techniques described by Fodor et al. (1991) and Lockhart et al. (1996), oligonucleotides are synthesized directly onto the microarrays (reviewed in (M. B. Miller & Tang, 2009)). Photolithographic techniques create these short chains (usually between 20-25 bp) (Fodor et al., 1991; Lockhart et al., 1996; M. B. Miller & Tang, 2009). First, masks are created to expose light to some chemical substrates, light-sensitive protecting agents. When these agents are exposed to light, they are released (Fodor et al., 1991), and the microarray is exposed to a nucleic acid bound to a new photolabile agent (M. B. Miller & Tang, 2009) (Figure 1.1). This process is repeated until the oligonucleotide probe sequence has been completed. Gene targets often have multiple probes associated with them, which increase sensitivity, specificity, and accuracy (M. B. Miller & Tang, 2009).

Affymetrix has multiple forms of oligonucleotide microarrays. The more established version (e.g., Affymetrix 3' *in vitro* transcription [IVT] platform) has traditionally used two types of probes: the perfect match and the mismatch. There are 11

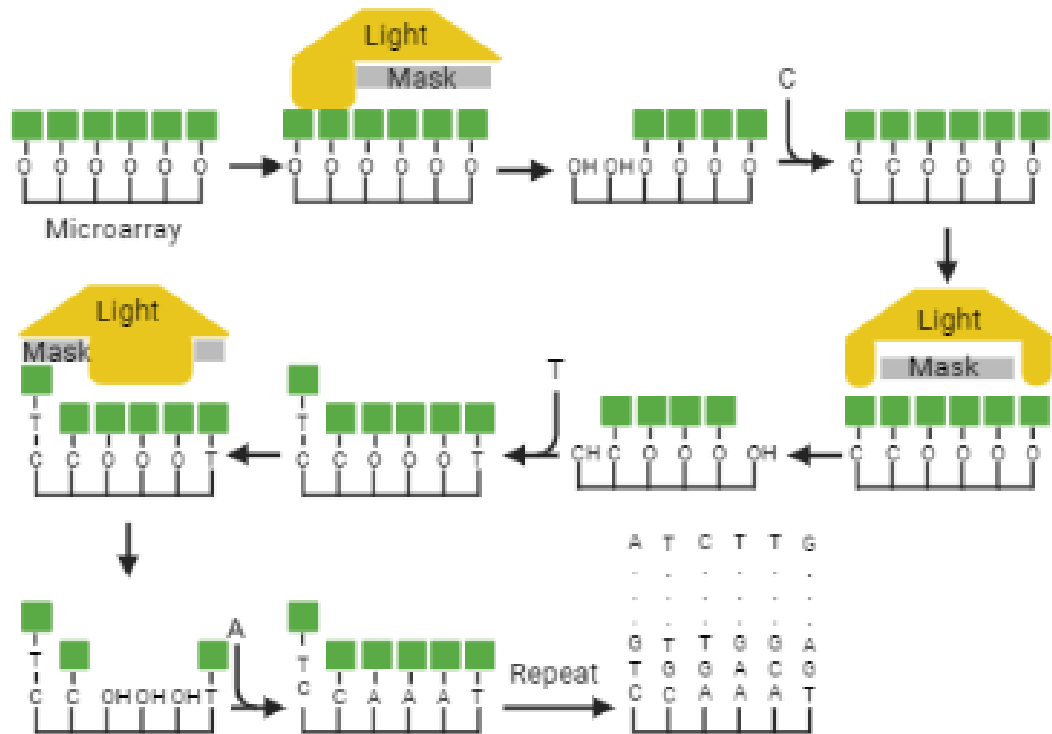


Figure 1.1. Chemical synthesis cycle of oligonucleotide microarray.

The lithographic mask allows for the UV light to only target specific regions of the microarray. The light removes the photolabile protecting agent from the surface of the microarray. Then it is washed with a nucleotide attached to another photolabile protector. A new mask is used, and the process repeats until the oligonucleotide probes are complete. (Probes are usually 20-25 nucleotides long.) Adapted from Miller & Tang (2009). Created with BioRender.com

sets of perfect match probes for each target, with each probe consisting of 25 nucleotides. Each of these sequences is usually chosen from a 600-nucleotide sequence near the non-coding 3' end of the target gene's coding region of interest (reviewed in (Jaksik et al., 2015; M. B. Miller & Tang, 2009)). Originally, there was an associated mismatch probe for each perfect match probe, which only differs by a single, non-complementary nucleotide in the middle of the probe (i.e., in the 25-nucleotide sequence, the 13th nucleotide will be a mismatch). These mismatched probes measure non-specific binding (Jaksik et al., 2015; M. B. Miller & Tang, 2009), although most modern probe level algorithms report better relative quantification if the mismatch data is omitted (Z. Wu & Irizarry, 2007).

In addition, Affymetrix also has exon-based microarrays (e.g., HuGene 1.0ST), which use similar probe designs but with some distinct differences. The first being that the perfect match probes are not associated with the 3' area of the target but rather are chosen to detect individual exons. Each exon probe set has about four probes, and these are grouped into sets of 25 for the individual genes. Another difference is that it does not use a mismatch probe. Instead, it relies on more Background Intensity Probes (BGP), about a thousand probes used to determine background intensity levels by binding to gene sequences that are non-complementary to human genes. This process allows for more perfect match probes on the microarray compared to the 3' IVT platforms, and these probes measure at the exon level can be algorithmically interpreted to produce gene level and splice variant intensities (Jaksik et al., 2015).

1.1.1.3 RNA isolation and processing

Once the company creates the microarrays, they may be sent to laboratories. The laboratories, which have selected a microarray for the species of their samples, prepare the samples for analysis. The first of these steps is RNA isolation (Jaksik et al., 2015). Once the RNA is isolated, its quality should be determined to ensure accurate readings from the microarray. One of the most common ways to measure RNA quality is through RNA integrity numbers (RINs; see section 1.2) (Jaksik et al., 2015; Schroeder et al., 2006).

An oligo-dT synthesizes the first strand of complementary DNA (cDNA) by first annealing to the mRNA's poly(A) sequence. Any RNA without the poly(A) tail is lost. The reverse transcriptase continues from the poly(A) sequence to copy the mRNA strand,

converting the RNA into cDNA (Jaksik et al., 2015; Nam et al., 2002). This strand of cDNA is then used as a template for other cDNA strands. Ribonucleases, which are also present, cause RNA cleavage at non-specific sites within the cDNA, causing fragmentation. These fragments act as primers for a polymerase, which creates a second strand of cDNA and removes the remaining RNA fragments (Figure 1.2).

This cDNA is amplified and transcribed into cRNA, which is fragmented into 50-100 nucleotides to increase the binding between short 20-25mer probes to longer cDNA strands. Another set of bacterial RNA is also introduced to biotinylate the cRNA. One is from the P1 bacteriophage and may integrate Cre, a common recombinase enzyme that inserts targets at a *Lox* site, into the system (Jaksik et al., 2015; Nagy, 2000; Sauer & Henderson, 1988). Cre allows for the insertion of biotin genes from *E. coli*, which are crucial for the fluorescence step (Figure 1.2) (Jaksik et al., 2015).

The cRNA is hybridized to the probes, and the degree to which probes are occupied is proportional to their concentrations, hybridization temperature, and GC content. Once the cRNA is bound to the probe, the unbound cRNA is washed from the microarray surface. Then a staining process occurs where the biotin binds to streptavidin-phycoerythrin, a protein with high affinity for biotin bound to a fluorescent protein (Figure 1.2) (Dundas, Demonte, & Park, 2013; Jaksik et al., 2015). The microarray is scanned, and the phycoerythrin becomes excited and emits fluorescent light that is used to quantify signal intensity. These excited levels are measured by the scanner and recorded as a single image for the microarray. This image is processed and returned as a .cel file, in which each probe has a single intensity value assigned to it. Probe level algorithms process the .cel file to adjust for background signal, normalize the signal, and then provide one expression value for each probe set (gene) (Jaksik et al., 2015). After this, the statistical analysis can begin to determine experimental or pathological effects.

1.1.2 RNA-Seq

While microarrays became more popular in the 1990s and early 2000s, another form of transcriptional profiling was also developing. Two methods for standard nucleotide sequencing were being developed: the Sanger method (cDNA is annealed to an oligonucleotide primer and continues to expand using a DNA polymerase and a solution

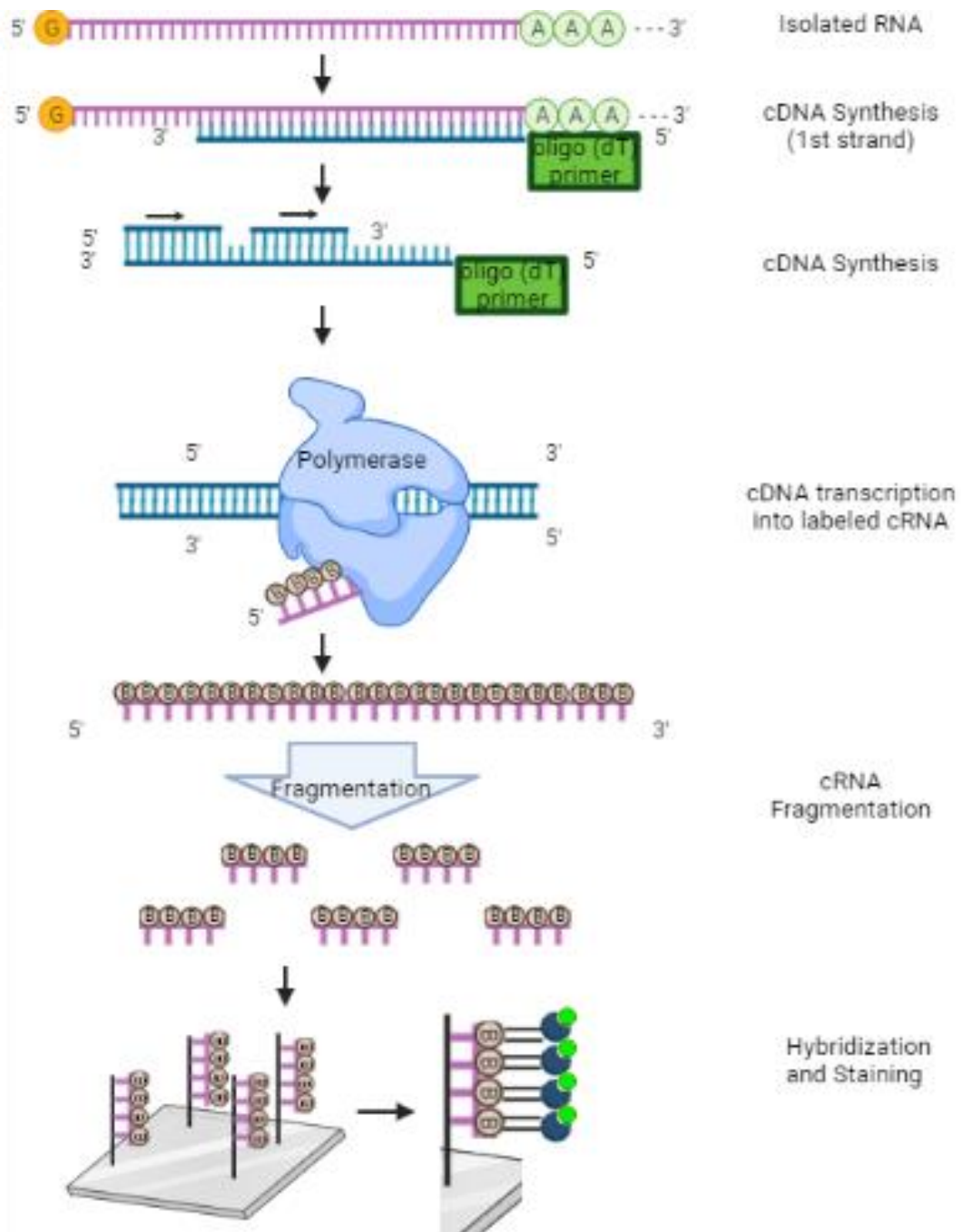


Figure 1.2. Microarray experimental steps.

RNA (pink) is isolated from its source, and then cDNA (blue) is synthesized. Once it is synthesized, the cDNA is transcribed into biotin (B) labeled cRNA. The cRNA is fragmented in 50-100 nucleotide sequences before hybridizing onto the microarray. The microarray is then washed and stained with streptavidin (dark blue circles) and phycoerythrin (neon green circles). When the phycoerythrin is exposed to the laser during scanning, it excites the machine to measure the fluorescence. Adapted from Jaksik et al. (2015). Created using BioRender.com.

of deoxynucleotide triphosphates or dideoxynucleotide triphosphates in a rate-limiting concentration (Crossley et al., 2020; Sanger, Nicklen, & Coulson, 1977)) and the serial analysis of gene expression (SAGE; a technique to gain direct and quantitative gene expression measurements (Velculescu, Zhang, Vogelstein, & Kinzler, 1995; Yamamoto, Wakatsuki, Hada, & Ryo, 2001). Based on advances in sequencing technology, Next Generation Sequencing (NGS) was introduced (reviewed by (Ansorge, 2009; Hrdlickova et al., 2017; Mardis, 2008)). NGS allows reading the nucleic acid sequence for millions of fragments in series (Ansorge, 2009). One of the most common NGS techniques today is RNA-Sequencing (RNA-Seq).

RNA-seq is a group of techniques that uses cDNA and determines the number of fragments associated with a specific gene. RNA-Seq has several advantages over microarrays. One of which is its higher dynamic range, as it counts each detected fragment and therefore does not saturate. In contrast, microarrays use hybridization approaches and have lower detection thresholds and upper saturability ceilings. Another is that RNA-seq can be done independent of a genomic reference, and therefore can more reliably find variants, measure mutations, and be used with organisms that do not have reference genomes (Sirbu, Kerr, Crane, & Ruskin, 2012; van der Kloet, Buurmans, Jonker, Smilde, & Westerhuis, 2020). However, because of its novelty, the bioinformatic pipeline to analyze the RNA-Seq findings has yet to be standardized, making it more difficult to compare across laboratories (Simoneau, Dumontier, Gosselin, & Scott, 2021). In addition, there are two types of RNA-seq: one that analyzes mRNA expression at the tissue level and one at the cell level. This discussion will focus on the former.

Preparing RNA-Seq samples is similar to preparing oligonucleotide microarray samples in some respects. In both cases, one starts by isolating the RNA, and ribosomal RNA must be removed lest it overwhelms the sequencer. This process involves enriching the RNA species of interest. One of the most common ways parallels that used in arrays, by separating the mature mRNA with long poly(A) tails from the remaining DNA, for instance beads coated with oligo-dT molecules (reviewed in (Hrdlickova et al., 2017; Voelker)). Another way to remove rRNA is rRNA depletion. This process can occur in one of two ways. The first is by using sequence-specific probes to hybridize rRNAs, bind with either biotinylated DNA or locked nucleic acid probes, and then deplete them with

streptavidin beads. The second is to use specific, not-so-random primers. These bind to the rRNA during reverse transcription, avoiding rRNA production (Hrdlickova et al., 2017).

One of two steps can come next. The first is the conversion of RNA to double-stranded cDNA, and the second is fragmentation. The RNA fragmentation, which has become the more popular option, occurs by enzymes (e.g., RNase III) or metal ions (e.g., Zn^{2+} , Mg^{2+}), though neither of these processes is entirely random. Meanwhile, cDNA can be fragmented with acoustic shearing or DNase, neither of which is random either (Hrdlickova et al., 2017; Voelker). Fragmentation is a crucial step for RNA-seq because the sequencers (i.e., Illumina) have size limitations (40-600 base pairs) as to how large of a fragment they can sequence at once (Hrdlickova et al., 2017; Voelker).

The cDNA fragments are used for the molecular cloning process. The fragmented nucleic acid no longer includes directional information. Adapters are added to the ends of the sequences, often in the RNA, to correct this problem (Hrdlickova et al., 2017). These adapters vary, depending on the platform. One of these approaches is the ligation of adapters on the 3' and 5' ends (Hrdlickova et al., 2017). The 3' and 5' ligation begins by removing the 3' phosphate group and adding a 5' phosphate group. Then the 5' adapter adenylated 3' adapter is added to the mRNA using an RNA ligase II, and a 5' adapter is ligated to the fragment with RNA ligase I. This mechanism allows the strand to be maintained during cDNA synthesis (Hrdlickova et al., 2017; Voelker). In order to prevent any bias from the adapter's sequence, random nucleotides have been added recently (Hrdlickova et al., 2017). After this, the cDNA library is then loaded onto a flow cell, a slide containing adapter-complementary oligos. Illumina Inc., the company, most commonly used for RNA-Seq, amplifies the cDNA fragments using bridge amplification cycles (Illumina, 2017) (reviewed in (Metzker, 2010)). Bridge amplification is a multistep process that begins when an adapter on a single strand of cDNA binds to its complementary oligo on the flow cell. A polymerase makes the complementary strand to the fragment. The double-strand is then denatured, and the original cDNA strand is removed (Illumina, 2016). The strand folds so that the other adapter is hybridized to its flow cell-bound complement, causing a bridge-like structure, and a polymerase produces another complementary strand. Again, these strands are denatured, creating two complementary fragments. This process is then repeated in order to create clusters of the

fragment. This process is repeated for each fragment (Illumina, 2016). An Illumina flow cell can have 100-200 million clusters (Metzker, 2010).

The reverse strands are then cleaved from the flow cell and washed away, and the 3' ends are blocked. Illumina uses a process called “sequencing by synthesis.” The first sequencing primer is then used to extend a new complementary strand. Fluorescently tagged nucleotides (each nucleotide bound with a different fluorescent) are added to the growing chain, and after they are bound, a light source excites the strand causing fluorescence. This excitement allows for sequencing based on the fluorescent signal emitted (Illumina, 2016). The wavelength and intensity are used to identify the base sequence (Illumina, 2017).

Once completed, the new strand is washed away, and an index-read primer is introduced (Illumina, 2016). Indexes are DNA sequences attached to the fragments for storage and identification (Illumina, 2017). This index fragment is created by sequencing synthesis and washed away after its completion. The 3' ends are unblocked, and the cDNA strand binds to complementary adapters again. Another index is then synthesized, only this one is extended to include the entire fragment, so there is a forward and reverse cDNA strand again. This time, the forward strand is removed, and the reverse strand is sequenced by synthesis (Illumina, 2016).

The sequences are then analyzed and grouped with similar fragments to determine the sequence of the bases, with forward and reverse reads paired. Each cluster is saved as a base cell (BCL) file until the sequencing is complete, then the BCL files are converted to a FASTQ file. These sequences are then aligned with the RNA-Seq library for variant identification (Illumina, 2016). While cDNA libraries can be created for each run, the process is time-consuming and requires higher read counts to create the library; otherwise, custom libraries may not identify mutations. Commonly used organisms (e.g., humans, mice, rats) often have libraries already compiled by the platform companies. The number of times a gene was measured is counted, and the mapped data is normalized (Costa-Silva, Domingues, & Lopes, 2017). At this point, differentially expressed genes (DEGs) can be determined statistically using one of many bioinformatic tools (Costa-Silva et al., 2017; McDermaid, Monier, Zhao, Liu, & Ma, 2019).

1.2 RNA integrity numbers

1.2.1 Role in transcriptional profiling

As previously described, unbiased RNA quantification is crucial for gene expression analysis (Schroeder et al., 2006). Multiple conditions can impact the gene expression, including RNA quality (Gallego Romero, Pai, Tung, & Gilad, 2014; Opitz et al., 2010; Stan et al., 2006). While RNA is a thermodynamically stable molecule, it can be digested quickly by endogenous enzymes. These enzymes cause RNA fragmentation. Early ways of measuring RNA quality were: 1) agarose gel electrophoresis to determine the ratio between the 28S and 18S bands from the ribosomal RNA (rRNA; high-quality RNA had a ratio > 2.0) (Schroeder et al., 2006); 2) using spectrometry determining the ratio between 260 nm band (specific nucleic acids) and 280 nm band (specific for proteins) (reviewed in (Fleige & Pfaffl, 2006)); or 3) the 3':5' ratio often determined during polymerase chain reaction (PCR) (Die, Obrero, González-Verdejo, & Román, 2011). However, the protocol for these measurements could vary depending on the laboratory, which did not allow for comparisons across laboratories and institutions, and were not always accurate predictors of RNA quality (Schroeder et al., 2006; Sonntag et al., 2016). To address this problem, Agilent Technologies introduced RNA integrity numbers (RINs) in 2004 using their 2100 Bioanalyzer RNA 6000 Nano and RNA 6000 Pico LabChip kits (Mueller, Lightfoot, & Schroeder, 2004; Schroeder et al., 2006).

By providing a tool to help standardize the reporting of RNA quality reporting, researchers were able to compare data more accurately. They could also determine correction methods to help remove the impact of RNA degradation in the samples. Currently, however, there is no universal or tissue-specific standard for considering the cells or tissue to be “too degraded” for experimental use. Mueller et al. claimed the effects of RNA quality might be more influential in specific transcriptional profiling techniques, and therefore procedures controlling for RIN might be method-specific too (2004). However, the most significant benefit of RINs is that it uses multiple measurements to determine a single value to determine the quality of the sample, while its predecessors tended only to use one measure (Mueller et al., 2004; Schroeder et al., 2006).

1.2.2 Determining RNA integrity number values

The RIN software algorithm was first developed using around 1,200 mammalian RNA samples of varying tissues and quality on the Eukaryote Total RNA Nano Assay from Agilent Technologies. These samples were then manually categorized into a numeric system ranging from 1 to 10, where increasing values indicate better quality (Mueller et al., 2004). The values are determined using measurements from an electropherogram (Figures 1.3, 1.4); these measurements include the marker peak, 5S region, fast region, 18S fragment, inter-region, and 28S fragment. Primarily, RINs are determined based on the quality of the rRNA as the 5S, 18S, and 28S, even though gene expression uses the mRNA because RNA degrading enzymes typically attack both (Hrdlickova et al., 2017; Jaksik et al., 2015; Mueller et al., 2004; Schroeder et al., 2006). The 5S region differs from the 18S and 28S peaks because it contains multiple smaller fragments (i.e., 5S and 5.8S rRNA and tRNA). Taken together, these measurements produce seven features that are input into an algorithm to determine the RIN for a given sample:

1. The total RNA ratio. The measurement of the fraction of the area in the 18S and 28S regions is compared to the total area under the curve. The ratio is largest in RIN scores of 6 - 10;
2. The 28S height. The 28S peak degrades more rapidly than the 18S peak and determines additional information about the degradation process. The 28S height is larger for RIN values of 9 - 10 and has a value of 0 for RIN scores of 1 - 3;
3. Fast area ratio. The measurement of the fast region area to the total RNA area;
4. The linear regression value at the endpoint of the fast region;
5. The number of detected fragments in the fast region. As rRNA degrades, there is a continuous shift towards smaller fragment sizes;
6. The presence or absence of the 18S peak. This allows the algorithm to determine between minimal or significant degradation;
7. The relationship between the overall mean value and the median value. The mean value is more sensitive to larger peaks. It contains information on totally degraded mRNA or abnormalities (Schroeder et al., 2006).

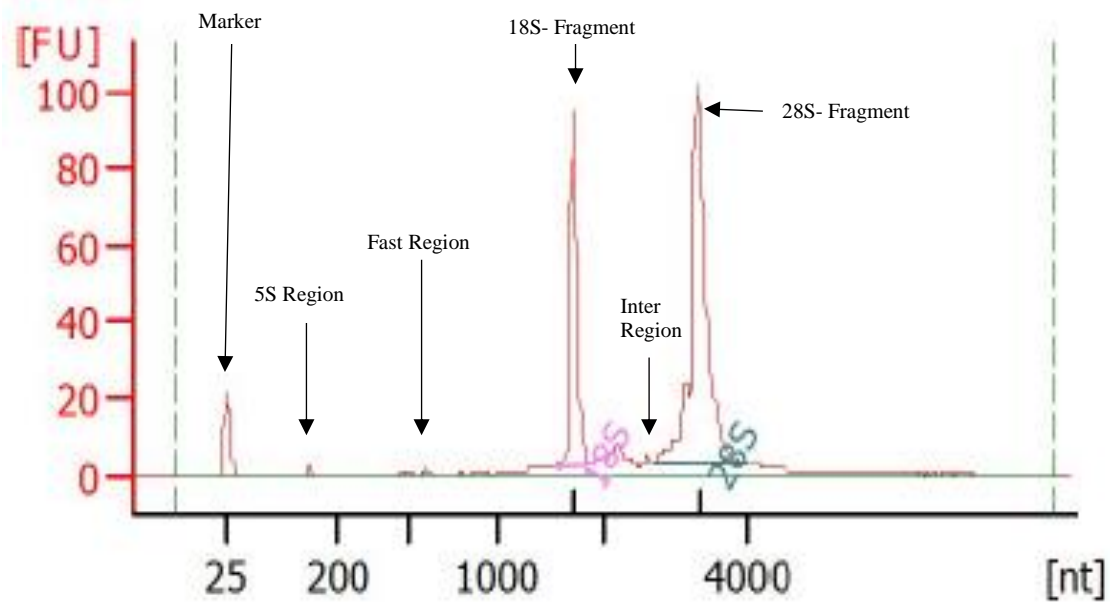


Figure 1.3. Parts of the RIN electropherogram.

Marker: this peak is used to determine strongly degraded samples since it is the only peak not influenced by RNA (highest peak at RINs of 1-2). 5S Region: this region contains smaller RNA fragments. Fast region: the area between 5S Region and 18S fragment; 18S fragment: the signal from 18S rRNA; Inter-Region: the region between the 18S and 28S fragments; and 28S fragment: the signal from the 28S rRNA.

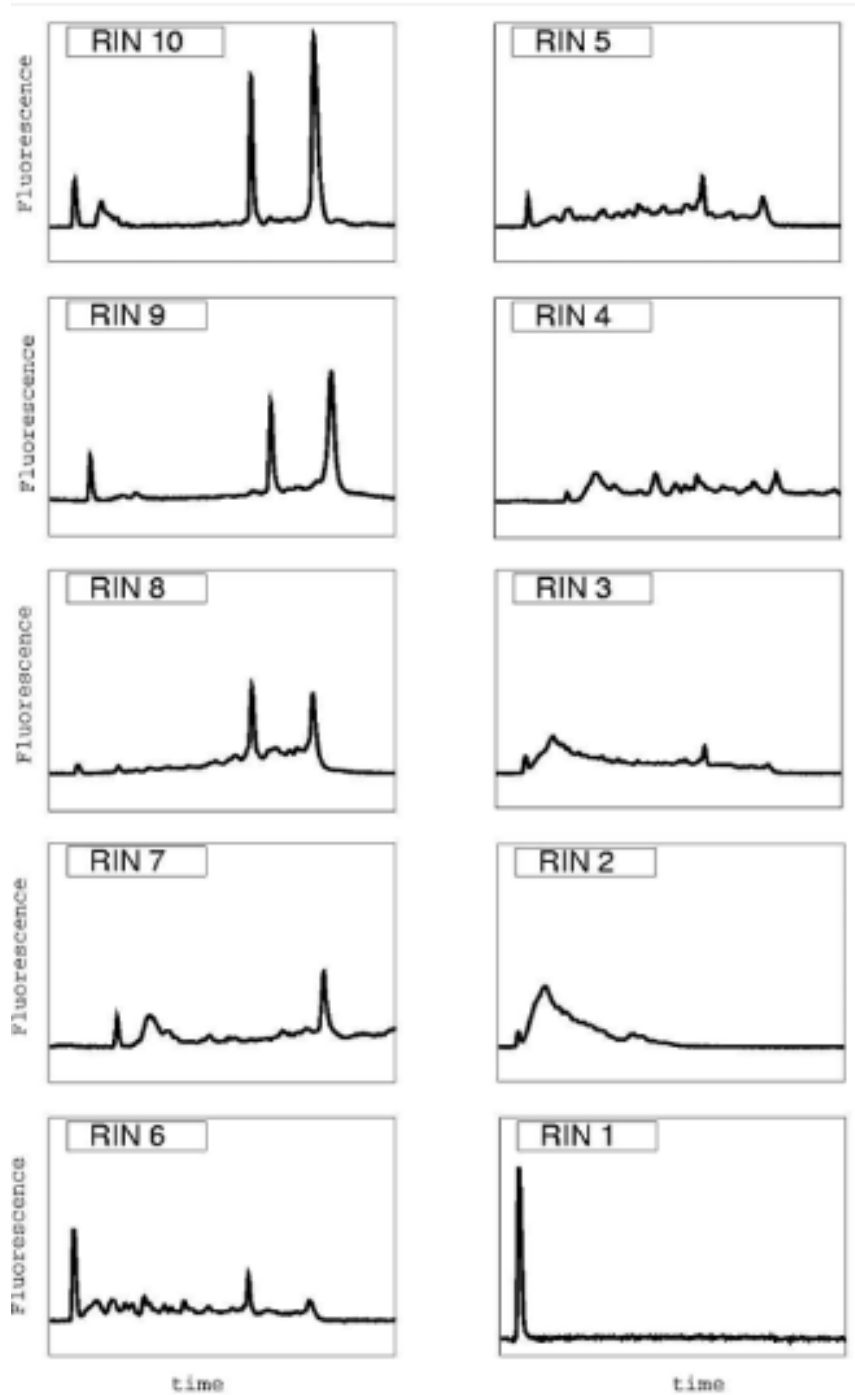


Figure 1.4. Representative electropherograms for each RIN integer.

These images show how the electropherogram readings change as RNA degrades. RINs of 10 include RNA with minimal degradation, while RINs of 1 are considered wholly degraded. Figure from Schroeder et al., 2006.

In addition to the RIN, the algorithm also produces the total RNA area, the RNA concentration, and the 28S / 18S ratio. While the total RNA area is used to determine the RIN and the 28S / 18S ratio is indirectly used, the RNA concentration is not used to calculate the RIN. Because of the standard protocol for determining RINs, the quantification of RNA degradation, and the abundant information provided, RINs have become a standard in the scientific community (Fleige & Pfaffl, 2006; Mueller et al., 2004; Schroeder et al., 2006).

RNA quality can vary due to pre-and post-mortem events (Durrenberger et al., 2010), and this can be seen in the quality between humans and animals (see Table 2.2). This difference is probably due to the more controlled conditions for tissue collection in the animals used for the study. In addition, there is evidence that lower RINs can be associated with disease states. For example, several studies have found that subjects diagnosed with Alzheimer's disease (AD) have significantly lower RINs than their controls post-mortem (Durrenberger et al., 2010; J. A. Miller et al., 2017). When one of the studies tried to remove the effect of the RINs, then their AD effect was removed as well (J. A. Miller et al., 2017). This indicates, at least in brain tissue, that the disease state may exacerbate the causes of RNA degradation. They may be influencing the same genes. There has been no prior work investigating how RNA degradations influence RNA expression in the brain of control subjects. However, the comparison of RNA decay's impact on human renal cancer tumors (Opitz et al., 2010) and peripheral blood mononuclear cells (Gallego Romero et al., 2014) found two different sets of influenced genes. This finding indicates that RNA degradation may impact specific genes and pathways and those genes and pathways may vary depending on tissue source.

Unfortunately, not understanding the impacts of RNA degradation, signified by lower RINs, can have significant implications. Since there is currently no widely accepted standard for a minimum RIN, the impact of RINs can vary across studies. Unfortunately, since studies do not often supply the RINs for individual tissue that has been transcriptionally profiled, it can be difficult or even impossible to tell how much of an effect it has had, leading to a lurking variable influencing data.

CHAPTER 2. DECLINING RNA INTEGRITY IN CONTROL AUTOPSY BRAIN TISSUE IS ROBUSTLY AND ASYMMETRICALLY ASSOCIATED WITH SELECTIVE NEURONAL WITH SELECTIVE NEURONAL SIGNAL LOSS

2.1 Summary

RNA integrity numbers (RINs) are a standardized method for semi-quantification of RNA degradation, and are used in quality control prior to transcriptional profiling analysis. Recent work has demonstrated that RINs are associated with downstream transcriptional profiling, and correction procedures are typically employed in bioinformatic analysis pipelines to attempt to control for RIN's influence on gene expression. However, relatively little work has been done to determine whether RIN's influence is random, or is specifically targeted to a subset of mRNAs. We tested the hypothesis that RIN would be associated with a robust transcriptional profile seen across multiple studies.

To test this, we downloaded subsets of raw transcriptional data from six published studies. We only included control, non-pathological post-mortem human brain tissue (n = 383 samples) in which independent subjects' RIN values were also reported. A robust set of mRNAs consistently and significantly correlated with RIN across multiple studies, appearing to be selectively degraded as RIN declines. Many of the affected gene expression pathways are related to neurons (e.g., vesicle, mRNA transport, synapse, and mitochondria), suggesting that neuronal synaptic mRNA may be particularly vulnerable to degradation. Subsequent analysis of the relationship between RIN and vulnerable mRNA expression revealed most of the decay occurred over a relatively narrow RIN range of 7.2-8.6, with RIN values > 8.6 showing a ceiling effect, and those < 7.2 showing a floor effect on gene expression. Our data suggests that the RIN effect is pathway selective and non-linear, which may be an important consideration for current bioinformatic RIN correcting procedures, particularly in datasets in which declining RIN is confounded with a pathology under study (e.g., in Alzheimer's disease).

2.2 Introduction

Transcriptional profiling in human brain tissue reveals that the gene signatures of aging and neurodegenerative diseases are robust and consistent across different independent samples using measurement platforms across different labs (Courtney,

Kornfeld, Janitz, & Janitz, 2010; K. E. Hargis & Blalock, 2017). However, disease-states and aging are not the only factors possibly impacting gene expression in transcriptional profiling. Tissue treatment, post-mortem interval (PMI), pH, etc. also have an impact on gene expression (Ferreira et al., 2018; Jia et al., 2021; Mistry & Pavlidis, 2010; Pozhitkov et al., 2017). Often, these factors are assumed to impact gene expression, since they damage RNA quality.

RNA quality, as measured through RIN, is known to impact transcriptional profiling (Copoio et al., 2007; Gallego Romero et al., 2014; Jaffe et al., 2017; Opitz et al., 2010). While there are many ways to determine RNA quality (i.e. gel optical density, NanoDrop, denaturing agarose gel-electrophoresis), but RNA integrity numbers (RINs) have become a standard in the last fifteen years (Fleige & Pfaffl, 2006; Mueller et al., 2004; Schroeder et al., 2006). This technology relies on several measures including the total RNA ratio (fraction of the area in the 18S and 28S region compared to the total area under the curve), 28S peak height, fast area ratio (fast area compared to the total area), and the marker height (Schroeder et al., 2006). In addition, the program used to determine RINs also provides the RNA area under the curve, RNA concentration, and rRNA ratio (28S/18S). It should be noted that though mRNA is typically the focus of most transcriptional profiling studies, RIN heavily relies on rRNA to infer the quality (Fleige & Pfaffl, 2006; Schroeder et al., 2006). Despite its prevalence and the importance of RNA integrity for transcriptional profiling, RINs are not often reported for individual subjects within published data. This is problematic, since often the tissue collection, storage, and handling can influence RNA quality (Gallego Romero et al., 2014; Jia et al., 2021). Often, human tissue samples are more variable and frequently have lower RINs than those in experimental animal studies (See Results).

Since RNA quality may impact gene expression, particularly in humans, multiple groups have published bioinformatic tools to attempt to correct for the influence of RNA degradation on gene expression. Three approaches for correcting include Surrogate Variable Analysis (SVA) (Viljoen & Blackburn, 2013), quality SVA (qSVA) (Jaffe et al., 2017), and regression (Gallego Romero et al., 2014; J. A. Miller et al., 2017; Parsana et al., 2019). SVAs use the gene expression data to determine which genes are impacted by sources of variability, depending on the metavariable being corrected. The factors are then

used in a linear model to adjust for noise (Viljoen & Blackburn, 2013). However, Jaffe et al. was concerned that this approach might include false-positives. Therefore, they created their own model, qSVA, which uses results from a defined independent tissue degradation experiment to identify genes most affected by degradation and correlate them in the experimental dataset based on factors calculated in the independent dataset (Jaffe et al., 2017). Regression approaches are most commonly used to correct for RIN (Gallego Romero et al., 2014; J. A. Miller et al., 2017; Parsana et al., 2019) since RNA degradation can influence genes and pathways at different rates (Gallego Romero et al., 2014; Jaffe et al., 2017).

However, these approaches may be problematic for two reasons. First, if RIN values above a certain threshold are considered ‘safe’ (i.e., do not influence gene expression), then defining that safe threshold would be important, as the simplest approach would be to retain samples that exceeded the safety threshold. Further, attempting to control for a metavariabile that is not associated with signal can cause artificially inflated variance (Williams, Grajales, & Kurkiewicz, 2013), thereby distorting the processed signal. Second, as Gallego-Romero et al. reported, half of the differentially expressed genes after 84 hours of room temperature degradation appeared to show increased expression after RIN correction, but this increase was a distortion caused by the RIN correction procedure itself (Gallego Romero et al., 2014). Thus, establishing a safe threshold for RIN, one above which transcriptional profiling data can be processed without correcting for RIN could be of use. Further, it is important to appreciate whether the influence of RIN 1) is randomly distributed across the transcriptome, and therefore would not replicate in samples in a study or across studies from different labs; or 2) is focused on certain genes and pathways. Finally, whether the RIN effect is exerted across the full spectrum of RIN values or is constrained to a narrow range would be important to know as regression tools are more well-suited to the former than the latter case.

If a condition such as neurodegenerative disease is associated with lower RINs, then the two variables would be confounded, complicating attempts to control for one variable without influencing the other. Indeed, this is a common issue, as prior work (Durrenberger et al., 2010; Jaffe et al., 2017; J. A. Miller et al., 2017) has shown that various insults are associated with significantly lower RINs in brain tissue. For instance, one study

investigating the influence of pre- and post-mortem variables on RIN (Durrenberger et al., 2010) found that ante-mortem variables such as agonal state, coma, and artificial ventilation had a cumulative downward influence on RIN, as did a diagnosis of Alzheimer's disease (no RIN corrections were employed, likely because of the presence of this confound). Another study determined that RIN scores decreased with a diagnosis of schizophrenia (Jaffe et al., 2017). Noting that multiple-regression RIN correction approaches would be confounded, the authors applied their novel RIN correction procedure, qSVA, that estimated decay based on observations in independent degradation datasets. Yet here, RIN-associated mRNA declines in the schizophrenic brain exceeded the correction, and therefore exceeded the amount of decline seen in control tissue (Jaffe et al., 2017). It is also important to note that the schizophrenic brains did not have a longer PMI than their controlled counterparts, yet had lower RINs, suggesting that some process other than PMI, and possibly influencing different pathways, plays a role. This indicated not only that schizophrenia was associated with a decline in RIN, but that the mRNA species associated with RIN in schizophrenia were targeted more aggressively than in control tissue. Finally, the last study established that there is a significant decrease in RIN with Alzheimer's disease (AD) (J. A. Miller et al., 2017). They also identified that a standard regression-based RIN correction procedure removed the well-established AD-effect from the transcriptional profile. While Jaffe et al., postulate an interaction between RNA quality and cellular composition (Jaffe et al., 2017), Miller et al. concluded the difference in RNA quality might be due pre- or post-mortem influences (J. A. Miller et al., 2017).

Due to the assumption that most post-mortem factors impact RINs, problems with current RNA correction methods, and the potential of biological factors playing a role in RNA degradation, we examined the role RINs play in gene expression in microarrays. In the current work, we investigate if RINs in control, post-mortem human frontal lobe tissue impacts gene expression in a non-linear fashion, targeting specific genes and pathways, and the thresholds of this impact. In addition, we investigated the relationship of other metavariabls with RIN and the effect of RIN on AD tissue to determine if they impact similar genes.

2.3 Methods

2.3.1 Identifying datasets and preparing cel files

The .cel files for the control subjects matching our criteria (see results) of the datasets were downloaded. Different datasets may have used different probe level algorithms in their published work, and many probe level algorithms are influenced by the total number of arrays selected for calculation (Gautier, Cope, Bolstad, & Irizarry, 2004). Further, in our approach, the total number of samples that would be used likely would change because our unique selection criteria would assess only control tissue from specified brain regions. These files were analyzed in R using the Robust Multi-array (RMA) (Bolstad, Irizarry, Astrand, & Speed, 2003; Irizarry et al., 2003) function in the oligo package (Carvalho & Irizarry, 2010) from Bioconductor. Therefore, we ran the RMA probe level summarization algorithm independently on .cel files of each dataset. These estimates of gene expression were transferred to flat files in Excel, and Gene Symbols and Titles (based upon the updated GEO platform IDs under which the original datasets were published), as well as sample-specific metadata (e.g. RIN, Age, pH, PMI, sex) were annotated.

2.3.2 Differences in brain RNA quality across species

To determine if there was a significant difference in reported RNA quality between human, rat, and mouse brains as most assume (keeping in mind that because RIN values are used to triage subjects, there is likely some bias in these reports), studies were identified that matched the following criteria: 1) include control brain tissue (for humans, only frontal lobe); 2) have disambiguated RNA integrity numbers (RINs); and 3) use Affymetrix platforms. Once studies were found, the RIN scores were separated by species and an unequal Mann-Whitney U-Test quantitatively tested the hypothesis (observed anecdotally in prior work) that human autopsy samples show lower RIN score than those from experimental animals. Subsequent work focuses completely on human, post-mortem brain tissue.

2.3.3 Pre-statistical processing and individual study analysis

Once the .cel files were analyzed, each study was independently processed as follows. We created signal intensity histograms to determine presence-call cutoffs (PCC).

The PCC was determined by analyzing the signal intensity histogram to determine the ‘saddle point’ at which signal values transitioned from noise to reliable signals. Then, within each dataset, probe sets were retained for analysis if $\geq 50\%$ of that probe set’s observations \geq PCC. To retain unique gene symbol representations, if > 1 probe set was annotated to the same gene symbol, then the probe set with the highest average signal intensity was retained.

2.3.4 Separate dataset approaches

2.3.4.1 Defining significant metavariate-correlated genes.

Once the pre-statistically filtered, uniquely annotated, and reliably expressed probe sets were selected, Pearson’s correlation (r) tests between different metavariates (i.e. age, PMI, and pH), and between metavariates and expression signals were performed, and the associated p-values and false discovery rates (FDRs) calculated. A liberal p-value cutoff ($\alpha = 0.05$) defined significant results to address the increased false negative rate anticipated to occur in subsequent cross dataset comparisons (Benjamini & Hochberg, 1995; Pawitan, Michiels, Koscielny, Gusnanto, & Ploner, 2005). To investigate the potential influence of sex on RIN-associated gene expression levels, the males and females from the data-subset with the largest number of subjects underwent independent RIN-associated gene expression analysis. In this dataset, males still represented $\sim 3/4$ of the total dataset. To address this statistical power imbalance, we also randomly resampled (1000 iterations) male subjects at the female n-level for comparison between sexes.

2.3.4.2 Comparing across separate datasets.

The influence of metavariates on independent data-subsets was assessed with a post-hoc proportional change analysis followed by binomial testing to determine whether there was significant agreement. The significant common probe sets were run through the WEB-based Gene Set Analysis Toolkit (WebGestalt) (Liao, Wang, Jaehnig, Shi, & Zhang, 2019) to statistically test functional categories in the Gene Ontology (Ashburner et al., 2000; Gene Ontology, 2021) for overrepresentation ($\alpha = 0.05$; GO Molecular Function, Cellular Component, Biological Process noRedundant; Redundancy reduction = affinity propagation).

2.3.5 Unified dataset analysis

2.3.5.1 Approaches for unifying independent datasets/ removing batch effects.

The ‘independent dataset’ approach described above treats each data set as an independent unit, therefore avoiding potential batch effects. However, the ‘independent dataset’ approach is also limited by the range of RIN values available in each study. To unify independent datasets, we tried three methods.

Method 1) Within-dataset standardization. Within each dataset, each row’s data is standardized, then those standardized results are combined across datasets

Method 2) Harmony. Using the Seurat package (Satija, Farrell, Gennert, Schier, & Regev, 2015) within the Bioconductor (Gentleman et al., 2004; Huber et al., 2015) subset of the R programming language, the Harmony function (Korsunsky et al., 2019) was applied to use PCA-based metrics to subtract batch-based variance.

Method 3) Mean-subtraction. Within each dataset, for each gene, the average gene expression for subjects with a RIN ≥ 8.3 were averaged. Then, that average was subtracted from all observations for that gene from that dataset.

2.3.5.2 Template analysis.

Unified dataset gene expression data were placed into a single worksheet and correlated with 356 user-defined templates. These templates were used to fit the gene expression signal across RIN values. Correlation was performed for each gene with all 356 templates, and the gene was assigned to the template with which the gene correlated most strongly and exceeded a stringent correlation criterion ($r \geq |0.69|$; $p = 9.61 \text{ E-}5$). Then, the number of genes observed per template was quantified. To determine if the number of genes assigned to each template was greater than expected by chance, a resampling procedure (1,000 iterations) was performed to estimate the number of genes per template. The probability that the number observed in the actual data was significantly higher than number estimated in the resampled data was tested for significance using the Z-score. Pathway analysis on selective templates with significant genes proceeded as described for ‘separate dataset approaches.’

2.3.6 Alzheimer's disease gene relationship

In order to determine if pathways associated with Alzheimer's disease (AD) are overrepresented among RNA degradation sensitive genes, two Alzheimer's disease transcriptional profile studies were used (K. E. Hargis & Blalock, 2017; J. A. Miller et al., 2017) (one examines the same tissue region as the present work (J. A. Miller et al., 2017), the second represents consensus AD signature across multiple brain regions from several labs (K. E. Hargis & Blalock, 2017)). From Miller et al., 2017, AD-significant gene expression levels were identified based analysis of the original publication ($p \leq 0.05$).

Hargis & Blalock (2017), a secondary data analysis study that summarized log₂ fold-changes (L2FCs) from 5 AD brain transcriptional studies across 8 different brain regions was used. In the present work, a consensus list of AD-significant genes from that secondary data analysis was determined by calculating the average L2FC ($\pm 99\%$ confidence interval) across all 5 of those studies. Results were considered significant if the 99% confidence interval did not cross the '0' L2FC line (e.g., 99% confidence the observation was upregulated or downregulated with AD). The binomial test was used to determine if the transcriptional profile of RIN-sensitive genes bore similarity to either AD profile (Miller or Hargis). The log₂ fold changes (L2FC) for the difference between AD and control subjects for each gene in Miller et al. was then compared to the correlation between gene expression and RIN from study with the most the subjects. The average L2FC for each unique probe set from Hargis & Blalock was compared with the genes significant in all data-subsets used in the cross-data comparison.

2.4 Results

2.4.1 Overview of dataset

Using the Gene Expression Omnibus, we identified 6 datasets which met our criteria (disambiguated RNA integrity number [RIN] values; human frontal lobe tissue; and Affymetrix platform technology): GSE22521 (Somel et al., 2011), GSE25219 (Kang et al., 2011), GSE45878 (Consortium, 2013), GSE46706 (Trabzuni et al., 2011), GSE53987 (Lanz et al., 2015), and GSE71620 (C. Y. Chen et al., 2016) (Table 2.1; Supp. Data 2.6-2.11).

From within each dataset, the .cel files that qualified for analysis (the qualifying "data-subset"- [tissue must be human frontal lobe tissue, must include disambiguated RNA

Table 2.1. Data-subset information

GEO Accession ID- The Gene Expression Omnibus (GEO) identifier for each dataset; *Representative Publication*- peer-reviewed citation for each dataset; *#Chips Used/ Total*- The subset of the total chips within original dataset that met criteria for inclusion in the present work (e.g., from control subject frontal cortex- subsequent data in table is for subjects that met criteria); *Age Range*- age (in years); *Age and RIN*: Results of correlation analysis (Pearson's test r and p -values) between age and RNA-Integrity Number; *Sex*: number of male (M) and Female (F) subjects; *Range of RIN*, *Mean of RIN* are as described; *FDRs for RIN, Age, PMI and pH*- False Discovery Rate (FDR) for the correlation between these metavariabes and global gene expression.

GEO Accession ID:	GSE22521	GSE25219	GSE45878	GSE46706	GSE53987	GSE71620
Representative Publication	(Somel et al., 2011)	(Kang et al., 2011)	GTE _x (2014)	(Trabzuni et al., 2011)	(Lanz et al., 2015)	(Chen et al., 2016)
# Chips Used/ Total	11/68	19/1139	16/837	119/1231	19/205	199/420
Age Range	22-98	3-70	-	16-102	22-68	16-96
Sex (M/F)	9/2	11/8	8/8	85/34	10/9	157/42
Range of RIN	7.3-9.2	7.7-9.4	5.7-8.5	2-7.7	6.6-8.7	5.9-9.6
Mean of RIN (\pm St. Dev.)	8.10 (\pm 0.58)	8.63 (\pm 0.53)	7.12 (\pm 0.79)	4.43 (\pm 1.59)	7.85 (\pm 0.62)	8.08 (\pm 0.67)
PCC	3.15	6.22	2.06	4.76	5.40	3.57
Correlation between RIN vs.						
<i>Age: r (p)</i>	-0.29 (0.38)	0.29 (0.23)	-	-0.049 (0.60)	-0.12 (0.62)	-0.10 (0.14)
<i>PMI: r (p)</i>	-0.61 (0.047)	-0.094 (0.70)	-	0.049 (0.59)	-0.093 (0.71)	-0.21 (0.0033)
<i>pH: r (p)</i>	-	0.0071 (0.98)	-	0.17 (0.066)	0.087 (0.72)	0.34 (7.8x 10 ⁻⁷)
FDR for Gene Expression vs.						
<i>RIN (0.05)</i>	0.437	0.138	0.271	0.992	0.295	0.149
<i>Age (0.05)</i>	0.127	0.248	-	0.121	0.216	0.112
<i>PMI (0.05)</i>	0.593	1.616	-	0.104	1.667	0.324
<i>pH (0.05)</i>	-	0.394	-	0.567	1.352	0.131

integrity numbers (RINs), and must use Affymetrix platform technology) were downloaded and reanalyzed at the probe level using Robust Multi-array (RMA; (Bolstad et al., 2003; Irizarry et al., 2003)). For each data-subset, a signal frequency histogram was plotted to remove low-intensity signal (Figure 2.1). Further, the gene annotations for each data-subset were downloaded from the platforms most recently associated with the studies on Gene Expression Omnibus (GEO) (Barrett et al., 2013). GPL6244 (last updated March 5, 2020) annotated GSE22521; GPL5175 (last updated February 18, 2019) annotated GSE25219 and GSE46706; GPL16977 (last updated September 2, 2014) annotated GSE45878; GPL570 (version updated June 16, 2016) annotated GSE53987; and GLP11532 (last updated November 8, 2016) annotated GSE71620. For each data-subset, if more than one row of data was annotated to the same gene symbol, then the row with the highest mean signal intensity was retained for further analysis.

For this secondary data analysis, two approaches are feasible. The first, and more conservative, approach would be to analyze each data-subset independently for correlation to RIN, and then, to compile the statically significant results from these independent tests. Using this approach, agreement among multiple independently analyzed datasets regarding RIN-sensitive genes could be used to test for consistent effects. This approach identifies robust effects and is less vulnerable to dataset-based batch effects. However, its conservative nature is both a strength and a weakness, reducing the likelihood of statistical false positives at the expense of increasing the likelihood of statistical false negatives. A second, more liberal approach would be to combine the data from these disparate sources to create a single dataset. This approach would have the advantage of increased discovery power but would also be more vulnerable to false positives, and would only be feasible in the absence of batch effects. To determine whether the first ('independent dataset') or secondary ('merged dataset') approach is more feasible for the initial analysis, a principle component analysis (PCA) was constructed. The PCA shows an intense batch effect among the different datasets (Figure 2.2A), strongly suggesting the 'independent dataset' approach would be more feasible for the data prior to any batch removal procedures.

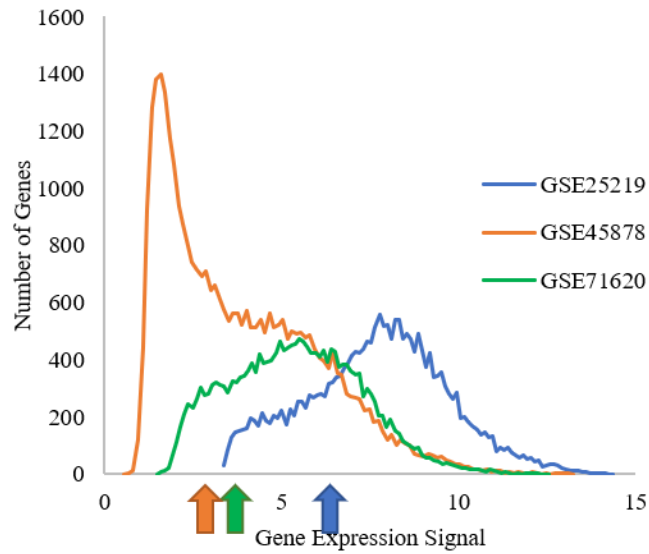


Figure 2.1. Presence cut-offs established in a dataset- dependent fashion.

Histograms of the average gene expression for datasets determine the cut-off value used. The gene expression signal varied significantly between the datasets. This prevented us from a single standardized cutoff value across all studies and combining the datasets, so each study had an independent cut-off value. Arrows represent the cut-off value for study of the same color.

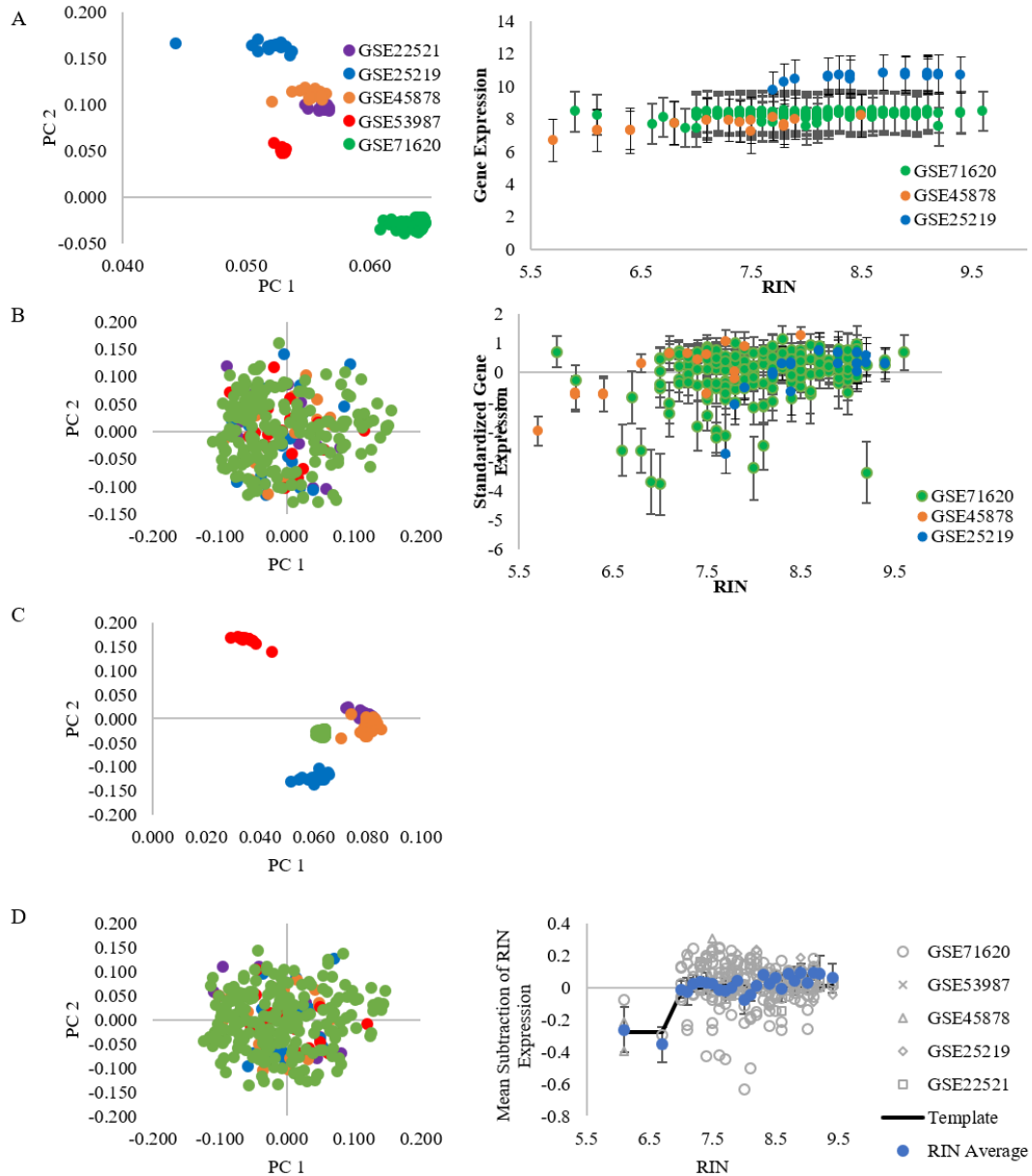


Figure 2.2 PCA plots and monovalent inorganic cation transmembrane transport pathway expression.

2,000 variable genes were used in the principle component analysis (PCA). The different datasets are distinct and separate from each other, not allowing for a single analysis. Genes for the monovalent cation transmembrane transport pathway (Table 2.4) were used to determine how gene expression decreased as RNA degrades. Here, we show the RMA values (A); a standardized gene expression (B); Harmony (C); and the mean-subtraction (D). Therefore, the mean subtraction approach (D) appeared to both remove the batch effect, while preserving original study deflecting points in the merged data. The raw data and Harmony did not remove the batch effect, and therefore did not allow for a merged data across datasets. The standardization method had each unique data-subset beginning to decline at different points, which may be due to the centering each dataset at zero, regardless of RIN range.

2.4.2 Differences in RNA quality across species

While reading prior studies, it came to our attention that no one had supported the claim that animal RINs were typically higher than those of humans. Therefore, we found ten studies which met our criteria (control brain tissue; disambiguated RINs; and Affymetrix platform technology) (C. Y. Chen et al., 2016; Consortium, 2013; Frazier et al., 2020; Gant et al., 2018; Kang et al., 2011; Lakatos, Goldberg, & Blurton-Jones, 2017; Lanz et al., 2015; Scarpa et al., 2018; Somel et al., 2011; Trabzuni et al., 2011) (Table 2.2). When disambiguated RINs are grouped by species (human, rat, and mouse), there is a significant difference between human and rat (unequal Mann-Whitney U-Test $p = 6.10E-4$) and human and mouse (unequal Mann-Whitney U-Test $p = 1.63E-6$), but not between rat and mouse (unequal Mann-Whitney U-Test $p = 0.301$).

2.4.3 Metadata correlation analysis of individual datasets

Pearson's correlations between published gene expression values and metadata (RIN, pH, post-mortem intervals [PMI], age) were calculated for each individual dataset where available (Table 2.1; Figure 2.3). 0/ 5 datasets had a significant ($p \leq 0.05$) age-to-RIN correlation (Figure 2.3A), while 2/ 5 had significant negative PMI-to-RIN correlations (Figure 2.3B). 1/ 4 datasets had a significant positive pH-to-RIN correlation (Figure 2.3C). Surprisingly, this lack of a robust relationship between RIN and PMI, or RIN and metadata traditionally associated with tissue quality suggests these measures may serve as poor proxies for estimating RNA quality.

However, just because metadata do not correlate with RIN scores does not mean they do not explain some degree of gene variability in their own right. To test this, the false discovery rates (FDRs) were calculated for the correlation between gene signal and: RINs; pH; PMI; or age (Table 2.1). Aging showed a strong and consistent influence on gene expression (average FDR = 0.165; 95% Confidence Interval [CI] = [0.110-0.220]) (Berchtold et al., 2013; Berchtold et al., 2008; Somel et al., 2011; Soreq et al., 2017). RIN appeared to have the second most prominent influence (average FDR = 0.380; 95% CI = [0.125-0.636]), while the influence of pH (average FDR = 0.611; 95% CI = [0.0960-1.13]) and PMI (average FDR = 0.861; 95% CI = [0.218-1.50]) were less stable. It should be noted that there are constraints on the data, determined by the original studies, which may be influencing the FDRs for RIN, pH, and PMI. Because our study focuses on the effects

Table 2.2. RIN comparisons across species.

GEO Accession ID- The Gene Expression Omnibus (GEO) identifier for each dataset; Representative Publication- peer-reviewed citation for each dataset; # of subjects- The number of subjects from a subsection that met our criteria in the present work (e.g. from human control subject frontal cortex- subsequent data in table is for subjects that met criteria) or a single tissue type from each dataset (rodents); Tissue- Reported tissue type analyzed; RIN Range, RIN Avg. + St. Dev. as described. Hipp.- hippocampus.

GEO ID	Publication	# of subjects	Tissue	RIN Range	RIN avg. \pm St. Dev.
<i>Human (see Table 1)</i>					
<i>Rat</i>					
GSE102054	Gant et al., 2018	23	Hipp.	8.9 - 9.8	9.40 \pm 0.22
GSE130098	Frazier et al., 2020	26	Hipp.	6.5 - 7.8	7.32 \pm 0.32
<i>Mouse</i>					
GSE63469	-	6	Hipp.	7.9 - 9.1	8.55 \pm 0.45
GSE95546	Lakatos et al., 2017	20	Striatum	9.2 - 9.7	9.42 \pm 0.15
GSE109112	Scarpa et al., 2018	98	Cortex	6.1 - 8.6	7.70 \pm 0.41

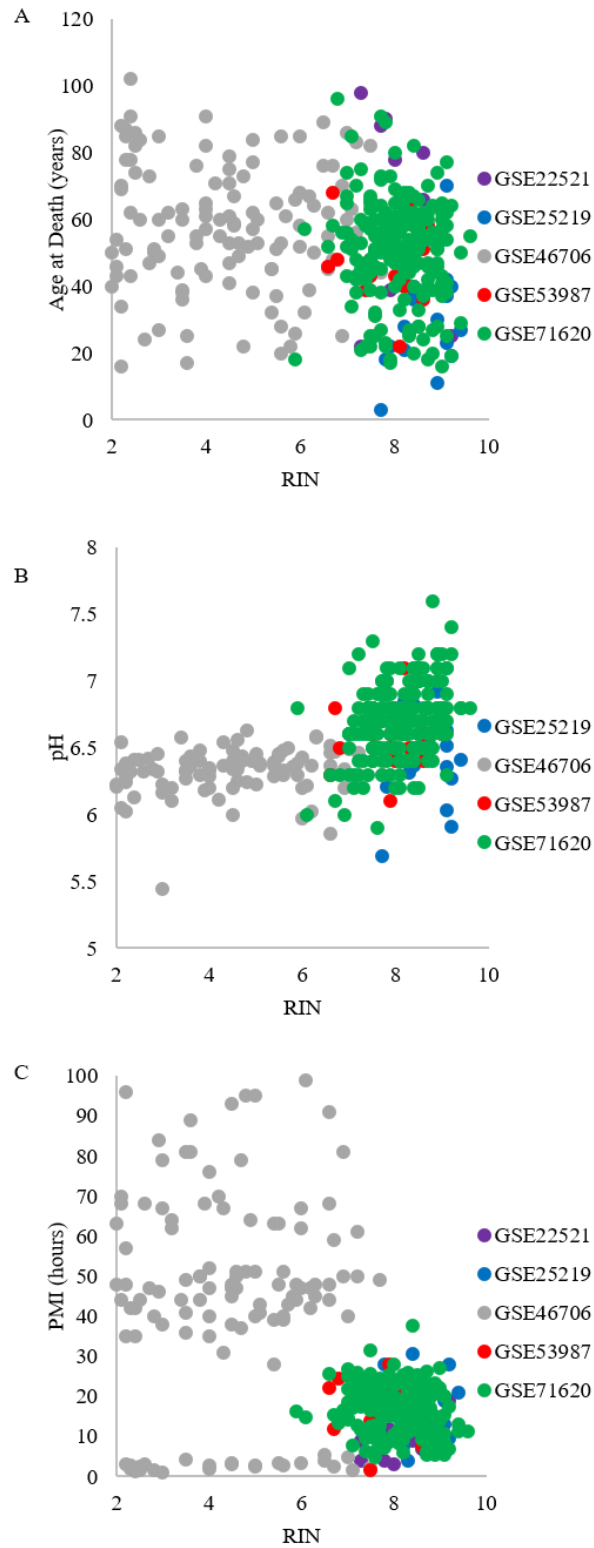


Figure 2.3. Metadata correlations to RIN.

(A) Age (in years) correlated to RIN. (B) Post Mortem Interval (in hours; PMI) correlated to RIN. (C) pH correlated to RIN.

of RNA degradation, we focused on data-subsets with the lowest FDRs (indicating statically effects that were less likely to be false positives) for RIN (GSE25219, GSE45878, and GSE71620) for further analysis.

Using the dataset with the most subjects, GSE71620, we investigated potential sex difference in RIN sensitivity. When separated into males and females, males had 3650 RIN-correlated genes while females had 3251 genes. However, there was an imbalance between the numbers of male and female subjects (157 males/ 42 females; male RIN = 8.08 ± 0.630 ; female discovered a non-significant (but trending) greater number of genes (3251 compared to 1719 [± 1065] resampled males, Z-test $p = 0.075$; Figure 2.4A). The females were also separated into young ($n = 14$; 16-46 years old; RIN = 8.32 ± 0.714) and aged ($n = 28$; 50-96 years old; RIN = 7.96 ± 0.840) groups and the aged subjects were randomized in the same manner. The young females had a significantly greater number of RIN- sensitive genes compared to their older counterparts (1972 young compared to 966 [± 526] resampled aged females, Z-test $p = 0.028$; Figure 2.4B). The males were separated into young ($n = 66$; 17-49 years old; RIN = 8.09 ± 0.651) and aged ($n = 91$; 50-89 years old; RIN = 8.08 ± 0.617) groups and the aged group was randomly resampled, as well. The young males had a significantly lower number of RIN-sensitive genes compared to their older counterparts (755 compared to 4932 [± 755] resampled aged males, Z-test $p < 1.0E - 5$; Figure. 2.4B).

Almost all of the significant genes in the aged male group had a positive correlation with RIN (total significant genes = 5853; positive significant genes = 4362; binomial test $p < 1.0 E -15$). To determine if this was by chance, the correlation was validated for these genes using in an additional study, GSE45878. GSE45878 contained 4356 genes out of the 4362 positive genes, out of which 2781 had a positive correlation between RIN and gene expression (binomial test $p < 1.0 E -15$). This indicates there is robust positive correlation between aged males' gene expressions and RIN.

2.4.4 Cross-Dataset analysis using individual datasets

A common list of total genes was determined from GSE25219, GSE45878, and GSE71620. This total gene list was comprised of probe sets annotated to unique gene symbols with sufficient signal intensity in all three studies (15,735 'total' genes). Using a P-value cut-off for the correlation between the RIN and gene expression signal ($p < 0.05$),

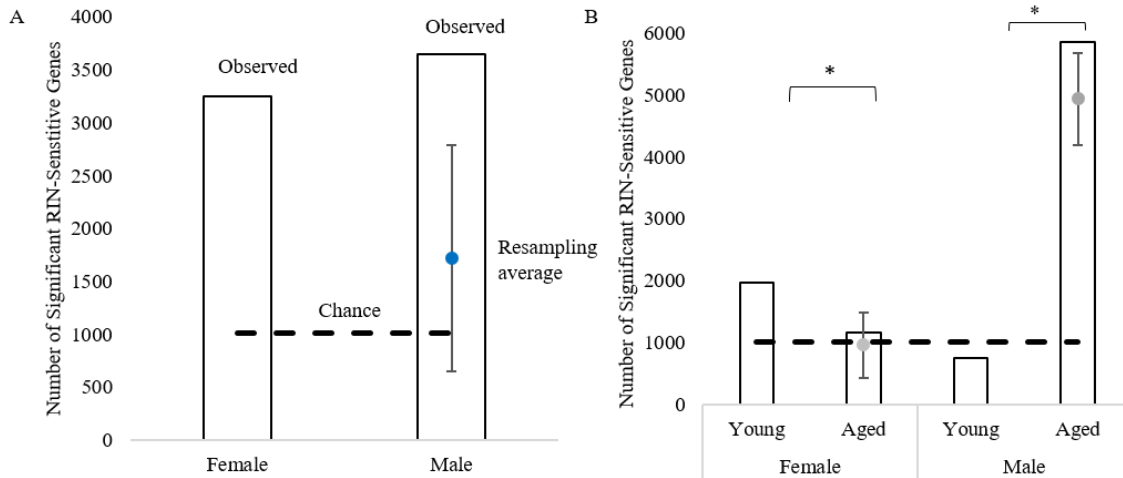


Figure 2.4. Sex effect on RNA degradation.

To equalize the estimated power between the number of male and female subjects in GSE71620, and young and aged for each sex, the group with the higher number of subjects was randomly resampled at the same n as the group with the lower number of samples. The number of significant genes for males and females (A). The blue dot represents average number of significant genes from 1000 resampling iterations. The hashed black line indicates the number of genes expected by chance (1013; A). The number of significant genes for young and aged males and females (B). The hashed black line indicates the number of genes expected by chance (1013). The gray dots represent the average number of significant genes found when the aged male and female groups were resampled at the same power as the young groups ($n = 66$, $n = 14$ respectively; B). * < 0.05 .

the number of genes significantly correlated with RIN in all 3 data-subsets was significant (609 compared to the expected 209; $p < 1.0E-15$; Binomial test; S1 Data) (Figure 2.5). Further, this overlapping agreement showed a strong direction-of-correlation agreement. The overlapping genes significant in all three datasets could have fallen into one of eight potential categories based on the correlation direction between RIN and gene expression (Figure 2.5). The subset of genes positively correlated with RIN in all three data-subsets (523/ 609) was highly significant ($p \leq 1.0E-15$), suggesting a consistent group of genes are robustly associated with RIN levels in multiple independent subjects. We validated the direction of change for these robust RIN-sensitive genes by comparing the correlative direction in a fourth dataset, GSE53987. Out of the 512 robust RIN-sensitive genes, 400 agreed in direction (binomial test: $p < 1.0E-15$; S2 Data) in GSE53987. Biological pathway overrepresentation analysis (WebGestalt) of these 523 robustly RIN-sensitive genes revealed consistent and selective pathways impacted, with the prominent positive correlation indicating a general decline in gene expression levels as RIN levels decreased (Table 2.3). These pathways appear to be related to vesicles, transporters, mitochondria, and synapses. This indicates mRNA housed in neurons may be particularly vulnerable to RNA degradation.

One consistent finding from the individual data-subsets analysis is the smaller r-values with larger data-subsets. When the data-subsets contain < 20 subjects, the maximum and minimum r-values (min $r = -0.8497$; max $r = 0.8737$) are more extreme than the data-subsets with > 100 subjects tend to have a lower $|r\text{-values}|$ (min $r = -0.3773$; max $r = 0.3343$). While the higher-powered data-subsets do not need higher r-values to show significance, it indicates the Pearson correlation's assumption of a linear relationship between gene expression level and RIN may not hold. This leads us to the hypothesis the relationship between gene expression and RINs may not be linear.

2.4.5 Merged datasets analysis

Using the independent dataset analysis approaches described above, we found a robust set of RIN-sensitive genes across multiple studies. However, this approach is limited by different ranges of RIN values in each dataset, and by the assumed linear relationship between RIN and gene expression that is implicit to the Pearson's correlation test. To address these issues, we employed two strategies: merging datasets to get a more

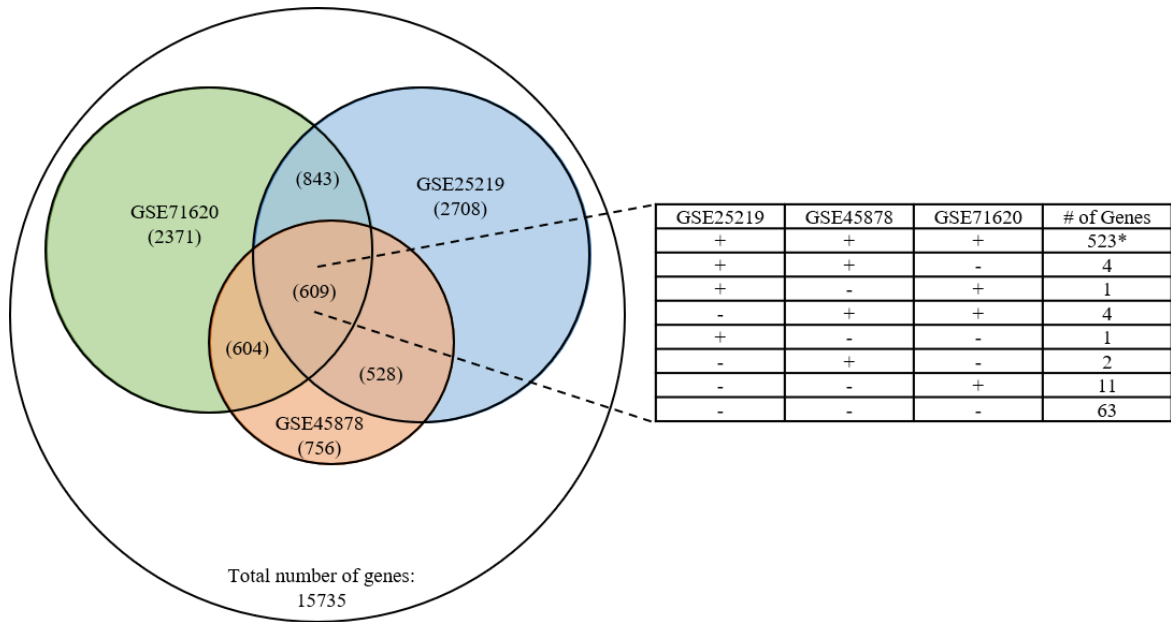


Figure 2.5. Overlapping significant genes between 3 datasets, and direction of significant genes.

Using GSE25219, GSE45878, and GSE71620, a common list of 15,735 genes was determined. The number of significant genes in each study and the overlap was determined. The expected number of genes significant in all 3 datasets was expected to be 209. *Left 3 Columns*- the direction of the RIN-correlation for the study listed in the top row; positive correlation (+), negative correlation (-). *# of Genes*- number of genes in each category. * $p \leq 0.05$.

inclusive range of RIN values; and using a template correlation approach on this merged dataset to evaluate potentially more complex relationships between RIN and gene expression.

2.4.5.1 Approaches for merging multiple datasets.

In order to merge the datasets, the batch effects (Figure 2.2) of each dataset were addressed. Three different approaches (described below) were considered.

1) Within-dataset standardization. Gene expression values from GSE25219, GSE45878, and GSE71620 were used. For each dataset, gene values were Z-scored for each subject. The PCA plot using this standardized approach shows the successful removal of the batch effect (Figure 2.2B). However, calculating the standardized average per dataset using 25 significant genes from one of the robustly overrepresented pathways, monovalent inorganic cation transmembrane transporter activity (Table 2.3), reveals an issue (Figure 2.2B). Each dataset shows the same significant positive correlation between gene expression and RIN, but different deflection points. GSE25219 begins its downward trend around a RIN of 8; GSE45878 begins to decrease around a RIN of 7; and GSE71620 begins to fall around 7.5 (Figure 2.2B). This shows that standardization effectively removes the batch effect, but centering at 0 biases the deflection range within the individual dataset's RIN range in the combined dataset approach, so that it is not appropriate to compare across studies.

2) Harmony. As a second attempt to remove batch effects from multiple datasets, the Seurat package with the Harmony algorithm (Korsunsky et al., 2019) in R, which uses multi-dimensional PCA-based variance to remove batch effects from disparate datasets, was used. However, this approach did not appear to substantially reduce the batch effect compared to that observed in the original datasets (Figure 2.2C).

3) Mean-Subtraction. As a third approach to remove the dataset-dependent batch effect while retaining a less-biased 'RIN deflection point' estimate, we used a signal subtraction strategy. It is well-understood hybridization-dependent mRNA quantification technology is strongly dependent on probe design (e.g., G-C content) (Kitchen et al., 2011; Swindell et al., 2014). Subtracting average signal intensity from each gene within each study would effectively address this probe-based variance, and it is this probe-based variance that likely contributes substantially to the batch effect. However, in the present work, signal

Table 2.3. RIN-sensitive pathways.

Description- name of the overrepresented pathway; *# of genes*- number of genes present in the group out of the 15,735 common list genes; *p-value*- p-value of finding this pathway by chance from our list; *Database*- functional group the pathway is associated with (Biological Process [BP], Cellular Component [CC], or Molecular Function [MF]); *genes (italicized)*- list of RIN-sensitive gene symbols associated with pathway.

GO IDs; Description; # of genes / Possible # of genes; p-values; Database; Genes
GO:0051648; vesicle localization; 33 / 280; 2.87E-09; BP; <i>APIAR, ARL6, ATP2A2, BBS7, CADPS2, GSK3B, KIF3A, KIFAP3, MKKS, NDEL1, NSF, PFN2, PPP6C, RAB27B, SEC22B, SEC23A, SNAP25, STXBPI, SV2A, SYBU, SYN2, SYNJ1, SYT11, SYT13, SYT4, TBC1D23, TMED2, TRAPPC3, TRAPPC6B, USO1, VPS33A, WASL</i>
GO:0099572; postsynaptic specialization; 27 / 292; 9.53E-06; CC; <i>ACTN2, ADAM22, ATP1A1, BMPR2, CACNG2, CAP2, CDH10, CRIPT, DNAJC6, GABRA1, GABRA3, GABRA4, GABRB2, GOPC, HTR5A, KCNAB2, KCND2, MAPK1, MTMR2, NSF, PJA2, RTN4, SIGMAR1, SLITRK3, SYN2, SYT11, VPS35</i>
GO:0016917; GABA receptor activity; 6 / 18; 7.92E-05; MF; <i>GABRA1, GABRA3, GABRA4, GABRB2, GABRB3, GABRG2</i>
GO:000135; coated vesicles; 22 / 83; 9.80E-05; CC; <i>AP2B1, APP, ARCNI, CLTC, COPA, COPB2, COPZ1, EPS15, GOPC, NECAP1, OCRL, RAB27B, SCAMP1, SCARB2, SEC22c, SEC23A, SH3GL2, SORT1, TMED2, USO1, VSP33A, YIPF5</i>
GO:0008565; protein transporter activity; 11 / 77; 1.06E-04; MF; <i>CSE1L, IPO5, KPNA6, SCARB2, SEC61A2, SEC63, TIMM23, TOMM20, USO1, VPS29, VSP35</i>
GO:0090150; establishment of protein localization to membrane; 21 / 238; 1.79E-04; BP; <i>ARL6, ARL6IP1, BLZF1, C16orf70, CACNG2, CHM, GD11, GOPC, NSF, PAK1, RAB3GAP2, SAMM50, SEC61A, SEC63, SNAP25, SRP68, TRAMIL1, VPS35, YWHAB, YWHAQ, ZDHHC15</i>
GO:0033178; proton-transporting two-sector ATPase complex; 6 / 9; 2.28E-04; CC; <i>ATP6AP1, ATP6V0D1, ATP6V1A, ATP6V1B2, ATP6V1C1, ATP6VID</i>
GO:0010008; endosome membrane; 29 / 398; 3.37E-04; CC; <i>ANXA6, AP2B1, ATP6AP1, ATP6V0D1, CLCN3, CLCN4, CLTC, EHD3, 3PS15, FIG4, ITCH, MTMR2, MTMR4, OCRL, RAB27B, RAP2A, SCAMP1, SCARB2, SLC30A4, SLC9A6, SORT1, STX12, TM9SF2, TMEM59, VPS29, VPS33A, VPS35, VPS4B, VTA1</i>
GO:0015077; monovalent inorganic cation transmembrane transporter activity; 25 / 328; 4.43E-04; MF; <i>ATP1A1, ATP2A2, ATP6AP1, ATP6V0D1, ATP6V1A, ATP6V1C1, ATPVID, CLCN3, CLCN4, HCN1, KCNAB2, KCNC2, KCND2, MTMR6, NALCN, NNT, SCN2A, SCN3B, SLC12A6, SLC4A10, SLC6A15, SLC8A1, SLC9A6, SNAP25</i>
GO:0006399; tRNA metabolic process; 15 / 159; 7.37E-04; BP; <i>AARS, DDX1, ELP3, EPRS, EXPSC2, FARBS, GRSF1, HARS, LARS, MTFMT, MTO1, NARS, RPP14, RPP30, USP14</i>

values are influenced by RIN, and different datasets have different RIN ranges. Therefore, subtracting the row average for each gene from each dataset would be less effective than conditionally subtracting only the average of signal from samples for which the RIN exceeded some cutoff. That cutoff should represent a RIN value above which the RNA is of such high quality, that RIN's association with gene expression is not detectable. To estimate what that RIN cutoff might be, data from GSE71620 was used.

The number of significant genes is plotted as a function of RIN (Figure 2.6), and each dot represents a step from a low (starting at 6.1) RIN to high RIN (ending at 9.4). For each step, the genes found to be significantly correlated with RIN at the prior step are subtracted. Thus, each step reflects the degree to which an increasing RIN range contributes to RIN-sensitive gene discovery. We found the correlation between RINs and gene expression is relatively flat from 6.1 to 7.1, increases markedly from 7.4 to 8.6, and additional new RIN-sensitive genes are rarely discovered by adding additional subjects with $RIN > 8.6$, suggesting a RIN cutoff of 8.3 would be sufficient for calculating a signal average relation for RIN influence.

Based on this, gene signal from subjects with a $RIN > 8.3$ appear less likely to contribute to the 'RIN effect' and their averages were calculated and then subtracted for each row of data in each dataset separately. Those 'mean-subtracted' datasets were then merged for subsequent analysis without a batch effect (Figure 2.2D).

2.4.5.2 Template Analysis

Three hundred and fifty-six templates were designed that could potentially fit the gene expression signal across RIN values from the merged, mean-subtracted data (Figure 2.7; S3 Data). However, some of these templates were highly similar to one another. A Pearson's correlation was run across the 356 templates, and those strongly correlated with one another were combined to simplify reporting. A single group of templates (from the S3 data, the linear climbs 6.1 to 7, 6.1 to 7.1, 6.1 to 7.2, exponential decline by 6.7, and plateau 6.1 to 6.7) were combined to make a "custom" template. Each gene was then correlated to all 352 templates, yielding 352 R values. Then, each gene was assigned to the template with which it most strongly correlated. If $r \geq |0.69|$ for its 'best match' template, then the gene was assigned to that template. 132/352 templates had genes assigned. Then, a resampling

Significant Findings at Different RIN Cutoffs

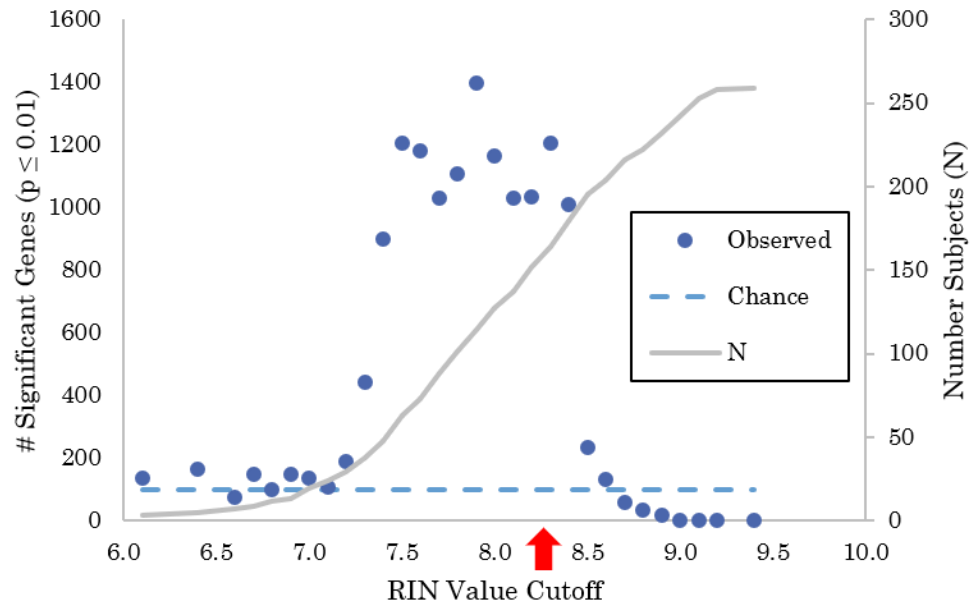


Figure 2.6. Number of significant genes associated with cumulative RIN.

The number of genes whose expression levels were significantly correlated with RIN (Pearson's test, $p \leq 0.01$) are plotted as a function of RIN cutoff. For the first cutoff (RIN = 6.1) there were only 3 observations, and the results were similar to chance (dashed line). Between RIN values of 7 and 7.5, there is a marked increase in number of significant correlations. Similarly, between 8.3 and 8.5, there is a marked decrease in number of significant genes. This suggests 1) lower RIN values (6.1 to 7.1) are not appreciably correlated with gene expression (or the data is significantly underpowered), 2) there is a strong linear relationship between gene expression and RIN between 7.3 and 8.3, and 3) this relationship falls off sharply at RINs higher than 8.3 as gene expression plateaus. Taken together, these results suggest a sigmoidal relationship between gene expression and RIN, or an exponential decay obscured by decreased statistical power at the lowest RIN range.

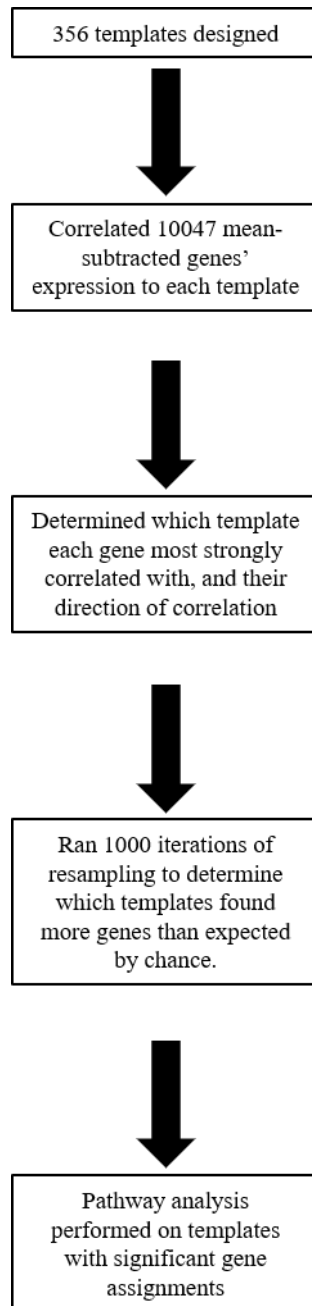


Figure 2.7. Flow chart of template analysis.
Summarized the different steps taken during the template analysis.

simulation (1000 iterations) was constructed to compare template assignment observed to estimated chance template assignment. Templates with significantly more gene assignments than estimated by chance ($p < 0.05$, Binomial test) were flagged for further analysis. Using this approach, 59 templates were identified as significant (Table 2.4, note that all template assigned genes are included in S1 Data) and the genes from the 6 templates with the largest number of gene assignments underwent pathway analysis (WebGestalt), and their normalized gene expression signals are graphed along with their idealized templates (Figure 2.8).

The “completely linear” template in this phase of the analysis (the one in which gene expression steadily rises as RIN improves) was designed to replicate the relationship ostensibly found by the Pearson’s test in the independent data-subset (e.g., Figure 2.5), yet it failed to do so. This follows the earlier observation that the independent data-subset Pearson’s correlation, although it found a robust set of genes across multiple studies, did not appear to entirely capture the nature of the RIN-to-gene relationship. For instance, in the data-subset with the largest n (GSE71620, $n = 199$), the r -value range, while significant, was also restricted, and rarely rose above $|0.34|$. This suggests a pattern was detected by the Pearson approach, but it is not entirely linear.

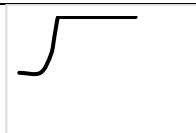
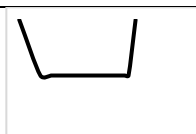
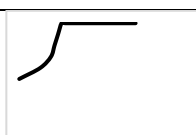
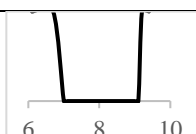
The overrepresented “exponential rise at 7” pathway reflected the monovalent inorganic cation transmembrane transport activity (GO: 0015077; 17 genes out of 420 genes; $p = 5.05 \times 10^{-3}$) found in the “independent data-subset” analysis, suggesting this may be a more accurate representation of a relatively narrow range over which RIN and gene expression are related. Therefore, we graphed the average gene expression for the genes present in the membrane-bound pathway as a function of RIN with the individual template superimposed (Figure 2.2D).

2.4.6 Relationship between Alzheimer’s disease and RIN-sensitive genes

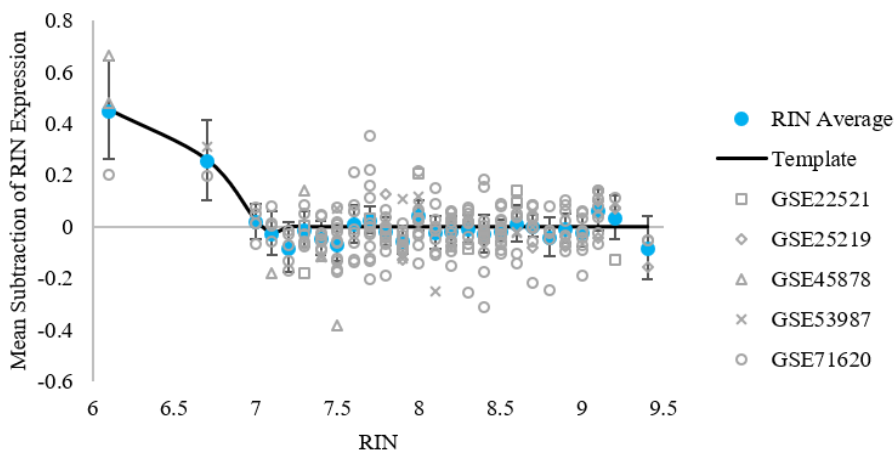
In order to compare RIN-sensitive genes to AD differentially expressed genes, two approaches were used. First, a comparison between two individual datasets, one reflecting RIN-sensitive and another reporting AD-associated genes was used. Second, consensus findings of RIN- sensitive vs. AD-associated genes from multiple datasets were compared. For the first approach, a common set of genes with sufficient signal intensity for testing was established between Miller et al (2017) and Chen et al (2016; GSE71260). Among

Table 2.4. Templates to which gene expression most commonly fit.

Each of these templates had more genes than expected by chance. The expected number of genes was found using a resampling (1000 iterations) and was considered to be significantly represented is Z-score ≥ 2 .

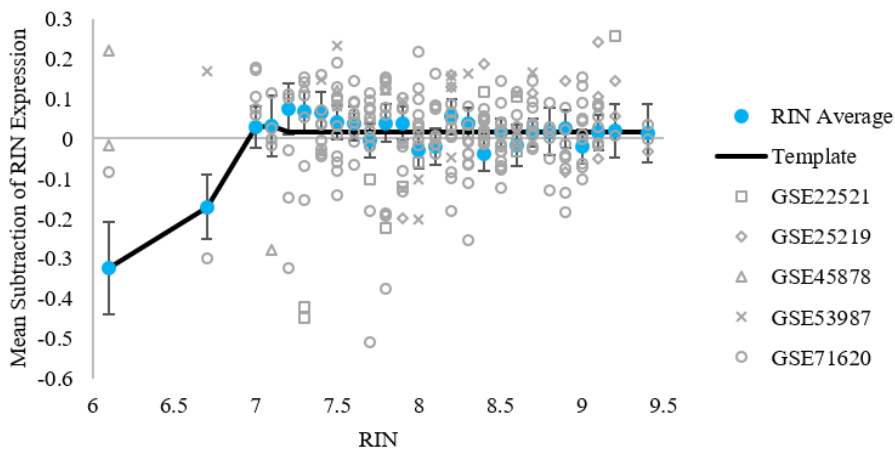
Name of Template	Shape	Resampling (Avg \pm STD)	Observed # of Genes	Z-Score
Spike at 6.7		0.0938 (\pm 0.305)	893	2926.562
Exponential decline by 7		0.626 (\pm 0.787)	782	992.5184
Spike at 6.1		0.0588 (\pm 0.240)	611	2548.499
Custom Group		0.575 (\pm 0.651)	533	818.0579
Linear Climb 6.7 to 7.1		1.18 (\pm 1.10)	62	55.43391
Boat 6.1 to 9.4		3.23 (\pm 1.84)	62	31.99302
Spike at 9.2		0.0828 (\pm 0.290)	30	103.199
Linear Climb 6.1 to 7.3		0.320 (\pm 0.573)	28	48.34277
Boat 6.7 to 9.2		16.4 (\pm 4.03)	27	2.62098

Custom List negative



Description	# of genes	p-value	Database
protein activation cascade	9	1.21E-06	Biological Process
cell-substrate adhesion	19	6.13E-05	Biological Process
angiogenesis	23	6.17E-05	Biological Process
positive regulation of defense response	18	8.29E-05	Biological Process
Golgi lumen	7	3.23E-04	Cellular Component
peptidase regulator activity	10	3.96E-04	Molecular Function
endoplasmic reticulum lumen	15	4.84E-04	Cellular Component
coagulation	15	0.001057	Biological Process
DNA-binding transcription repressor activity, RNA polymerase II-specific	14	0.001822	Molecular Function
cell chemotaxis	11	0.002784	Biological Process

Custom positive



Description	# of genes	p-value	Database
myelin sheath	12	3.17E-05	Cellular Component
dephosphorylation	17	6.57E-04	Biological Process
transporter complex	12	0.001187	Cellular Component
sleep	3	0.004187	Biological Process
ATP hydrolysis coupled transmembrane transport	3	0.004187	Biological Process
synaptic transmission, GABAergic	4	0.006812	Biological Process
regulation of microtubule-based process	8	0.013638	Biological Process
active transmembrane transporter activity	9	0.017855	Molecular Function
synaptic membrane	13	0.024409	Cellular Component

Figure 2.8. Representative gene expression templates.

Each figure represents a template associated with a significant number of genes. The table under each figure is the overrepresented pathways corresponding to the template.

Custom negatively correlated (A). Custom positively correlated (B). The blue dots represent average of gene expression. Each gray shape represents a subject, and each corresponds to a study. The black line represents the template.

these 11,631 genes, Chen found 4,173 RIN-sensitive genes while Miller found 3,238 AD-significant genes. The log₂ fold changes (L2FCs) for the ‘AD-effect’ and the *r* values for the ‘RIN-effect’ are plotted (Figure 2.9A) and revealed a strong directional agreement. More genes were found significant by both AD and RIN (1,531 genes significant by both AD and RIN; Data S4) than expected by chance (expect 1,162 genes, $p < 1.0E-15$), consistent with prior reports (J. A. Miller et al., 2017) noting the relationship between AD-associated and RIN-sensitive gene expression. Further, the direction of these changes appeared consistent, with genes downregulated with AD also showing a positive correlation with RIN (indicating gene expression decreases as RIN is lowered). Of the 1,531 genes significant by both RIN and AD, we determined if any directional groups (i.e. positive AD-associated genes and positive RIN-sensitive genes, positive AD-associated genes and negative RIN-sensitive genes) were overrepresented. In fact, genes whose expression was both decreased with AD and positively correlated with RIN, formed the majority of all commonly significant findings and were significantly overrepresented ($n = 1223$, binomial test, $p < 1.0E-15$; Figure 2.9A). This indicates the downregulated (although not upregulated) component of AD-associated gene expression is associated with RIN-based measures of RNA degradation.

For the second approach, we then repeated this process, but used a more generalized approach by applying the Hargis and Blalock (2017) and current data (Figure 2.5) were indexed to find a common set of 12,144 genes. There were 6247 significant AD-associated genes and 571 RIN-sensitive genes (binomial $p = 4.64E-08$, $p < 1E-15$, respectively). There were more genes that were both AD-associated and RIN-sensitive than expected by chance as well (expected: 294; found: 438; binomial $p = 6.66E-16$; Data S5; Figure 2.9B). We found the majority of these genes (383/438) had expression that was both decreasing with AD and positively correlated with RIN (expected: 110; binomial $p < 1.0E-15$; Figure 2.9B), supporting a relationship between RIN-sensitivity and AD influence on gene expression, although the AD effect appeared to encompass more genes than could be explained by the RIN effect.

This analysis supports prior findings (J. A. Miller et al., 2017) that RIN is associated with gene expression levels, especially for AD-associated genes. However, our findings also support the hypothesis that the influence of RIN extends beyond AD and influences AD-

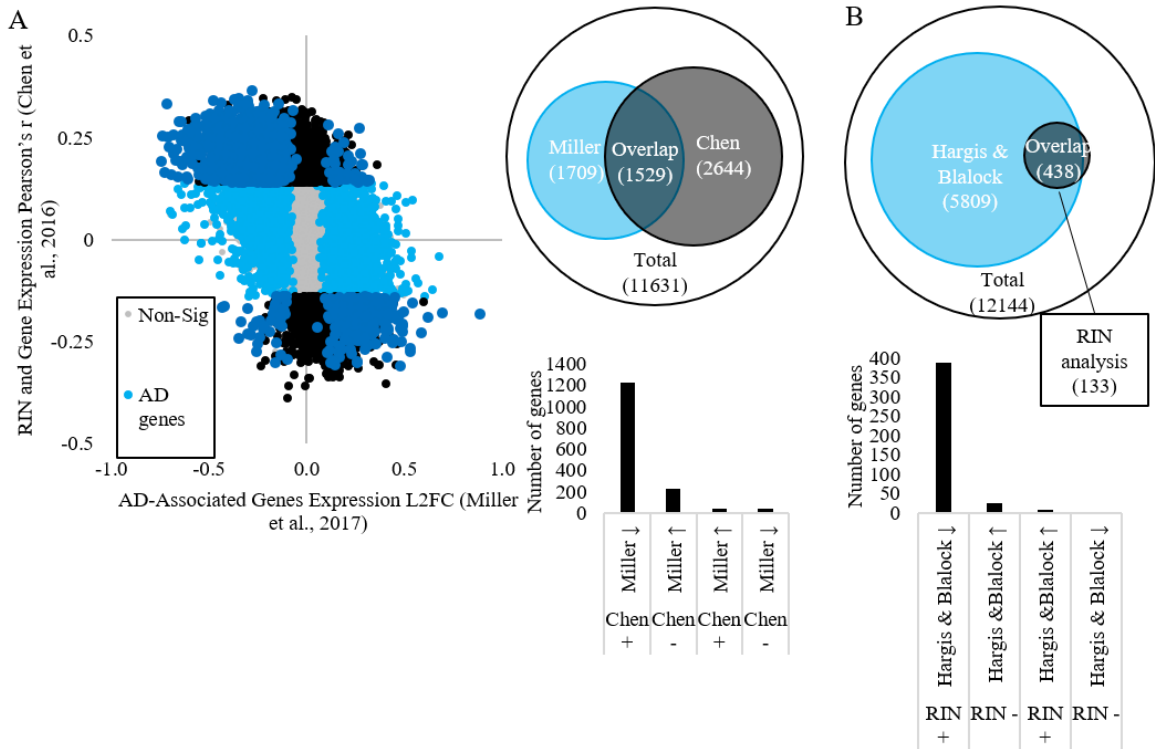


Figure 2.9. Relationship between RIN-sensitive genes and AD-associated genes. Single study comparison between the L2FC for AD genes (Miller et al., 2017) and correlation of RIN-sensitive genes (GSE71620; Chen et al., 2016). The Venn diagram also indicates the number of significant AD-associated genes, significant RIN-sensitive genes, and the overlap from the Miller et al. and Chen et al. analysis. The bar graph shows the number of significant overlapping genes and the Pearson's correlation direction for RIN and direction of the L2FC (A). An analysis of the commonalities between a consensus of AD-associated genes (Hargis & Blalock, 2017) and the agreement of multiple RIN-sensitive datasets (Figure 2.5). The Venn diagram indicates the number of significant AD-associated genes, significant RIN-sensitive genes, and the overlapping genes. The bar graph shows the number of significant overlapping genes separated by the unanimous direction of the Pearson's correlation for RIN and the average L2FC direction (B).

associated gene expression even in normal, non-pathological brain tissue. This suggests AD may amplify some general property of RNA degradation present pre-mortem even in non-pathological samples.

2.5 Discussion

RNA integrity numbers (RINs) have been important tools in determining RNA quality for nearly fifteen years, however the relationship between RIN and gene expression is still not well understood. Changes in RIN values may reflect the combined influence of multiple insults (e.g, RNase activity, oxidative stress, tissue injury) (Copoio et al., 2007; Feyzi et al., 2007) to which different mRNA species may be selectively vulnerable. For the present work, we designed an analysis that tested individual, post-mortem, human frontal cortex data-subsets independently (secondary data analysis), and as a single dataset (meta-analysis). We hypothesized that, despite multiple possible mechanisms of insult, consistent genes and pathways would associate with RNA quality in post-mortem brain samples from control subjects with no diagnosed neuropathology. Our findings support this by showing specific genes and pathways are consistently associated with RNA degradation across multiple studies. However, while we hypothesized a linear relationship between RNA integrity numbers (RINs) and gene expression, our template analysis found that an exponential (or possibly sigmoidal) relationship better describes individual gene relationships to RIN. In addition, we found a surprising difference between RNA degradation's influence with sex and age (aged males tended to show the strongest relationship). Based on the present work and prior publications (J. A. Miller et al., 2017), we propose that the apparently neuron-selective RNA degradation in control tissue is the result of selective damage to mRNA localized in synapses, and is similar to the influence seen in Alzheimer's disease (AD).

Regarding other metavariabiles commonly used to assess tissue quality, RIN values in healthy control brain tissue appears to correlate inconsistently with post-mortem interval (PMI) or tissue pH. Since our analysis does rely on the information published by others, there could be selection criteria we are unaware of that limit the range of variables. This 'floor-effect' could be impacting our results. With the information available to us, only 2 out of the 5 datasets report PMIs with a significant correlation between PMI and RINs, and they correlate in opposite directions. This is particularly of note since several

studies investigating the influence of RIN in controlled experimental settings have manipulated PMI to drive changes in RIN (Jaffe et al., 2017; Sampaio-Silva, Magalhaes, Carvalho, Dinis-Oliveira, & Silvestre, 2013), which may represent a component of the process observed here or an entirely separate process. Pre-mortem changes in control tissue that are not associated with known pathology or mishandling may also play a role. A study from the University of Maryland used human brain cortices from the NIH found the quality of RNA did not significantly drop until 36 hours post-mortem (White et al., 2018). With the exception of subjects from GSE46706, the longest PMI for any subject was 37.5 hours; this may explain why there is not a clear relationship between PMI and RIN in the present work. Our analysis is in line with others (Ervin et al., 2007; Johnson, Morgan, & Finch, 1986; Stan et al., 2006) that have found a lack of a relationship between RIN and PMI (however, see (Birdsill, Walker, Lue, Sue, & Beach, 2011)). It has also been established the PMI and RIN correlation is tissue-dependent, and possibly region-specific as well (Ferreira et al., 2018). One study found subjects with Alzheimer's disease had a significant negative correlation between PMI and RIN, but the control subjects did not (Preece & Cairns, 2003). Therefore, more investigation needs to be done on the relationship between PMI and RNA quality. Like PMI, tissue pH does not show a robust relationship with RIN in control brain tissue in this study. Only one out of the four studies reporting pH finds any significant correlation. However, other studies have found a significant relationship between RIN and pH (Atz et al., 2007; Durrenberger et al., 2010; Sonntag et al., 2016) and it is possible, since pH is also used as a preliminary triage variable, that the work we analyze had a constrained pH range. It should be noted that even though these metavariabes did not have a robust impact on RIN, on their own they did show a significant association with transcriptional profile (albeit different sets of genes). This suggests these metavariabes may have mechanistically distinct influences. Because of this, PMI and pH appear to be unreliable proxies for RIN-assessments.

In females, younger subjects are moderately more sensitive to RNA degradation than aged. But in males, there is a strong increase in RIN-sensitivity with age (Figure 2.4B). Age itself does not significantly correlate with RIN, even when young males, young females, aged males, and aged females from the GSE71620 data-subset are analyzed separately. One possibility is that aging genes could be indirectly influencing

RNA degradation since aging can play a role in mRNA turnover (Borbolis & Syntichaki, 2015). Future work could focus on whether aging itself confers a differential sensitivity of mRNA to RIN variability, and what the potential mechanisms of such an effect would be and what the potential mechanisms of such an effect would be.

Our data indicates RNA degradation is strongly associated with specific genes and pathways in post-mortem human frontal lobe tissue in control subjects. We find the same outcomes using two types of analyses: comparing individual datasets and merging datasets for a single analysis. In both cases, there is a highly consistent subset of genes that reliably showed lower expression as a function of decreasing RIN. The functional pathways with which these genes are associated included vesicles, transport activity, synapses, and mitochondria, implying neuronal mRNA may be particularly sensitive to degradation.

There are two thresholds to consider for RIN's influence on mRNA expression- 1) where RIN begins to have a significant effect on gene expression; and 2) where RIN becomes so severe that gene expression reaches a floor effect and is no longer impacted by further RNA degradation. Although individual RIN-sensitive gene sensitivities vary for both of these thresholds, there are some general consensus values that may be useful to consider in future work. As RNA degrades and the RIN begins to decrease, there is a marked increase in the number of genes whose expression correlates with RIN (Figure 2.6). This indicates that if experimental tissue has a RIN above 8.6, then in general, there is no reliably detectable effect of RIN on gene expression and RIN correction would not be necessary in human post-mortem neocortical tissue. Between RINs of 7.2 and 8.6, there is a strong increase in RIN-sensitive mRNA detection, and below 7.2, detection again falls below statistically significant thresholds. However, our analysis also suggests that specific pathways (e.g., monovalent cation transporter- Figure 2.2) are more impacted at lower RINs. Thus, it is possible that different pathways are impacted at different points along the continuum of mRNA degradation.

In this work, RNA degradation also appears to exert a floor effect on gene expression. The point at which a gene reaches its floor effect can vary from gene to gene, but is critical to consider. Beyond this threshold, the application of a RIN correction procedure would appear to provide data but instead would provide nonsense as its starting value cannot be estimated based on the RIN score. Often, a RIN of 6 is used as a criterion

for inclusion in a study, though there is no clear consensus in the literature (Sonntag et al., 2016). Based on our findings using 6 data-subsets, a RIN of 6.7-7 appears to represent a generalized ‘point of no return’ for RIN-sensitive genes. This floor effect is also indicated by GSE46706, a data-subset with an unusually high RIN-to-gene expression false discovery rate (FDR) > 0.75 and an unusually low range of RIN values (2-7.7; only 26 of the 119 subjects had a RIN \geq 6). This supports our hypothesis that lower RINs are associated with flattened gene expression, and suggests that low range RIN corrections are unreliable for expression adjustment.

Taken together, the upper and lower thresholds for RIN-sensitivity suggest that there is an interior RIN range between 7.2-8.6 in which RIN may have a fairly linear effect on gene expression that is amenable to correction. However, when considering RIN-sensitive genes, for RIN values above this range, RIN correction may inappropriately add to variance, since these genes do not need correcting. For RIN values below this range, we argue that the signal is not rescuable.

Although there is strength to secondary and meta-analyses such as the present work, especially regarding robust findings, there are important caveats. These findings are correlative, and therefore we cannot determine if the associations are causal, consequential, or epiphenomenal. Further, while it is tempting to speculate that RNA degradation is impacting genes/ pathways at different rates (perhaps even forming a ‘meta-pathway’ of progressive decay), this would require more observation and interventional experimentation. In addition, there is evidence that different pathways regarding mRNA transcription and transport are impacted at differing rates in post-mortem mice and zebrafish (Pozhitkov et al., 2017), giving more credence to the possibility that RNA degradation results in a cascading effect on the transcriptome. Although it is expected that available datasets would have restricted RIN ranges (RIN is typically used to establish a quality control cutoff; similar issues exist for other metavariabes like pH and PMI), a more complete idea of RNA degradation’s effects could be achieved by examining the transcriptional influence across the entirety of the RIN range and with more attention given to the different measures (e.g. Total RNA ratio, 28S peak height, fast area ratio, and the marker height) that contribute to the RIN score (Schroeder et al., 2006). However,

another consideration is the subject-to-subject normal variation, and RIN may not reach such low values in the absence of severe pathology.

Our findings that pathways relating to neurons are most vulnerable to RNA degradation suggests concerns with use of common regression approaches to control for RIN in transcriptional profiling of neural tissue, particularly with regard to neurodegenerative disease. First, we report a consistent set of genes sensitive to both RIN and Alzheimer's disease (AD). These RIN/AD genes predominantly have lower expression with worsening AD and with lower RNA quality (e.g., are decreased with AD and show a positive correlation with RIN). These results support Miller et al., where RIN correction procedures removed the apparent Alzheimer's disease effect (J. A. Miller et al., 2017). Miller et al. reported RNA degradation was a confounding variable worsened in AD samples, and proposed this might be due to improper handling of tissue (J. A. Miller et al., 2017). However, questions remain regarding whether it is reasonable to assume that pathologists would be selectively indelicate with AD compared to control tissue, and it should be considered that the RNA could decay appreciably in living tissue prior to death and independent of post-mortem procedures.

Second, in a disease state where both RIN and AD gene expression are declining, attempting to control for one issue may inadvertently remove clinically relevant findings from the other. We found similar results when we compared an AD dataset consisting of the robust AD changes observed in multiple independent studies (K. E. Hargis & Blalock, 2017) along with the consistent RIN-sensitive genes identified in 3 control tissue data-subsets (see cross-dataset analysis using individual datasets in Results). This supports the observation (J. A. Miller et al., 2017) that specific AD genes are RIN sensitive. This may indicate correcting and/or normalizing RIN may actually be removing a true effect within AD subjects, as the RIN degradation itself may reflect in situ degradation.

There are still many unanswered questions regarding the RNA degradation and its impact on gene expression. To our knowledge, this is the first study to look across multiple datasets at the relationship between RIN and gene expression in human post-mortem control brain tissue. However, other studies have looked at RNA degradation's impact in other tissues and species. For example, when Opitz et al. investigated RNA degradation in RNA extracted from renal cancer tumors, they found overrepresented

translation, GTP, and RNA activity (Opitz et al., 2010) pathways. Gallego-Romero et al. found inflammatory, immune, and clotting factors are most vulnerable to rapid RNA degradation in human peripheral blood mononuclear cells (Gallego Romero et al., 2014). Jaffe et al. also presented evidence that RNA from different cell types may have different susceptibility to degradation (Jaffe et al., 2017). This indicates cell and tissue type plays a role in which pathways are sensitive to RNA degradation. Indeed, this suggests that the mRNA associated with the principal functional cells of a tissue are the most vulnerable to degradation.

In conclusion, transcriptional profiling reveals that neuronal, especially synaptic, pathways appear more strongly and consistently associated with RNA integrity than other pathways in control, post-mortem, human frontal lobe tissue from multiple independent datasets. This suggests that mRNA localized to synaptic regions may be particularly vulnerable, possibly due to its close association with mitochondria. Further, RNA integrity number (RIN) does not reliably correlate with two other measures commonly associated with post-mortem tissue quality, PMI and pH, suggesting PMI and pH would be poor proxies for RIN. Interestingly, there does appear to be an age-based shift in RIN-sensitive gene expression. Despite the fact that the range of RIN values was roughly the same in young and aged subjects, the association between RIN and gene expression increased markedly with age in males, and to a much lesser extent, decreased with age in females. In addition, and in support of prior work (J. A. Miller et al., 2017), there is strong overlap between RIN and AD's influence on gene expression. For example, we also found that nearly half of all AD-sensitive genes identified in Miller et al. (2017) were also correlated with RIN (in Chen et al. (2016), completely independent dataset of control-only post-mortem brain tissue). In datasets where RIN and AD are confounded (e.g., where RIN is significantly lower in AD samples), procedures such as multiple regression that are designed to correct for RIN's influence may inadvertently remove the effect of AD. Indeed, one of AD's effects may be to lower RIN. Therefore, we suggest avoiding RIN-correction if such a confound exists, as have prior researchers (Gallego Romero et al., 2014). Reporting the confound may be more appropriate than obfuscating it with RIN normalizing procedures. We also found that the relationship between RIN and gene expression more closely reflects a sigmoidal (or stepped) relationship across a narrow RIN

range of 6.7-8.6, rather than a continuous linear relationship across the entire RIN range. This suggests that RIN correction tools using regression may over-correct values outside of the linear range, and under-correct values within it.

CHAPTER 3. RNA DEGRADATION, GLUCOCORTICOID, AND GLUCOCORTICOID RECEPTORS

3.1 mRNA degradation pathways

As the previous chapter indicates, RNA degradation impacts gene expression, even in control tissue. While RNA degradation is increased post-mortem, there are internal mechanisms designed to degrade mRNA. To prevent continuous overexpression of gene or to prevent aberrant mRNA from being translated into dysfunctional proteins, mRNA decay pathways have evolved. While ribonucleases are often responsible for mRNA degradation and ensure mRNA stability, other mechanisms also play a role and are probably more instrumental when an external stressor occurs.

Messenger RNA (mRNA) stability is mRNA species-dependent and can be expressed in mRNA half-lives. mRNA half-life (the amount of time of time it takes for one half of the amount of mRNA species to be metabolized or degraded) may range from less than one hour to days (Meyer, Temme, & Wahle, 2004; Thapar & Denmon, 2013) and is directly tied to the abundance of the mRNA available for transcription (Thapar & Denmon, 2013), length of 3' untranslated regions, the number of mutations in the AT-rich sequences, and the presences of proteins and microRNA binding sites (Tutucci, Livingston, Singer, & Wu, 2018). When the mRNA is no longer able to be transcribed into protein, it is considered degraded. Thus, the RIN score, which depends in large part on rRNA measures, is a proxy for assessing mRNA degradation.

Most mRNA decay occurs in the cytoplasm of the cell. After being transcribed from the DNA, nascent mRNA is spliced and polyadenylated before being exported into the cytoplasm. After the mRNA has been used to translate a protein, the post-translational mRNA may be sent to processing bodies (P-bodies) or stress granules for storage to be used again. Recent work shows decreases in P-bodies do not impact mRNA degradation, as previously hypothesized, and single-molecule studies indicate degradation occurs throughout the cell (Zhang & Herman, 2020). P-bodies are a ribonucleoprotein structure containing proteins and enzymes used to process, store, and degrade mRNA (reviewed in (Decker & Parker, 2012; Zhang & Herman, 2020)). This degradation is essential for maintaining mRNA homeostasis, which is important for regulating individual protein homeostasis. Although the specific ways to activate the decay of post-translational mRNA are still unclear, the basics have been described.

RNA decay is typically initiated by deadenylation of the 3' tail. Most of this activity is driven by the Ccr4-Not deadenylase complex followed by the Pan2-Pan3 enzyme (reviewed in (Labno, Tomecki, & Dziembowski, 2016; X. Wu & Brewer, 2012)). There are two decay pathways following the deadenylation, 3' – 5' or 5' – 3' decay. In the 3' – 5' pathway, the deadenylation process releases poly(A)- binding proteins (PABPs), which allows for an exoribonuclease, such as the RNA exosome complex, to bind to the 3' end of the mRNA. Once most of the mRNA has been degraded, the 5' cap and remaining fragments are also degraded using the scavenger mRNA decapping enzyme, DcpS (in humans) (Labno et al., 2016; Liu, Rodgers, Jiao, & Kiledjian, 2002). The 5' – 3' pathways start with the mRNA's decapping using the decapping enzymes Dcp1-Dcp2, and Lsm1-7, Edc3, Ddx6, and Hedls (Fenger-Gron, Fillman, Norrild, & Lykke-Andersen, 2005). Then Xrn1 degrades the mRNA (X. Wu & Brewer, 2012). In both cases, the mRNA is degraded, allowing for mRNA homeostasis to be retained.

Although, these degradation pathways are essential for understanding the stability of individual mRNA species, and the variability between them, they are not the most commonly studied mRNA degrading pathways. Most of the well-understood degradation pathways survey mRNA quality and cause mRNA degradation to occur when there is a problem during translation. One of the most understood is the non-sense mediated decay pathway (Thapar & Denmon, 2013).

3.1.1 Non-sense mediated decay

Non-sense mediated decay (NMD) (reviewed in (Schoenberg & Maquat, 2012; Thapar & Denmon, 2013; Weskamp & Barmada, 2018)) is a surveillance pathway that degrades mRNA with a premature translation stop codon to prevent potentially detrimental effects (Borbolis & Syntichaki, 2015; Schoenberg & Maquat, 2012). It may also regulate some normally sequenced mRNA, particularly species with alternatively spliced exons in the 3' UTR (X. Wu & Brewer, 2012). However, it should be noted that there is no evidence that mammalian NMD degrades "old" mRNA; it is believed to primarily target mRNA recently bound at the 5' end to cap-binding proteins (Schoenberg & Maquat, 2012). The NMD pathway removes aberrant transcripts and helps to maintain telomeres during cell cycle progression (Thapar & Denmon, 2013).

After nascent mRNA splicing occurs in the nucleus, an exon-exon junction complex is placed 24 nucleotides upstream from the splice site to mark where an intron was removed. If this exon-exon junction complex is more than 50 nucleotides downstream of a stop codon, it is considered a premature termination codon, and the NMD is activated (Thapar & Denmon, 2013). During translation, the ribosome stalls at the premature termination codon. Then Upf1, eRF1, and eRF3 form a surveillance complex and bind to the adjacent premature termination codon (Weskamp & Barmada, 2018). The surveillance complex then interacts with the exon junction complex, particularly the Upf2 and Upf3, triggering the phosphorylation of the Upf1 by Smg1 (Schoenberg & Maquat, 2012; Weskamp & Barmada, 2018). This mechanism prevents further mRNA transcription prevent the inhibition of degradation (Schoenberg & Maquat, 2012; Weskamp & Barmada, 2018). In addition, the phosphorylated Upf1 binds to Smg5-7, which cleaves mRNA and triggers adenylation and decapping (Weskamp & Barmada, 2018). This process allows for 3' – 5' degradation through the Ccr4-Not deadenylase complex (Kim & Maquat, 2019). Smg5-7 promotes the dephosphorylation of Upf1 via protein phosphatase 2A, enabling Upf1 to be reused (Schoenberg & Maquat, 2012). 5' – 3' degradation occurs if, in addition to the Smg5-7 proteins, the proline-rich nuclear receptor coregulatory protein 2 (Pncr2) is activated (Cho et al., 2015; Kim & Maquat, 2019). Pncr2 binds to Dcpa1, part of the decapping enzyme, which causes 5'- 3' exoribonuclease cleavage via Xrn1 (Kim & Maquat, 2019).

It should be noted that NMD efficiency in the brain is decreased due to miRNA-128. miRNA-128 is a microRNA associated with neuronal excitability and motor behavior (Tan et al., 2013) that targets Upf1 and the exon junction complex's MLN51 protein, particularly during neuronal development (Schoenberg & Maquat, 2012). This activity may indicate non-sense transcripts occur at higher rates in the brain compared to other tissues. However, the model for amyotrophic lateral sclerosis (ALS) shows overexpression of Upf1 and Upf2, causing an increase in NMD and preventing neuronal death in ALS by inhibiting RNA binding proteins Tdp43 and Fus (Barmada et al., 2015).

3.1.2 Glucocorticoid receptor mediated mRNA decay

Recently, a new degradation pathway was identified, the glucocorticoid receptor-mediated decay pathway (GMD). First described in 2015, the glucocorticoid receptor

initiates the degradation by acting as an RNA-binding protein in monocytes. This mRNA decay pathway's independence from both translation status and exon junction complex signals of the target mRNA distinguishes it from the other degradation pathways like NMD (Cho et al., 2015; O. H. Park et al., 2016). It is only known to degrade selected mRNAs in monocytes, such as chemokine (C-C motif) ligand 2 (CCL2) (Cho et al., 2015) and interleukin 8 (IL8) (O. H. Park et al., 2016), which may help to explain some glucocorticoid anti-inflammatory actions. In mechanosensory cells the pathway can be triggered by a long noncoding RNAs to promote the degradation of early growth response protein 1 (EGR1) mRNA (Zhu et al., 2021). Currently, this newly identified pathway has not been identified in other cell types or studied outside of cell culture settings. Two particular aspects of this pathway that would be of great interest to this work would be: 1) if this pathway was found in the brain and, if so, what brain regions, cell types, and mRNA species it might degrade; and 2) if this pathway can be triggered by stress. Cho et al. used dexamethasone, a synthesized glucocorticoid, to activate the pathway (2015).

Because of the novelty of the pathway, there are still some unknowns regarding its process. However, a model has been proposed (Cho et al., 2015). Before a ligand binds to the glucocorticoid receptor, the receptor is preloaded to a binding site on a target mRNA. When the glucocorticoid ligand binds to the glucocorticoid receptor, Pnrc2, Dcp1, and Upf1 are recruited. This complex then associates with the 5' UTR. Upf1 is then phosphorylated with ataxia-telangiectasia mutates (Atm), a nuclear protein activated by phosphatidylinositol 3-kinase-related kinases (PI3KK) after DNA damage, which can be caused by stress hormones such as glucocorticoids (Flint, Baum, Chambers, & Jenkins, 2007; O. H. Park et al., 2016). This phosphorylation causes Upf1 to remodel the ribonucleoprotein through its helicase activity (Cho et al., 2015). Next, Y-box-binding protein (Ybx1) and heat-responsive protein 12 (HRSP12) stabilize the GMD complex. In addition, HRSP12 is known to have endoribonucleolytic activity (O. H. Park et al., 2016). Upf1 and HRSP12 would then trigger 5' decapping and 5'-3' degradation (Cho et al., 2015; O. H. Park et al., 2016) (Figure 3.1).

Since psychological stress releases glucocorticoids that cause DNA damage (Flint et al., 2007), upregulate Atm and its phosphorylation of Upf1 (O. H. Park et al., 2016), increased stress may lead to more GMD activity. Since there is evidence that GMD targets

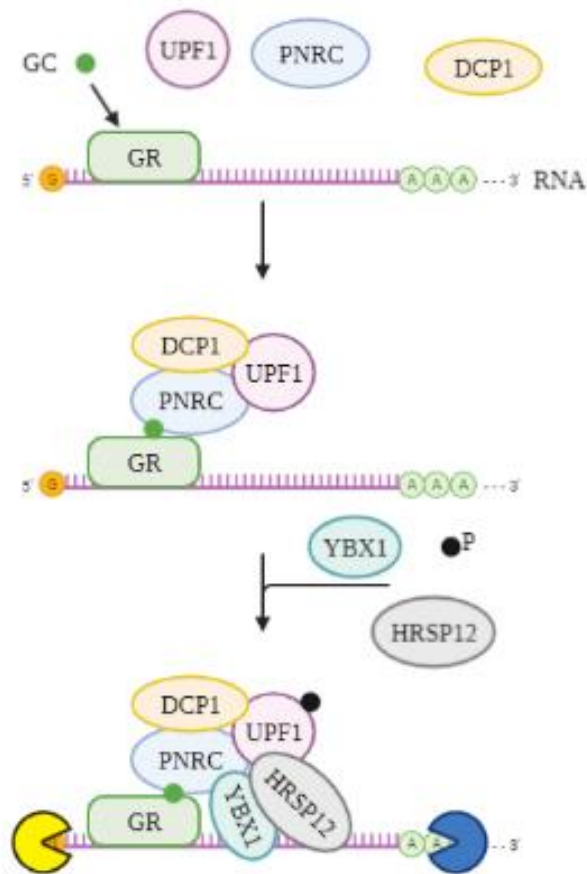


Figure 3.1. Glucocorticoid receptor mediated mRNA decay

The glucocorticoid receptor (GR) is preloaded onto the mRNA. Once a ligand (i.e., GC) binds, Upf1, Pnr, and Dcp1 are also recruited. When Upf1 is phosphorylated, it recruits Ybx1 and HRSP12 to provide stability to the GR complex. Upf1 and HRSP12 also trigger the 5' decapping and the 3'-5' degradation. Adapted from Park et al. (2016). Created using Biorender.com.

some inflammatory mRNA (e.g., IL8) (O. H. Park et al., 2016), this could be a potential mechanism for glucocorticoid's anti-inflammatory effects.

3.2 Glucocorticoid receptors

Glucocorticoid receptors are a member of the nuclear receptor family (Ismaili & Garabedian, 2004), including mineralocorticoid and progesterone receptors (Smoak & Cidlowski, 2004). Glucocorticoid receptors are ubiquitously found throughout the body. Still, the glucocorticoid receptor concentration and its DNA binding vary based on the tissue or cell type (Oakley & Cidlowski, 2013). These receptors regulate various systems (e.g., cardiovascular, immune, musculoskeletal, nervous, respiratory, reproductive, adipocyte, and hepatic) (Garabedian, Harris, & Jeanneteau, 2017). One place that glucocorticoid receptors are well-documented to be expressed is in the nervous system, particularly the brain. One of the most studied regions for glucocorticoid receptors is the hippocampus, a primary structure for memory (Caudal, Jay, & Godsil, 2014; Garabedian et al., 2017). The hippocampus and other limbic structures have the highest density of glucocorticoid receptors in the brain, along with the paraventricular nucleus of the hypothalamus and ascending aminergic pathways (Gadek-Michalska, Szyrka, Rachwalska, Tadeusz, & Bugajski, 2013). In addition, the nuclear levels of glucocorticoid receptors increase within an hour of stress exposure (Caudal et al., 2014).

3.2.1 Structure

There are multiple glucocorticoid receptor isoforms in humans (Vandevyver, Dejager, & Libert, 2014), the canonical version being GR α . GR α , which will be identified throughout this work as glucocorticoid receptor, has 777 amino acids and promotes the transcription of glucocorticoid-responsive genes (Smoak & Cidlowski, 2004).

Like most other nuclear receptor family members, glucocorticoid receptors have three functional domains (Ismaili & Garabedian, 2004; Oakley & Cidlowski, 2013). The first is the 421 amino acid N-terminal region, which contains the ligand-independent transcriptional activation function (AF-1) (Ismaili & Garabedian, 2004; Vandevyver et al., 2014). The AF-1 region is one of the most variable areas between the nuclear receptor family members and is responsible for gene regulation. It is also a common phosphorylation target for ligand-dependent activity since it has 6-7 phosphorylation sites

in rodents and 5 phosphorylation sites in humans (Ismaili & Garabedian, 2004). It also directly interacts with the basal transcription machinery, which begins the transcription process from DNA (Heitzer, Wolf, Sanchez, Witchel, & DeFranco, 2007). It is encoded on exon 2 (Oakley & Cidlowski, 2013).

The second functional domain is the central part of the protein, which contains a DNA binding domain (DBD), a nuclear localization signal, and a dimerization motif (Ismaili & Garabedian, 2004). The DBD contains eight cysteine residues tetrahedrally organized around two zinc atoms, which confer binding specificity to glucocorticoid response elements (GREs) on target DNA (Heitzer et al., 2007). It also functions to allow dimerization of the glucocorticoid receptor and interaction with cofactors and transcription factors (Vandevyver et al., 2014). The DBD is encoded on exons 3 and 4 to become a 65-residue region of the glucocorticoid receptor (Oakley & Cidlowski, 2013; Vandevyver et al., 2014). In addition, the nuclear localization signal acts as a hinge to allow the receptor to change its conformation (Heitzer et al., 2007).

The third domain, the C-terminal region, contains the ligand-binding domain (LBD) which binds to both the ligand and to the heat shock protein 90 complex, along with other transcriptional activation sites (AF-2) (Ismaili & Garabedian, 2004; Smoak & Cidlowski, 2004). The LBD consists of 12 α -helices and four β -sheets which are involved in forming a hydrophobic ligand-binding pocket. The LBD is encoded by exons 5-9, along with the hinge. The AF-2 can go through a conformation change when a ligand binds, allowing accessory proteins (e.g., coactivators, co-repressors) to bind (Oakley & Cidlowski, 2013; Stahn, Lowenberg, Hommes, & Buttgerit, 2007).

3.2.2 Mechanisms of action

Before ligand binding, glucocorticoid receptors are predominantly found in the cytoplasm of a cell (Vandevyver et al., 2014), where they are bound to heat shock protein 90 (hsp90)- chaperone complex, which consists of hsp90, hsp70, hsp56, hsp40, p23 and immunophilins (Ismaili & Garabedian, 2004; Smoak & Cidlowski, 2004; Stahn et al., 2007). Once an agonist binds to it, the receptor changes conformation, releasing from the hsp90 complex and translocating into the nucleus via the microtubule network, which takes around 20 minutes (Ismaili & Garabedian, 2004; Stahn et al., 2007). Once in the nucleus, the glucocorticoid receptor binds to the GRE motif GGAACAnnnTGTTCT,

where 'n' represents any nucleotide on the DNA, in the promoter regions of the target genes, recruiting coactivators to the glucocorticoid receptor-DNA complex and starting the "transactivation" of genes (Almawi & Melemedjian, 2002; Ismaili & Garabedian, 2004; Oakley & Cidlowski, 2013; Smoak & Cidlowski, 2004; Stahn et al., 2007). The coactivators contain histone acetylase (HAT) activity, which may be necessary for remodeling chromatin structure, unwinding the DNA, and exposing the gene's DNA sequence for transcription. Once unwound, the basal transcription machinery has access to the promoter (Smoak & Cidlowski, 2004).

One example of this is the transcription of serum-glucocorticoid-inducible kinase 1 (Sgk1). Sgk1, identified initially as a cell volume regulator, has many functions, including modifying phosphorylation of ion channels, transporters, and enzymes (Lang & Shumilina, 2013; Lang, Strutz-Seebohm, Seebohm, & Lang, 2010) and influencing glutamate transmission (Finsterwald & Alberini, 2014). Sgk1 activates the Rab4-GDI complex, which regulates AMPA receptor recycling at the synapse. This increases the expression of GluA2, a component of AMPA receptors (Wright & Vissel, 2012), causing an increase in hippocampal synaptic transmission, spine formation, and long-term memory (Finsterwald & Alberini, 2014).

Apart from transcription, glucocorticoids can act through negative GREs (nGREs), inhibit transcription via protein-protein interactions ("transrepression"), activate signaling pathways, and activate glucocorticoid receptor-mediated decay (GMD; see Section 3.1.2) (Cho et al., 2015; Ismaili & Garabedian, 2004; O. H. Park et al., 2016; Smoak & Cidlowski, 2004; Stahn et al., 2007). One example of the nGRE is the proopiomelanocortin gene, which inhibits corticotropin-releasing hormone (CRH) and adrenocorticotrophic hormone (ACTH) in the hypothalamic-pituitary-adrenal (HPA)- axis (see Section 3.3.2). The nGRE acts in a similar manner as the positive GREs, though they have a different motif with 0-2 spacers (CTCC(n)₀₋₂GGAGA) (Oakley & Cidlowski, 2013). In addition, the glucocorticoid receptor complexes can cause transrepression by blocking access of other promoters to their promoter regions (Heitzer et al., 2007).

Glucocorticoid receptor transrepression occurs in either of the promoter regions of pro-inflammatory, such as activator protein 1 (AP1) and nuclear factor- κ B (NF- κ B) (Stahn et al., 2007). The glucocorticoid receptor can heterodimerize to the Jun subunit of

AP1 and the p65 subunit of the NF- κ B, preventing their ability to act as pro-inflammatory cytokine transcript promoters (Bolshakov, Tret'yakova, Kvichansky, & Gulyaeva, 2021; Oakley & Cidlowski, 2013). These heterodimers can also promote anti-inflammatory cytokine, such as Il-4 and Il-10, transcription (Walker & Spencer, 2018).

Glucocorticoid receptors have several gene transcription roles and through the direct mechanism described above, as well as through downstream consequences of that activity, impact the expression levels of 10-20% of the human genome (Oakley & Cidlowski, 2013). Post-translational modification can also have a remarkable impact on the functions of the glucocorticoid receptor. Phosphorylation, the most well understood modification in glucocorticoid receptors, involves at least six kinases: 1) cyclin-dependent kinases (CDKs); 2) p38 mitogen-activated protein kinase (MAPK); 3) c-Jun N-terminal kinase (JNKs); 4) glycogen synthase kinase 3 β (GSK-3 β); 5) extracellular signal-regulated kinase (ERK); and 6) casein kinase II (Vandevyver et al., 2014). MAPK (including JNKs, p38 MAPK, and ERK) are responsive to several factors, including stress, while CDK reacts to cyclin subunits, binding inhibitory polypeptides, and regulating phosphorylation. (Ismaili & Garabedian, 2004). For the present review, I will focus on MAPK and its response to stressful stimuli.

MAPK has low basal phosphorylation activity until the glucocorticoid receptors are bound by agonists, ligands bind, causing the receptors to become hyperphosphorylated. This is due to changes in the conformation of the glucocorticoid receptor (with the exception of Ser-134 in humans that can be phosphorylated in a ligand-independent manner through cellular stress-activating stimuli (Oakley & Cidlowski, 2013)). p38 MAPK phosphorylates Ser-134 in response to stressors, leading to an increase in transcriptional activity (Vandevyver et al., 2014). The phosphorylated Ser-404 also impactions the function of the receptor by diminishing its binding capability (Oakley & Cidlowski, 2013).

Both acute and chronic stress promote histone modifications, which can repress or activate genes related to memory. One example of this was discovered using the Morris water maze and forced swim tests. Glucocorticoids, via glucocorticoid receptors, cause the ERK-MAPK pathway to signal to MSK1 and Elk1, two nuclear kinases, in the dentate gyrus. This process activates phosphorylation and acetylation of residues in histone H3,

inducing c-Fos (Chandramohan, Droste, Arthur, & Reul, 2008), an immediate-early gene that are a neuronal activity marker (Bullitt, 1990).

In addition, glucocorticoid receptors also regulate the endocannabinoid system through non-genomic actions. By releasing endocannabinoids in the hypothalamus (part of a retrograde neurotransmitter system), glucocorticoids suppress HPA-axis activity, thereby feedback inhibiting glucocorticoid release (Bolshakov et al., 2021; Finsterwald & Alberini, 2014; McEwen et al., 2015). Chronic stress and corticosterone treatments downregulate cannabinoid 1 receptor and decrease endocannabinoid levels, impairing the endocannabinoid feedback inhibition system (McEwen et al., 2015). In the hippocampus and the amygdala, endocannabinoids impact cognition and emotional memory encoding (Finsterwald & Alberini, 2014). Endocannabinoids themselves also have anti-inflammatory properties by inhibiting the release of pro-inflammatory cytokines (Bolshakov et al., 2021)

Glucocorticoid receptors also can translocate to the mitochondria with the B-cell-lymphoma 2 (Bcl-2) protein, promoting Ca^{2+} sequestration, reducing mitochondrial oxidation and free radical formation, and hyperpolarizing mitochondrial membrane potential, promoting mitochondrial function. However, high glucocorticoid levels cause this process to fail within 72 hours, leading to increased free radical formation (McEwen et al., 2015).

3.3 Glucocorticoids

Glucocorticoids, a class of hormones that act as the primary ligands for glucocorticoid receptors, are synthesized from cholesterol in the adrenal glands. The most common inactive glucocorticoids are cortisone (primates) and 11-dehydrocorticosterone (rodents), converted by 11 β -hydroxysteroid dehydrogenase 1 into the active cortisol and corticosterone, respectively. However, 11 β -hydroxysteroid dehydrogenase 2 deactivates the hormones (Mifsud & Reul, 2018). After being secreted into the bloodstream by the adrenal gland, 90% of glucocorticoids are bound to glucocorticoid-binding globulins (GBC). The remaining 10% can transverse the blood-brain barrier and cell membranes. Glucocorticoids can bind to two receptors, mineralocorticoid receptors and glucocorticoid receptors (see section 3.2). Mineralocorticoid receptors are another member of the nuclear receptor family. They share characteristics with the glucocorticoid receptor (Baker &

Katsu, 2020); however, they do not share their transactivation domains and target different genes (Datson, van der Perk, de Kloet, & Vreugdenhil, 2001). While their classical ligand is aldosterone, glucocorticoids, and several other hormones have similar affinities for the mineralocorticoid receptors (Baker & Katsu, 2020).

Interestingly, glucocorticoids have a 5-10-fold higher affinity for mineralocorticoid receptors ($K_D \sim 0.5$ nM) than glucocorticoid receptors ($K_D \sim 2.5 - 5$ nM). At basal glucocorticoid levels, mineralocorticoid receptor occupancy is saturated, while increased levels of glucocorticoids cause the activation of the glucocorticoid receptors (Sorrells, Caso, Munhoz, & Sapolsky, 2009; Tanaka et al., 1997). Because of their higher affinity for glucocorticoids and other hormones, mineralocorticoid receptors are constantly in a bound and active state (Mifsud & Reul, 2018). While glucocorticoid receptors are ubiquitously found through the brain, mineralocorticoid receptors are primarily found in the limbic system. Interestingly, RNA-Seq has identified mineralocorticoid receptor mRNA in most neural cells, with microglia the only exception (Bolshakov et al., 2021). This dual-receptor model is thought to, at least in part, confer an "inverse-U" pattern of activation for glucocorticoids on their downstream markers, since mineralocorticoid and glucocorticoid receptors can have opposing effects (Sorrells et al., 2009). This inverse-U pattern shows that stress intensity impacts learning memory and causes fewer deficits with intermediate stress. The glucocorticoid receptors typically mediate high-stress situations that impact spatial memory in the hippocampus and amygdala (Finsterwald & Alberini, 2014). In addition to the stress response (see section 3.3.2), glucocorticoids, in the absence of stress, are released in a circadian fashion and play a role in modulating circadian rhythm and sleep.

Glucocorticoids have a strong anti-inflammatory effect on the immune system throughout the body (Stahn et al., 2007). Acute stress can prime the immune response if the glucocorticoid exposure occurs before stress, producing an exaggerated pro-inflammatory cytokines response (Frank, Watkins, & Maier, 2013; Sorrells et al., 2009). However, glucocorticoids can also attenuate stress-induced defense mechanisms, including pro-inflammatory cytokines (Munck & Naray-Fejes-Toth, 1994), and suppress the pro-inflammatory immune mediators, such as NF- κ B if it occurs consequent with, or after, the stress (De Bosscher, Vanden Berghe, & Haegeman, 2003). Essentially, the stress

exposure post-pro-inflammation attenuates the response (Goujon et al., 1995). Most anti-inflammatory effects have been studied within the brain using bacterial lipopolysaccharides (LPS) injections as a pro-inflammatory challenge. Acute restraint stress immediately after these injections prevented the inflammatory response (Goujon et al., 1995). Corticosterone also inhibited the expression of pro-inflammatory $IL-1\alpha$ and $IL-1\beta$ mRNA in the hypothalamus and hippocampus, though it increased the mRNA levels of $IL-6$ (Chai, Alheim, Lundkvist, Gatti, & Bartfai, 1996). Glucocorticoids also impact microglia, the primary immune cell in the central nervous system. Glucocorticoids, aldosterone, and progesterone attenuate the proliferation of microglia (Ganter, Northoff, Mannel, & Gebicke-Harter, 1992). Microglia can be activated during stress, though glucocorticoids tend to inhibit this effect. Once activated, microglia can phagocytose damaged neurons and release pro-inflammatory factors, such as $IL-1$ (Sugama et al., 2013). Interestingly, when glucocorticoids are given before an inflammatory event, it primes the microglia and increases pro-inflammatory effects of subsequent insults (Dinkel, MacPherson, & Sapolsky, 2003).

Glucocorticoids regulate the circadian clock in multiple brain regions and the liver (McEwen et al., 2015). For example, hippocampal mineralocorticoid receptors control the basal HPA-axis during circadian rhythm (Gadek-Michalska et al., 2013). Additionally, glucocorticoid secretions are higher during the active than inactive periods (Chung, Son, & Kim, 2011), reaching their peak just before waking (Sorrells et al., 2009). A correctly-functioning circadian rhythm allows for normal regulation of ACTH, while a disrupted circadian rhythm can lead to increased risk of psychiatric, cardiovascular, and physiological disorders (McEwen et al., 2015). Interestingly, in aged animals, glucocorticoid levels were elevated during the inactive phase and glucocorticoid receptor expression was reported to be elevated (Barrientos et al., 2015).

3.3.1 Interactions with progesterone and allopregnanolone

Progesterone and glucocorticoids have higher blood plasma levels during mild or acute physical stressors than in severe chronic stress (Ladisich, 1975). Chronic stress (48 hours of social isolation) also decreases the cerebrocortical and hippocampal levels of progesterone and allopregnanolone; they appear to have a floor effect at this point since the concentrations do not continue to fall even with continued stress (Barbaccia, Serra,

Purdy, & Biggio, 2001). Progesterone helps regulate the development of neurons and glial cells, particularly the oligodendrocytic myelination process, and has neuroprotective effects for neurodegenerative diseases (Melcangi & Panzica, 2014).

Like glucocorticoid and mineralocorticoid receptors, progesterone receptors are also members of the nuclear receptor family. Because of this, progesterone, like glucocorticoids, is also able to bind to mineralocorticoid receptors. In fact, progesterone, cortisol, corticosterone, 11-deoxycorticosterone, and aldosterone (the classic ligand for mineralocorticoid receptors) all have similar affinities for the receptor. Interestingly, however, progesterone is an antagonist to the receptor. The interaction between progesterone and the mineralocorticoid receptor is not well understood, especially in its relationship to its effects on glucocorticoids and the stress system (Baker & Katsu, 2020). Based on knowledge of mineralocorticoid receptors' impact on the stress response, it is tempting to speculate that progesterone antagonizing glucocorticoid action on mineralocorticoid receptors would serve to inhibit glucocorticoid's mineralocorticoid receptor-driven effects on the HPA-axis. In addition, if progesterone is in high enough concentrations, it could disrupt in glucocorticoid binding to the glucocorticoid receptor.

5 α -reductase reduces progesterone into dihydroprogesterone, which is then reduced by 3 α -hydroxysteroid oxidoreductase into allopregnanolone (also called 3 α , 5 α -tetrahydroprogesterone) (Guennoun, 2020; Melcangi & Panzica, 2014). Allopregnanolone is a 3 α -, 5 α -reduced metabolite of progesterone, which acts to promote GABA_A receptor activity, and its levels are increased during acute stress (Pluchino et al., 2006). This neuroactive metabolite has anxiolytic properties similar to those of the benzodiazepine class of agents, and the FDA recently approved brexanolone (an exogenous form of allopregnanolone) for the treatment of post-partum depression. Acute treatment can improve memory and learning, and increase neuronal progenitor cells in the hippocampal subgranular zone, in 3xTg-AD mice if administered before pathology develops (Wang et al., 2010). Meanwhile, chronic administrations of allopregnanolone can cause neurogenesis, oligodendrogenesis, reductions in neuroinflammation and β -amyloid burden, and increases in white matter generation and cholesterol homeostasis (Melcangi & Panzica, 2014).

3.3.2 Role in stress and Hypothalamus-Pituitary-Adrenal-Axis

3.3.2.1 Mechanism

When a stressor (e.g., cytokines, nociception, behavioral insult) activates the stress response, the hypothalamic-pituitary-adrenal (HPA)-axis activates a rapid, epinephrine based response, and a slower glucocorticoid-based response in the adrenal gland (Walker & Spencer, 2018). The HPA- axis starts with the paraventricular nucleus (PVN) of the hypothalamus secreting corticotrophin-releasing hormone (CRH) and vasopressin into the pituitary portal (Gadek-Michalska et al., 2013; Sorrells et al., 2009). CRH, whose release is inhibited by GABA_A activity and retrograde endocannabinoid signaling (Barbaccia et al., 2001), also plays a role in dendritic remodeling in the CA1 region of the hippocampus (McEwen et al., 2015). The release of CRH and vasopressin causes the pituitary to release adrenocorticotropin hormone (ACTH) into the bloodstream. ACTH travels to the adrenal glands, which are then stimulated to secrete glucocorticoids. Since females have higher levels of ACTH than males, it follows that they also have higher levels of glucocorticoids (Le Mevel, Abitbol, Beraud, & Maniey, 1978). The glucocorticoids then enter the bloodstream and travel throughout the body. Since they are lipophilic (Timmermans, Souffriau, & Libert, 2019), the free glucocorticoids can easily transverse the blood-brain barrier and plasma cell membranes, where they can bind to cytosolic glucocorticoid and mineralocorticoid receptors, some of which are in the hippocampus (Gadek-Michalska et al., 2013; Sorrells et al., 2009). This binding both stimulates action and begins a negative feedback loop, where ventral hippocampal neurons send inhibitory input to the anterior pituitary (A. H. Miller et al., 1992) and the PVN of the hypothalamus (Garrido, de Blas, Del Arco, Segovia, & Mora, 2012) (Figure 3.2). Meanwhile, the mineralocorticoid receptors rapidly increase the hippocampal and amygdala excitability in the neurons via non-genomic mechanisms; this occurs upstream of the PVN, indicating that both receptors attenuate HPA-activity (Pasricha, Joels, & Karst, 2011). Interestingly, injections of corticosterone do not cause the same effects as acute stress, indicating that other signaling molecules, such as epinephrine in the periphery and CRH centrally, play a role in the stress response (McEwen et al., 2015). There are also sex differences in response to stress stimuli. Females tend to be more responsive to stress during the luteal phase of the estrous

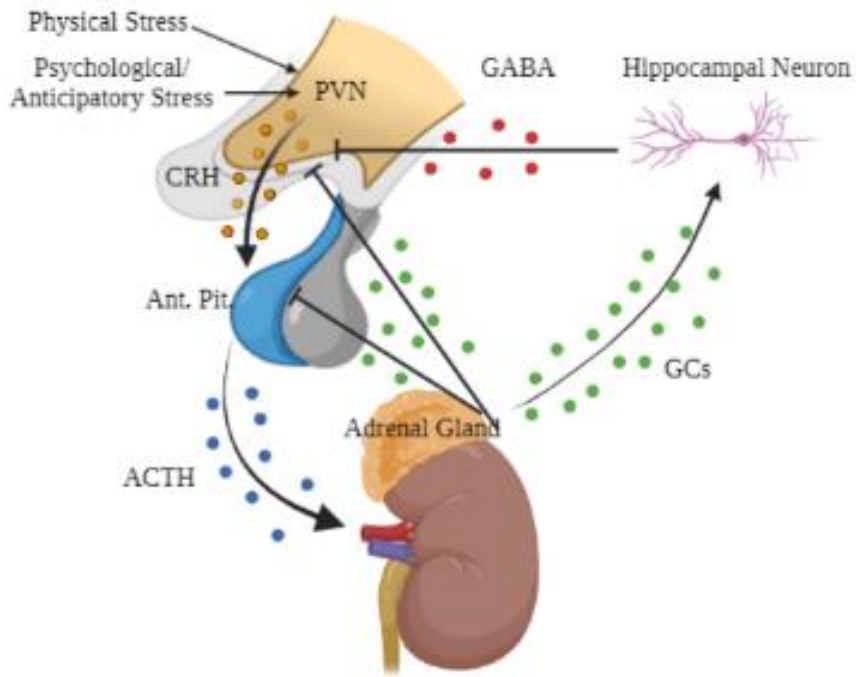


Figure 3.2. Hypothalamus-pituitary-adrenal-axis.

Physical or psychological stress stimulates the paraventricular nucleus (PVN) of the hypothalamus to release corticotrophin-releasing hormones (CRH), which then move to the anterior pituitary. This stimulates the release of adrenocorticotropin hormone (ACTH) into the blood stream, where it travels to the adrenal gland and stimulates the secretion of glucocorticoids (GCs) into the blood stream. Some GCs return to the brain and bind to GC receptors on the neurons. This releases GABA and causes attenuation of the PVN and the anterior pituitary, creating a negative feedback loop on the HPA-axis. Created using BioRender.com.

cycle (Kajantie & Phillips, 2006). However, males' memory consolidation appears to be more affected by stress than females (de Quervain, Schwabe, & Roozendaal, 2017).

3.3.2.2 Stress Response

The stress response is an essential biological function that varies depending on the stressor, its duration, and the subject's age, sex, and species (Atrooz, Alkadhi, & Salim, 2021; von Dawans, Strojny, & Domes, 2021). Stress disrupts multiple systems by activating the HPA-axis, leading to cardiovascular, immune, and mental disorders (Campbell & Ehlert, 2012; Gjerstad, Lightman, & Spiga, 2018). For this study, we will be focusing primarily on the effects on the brain.

Stress can be divided into two groups, physical and psychological. Physical stressors are caused by stimuli that activate nociceptors and lead to an unconscious reflexive activation of the HPA-axis (such as foot shock in rodents or the cold compressor test). Psychological and psychosocial stressors require consciousness to be activated because they rely on anticipatory or predictive brain circuitry (e.g., restraint stress in rodents or the Trier social stress test) (Herman, 2013). Stress can also be subdivided on whether it is acute or chronic. Acute stress is often identified as a stressor that lasts minutes to hours, while chronic stress lasts days to months. In addition, the age and sex of an organism can impact its stress response as well. Most work in stress has been in males, at least in part due to the female estrous cycle affecting stress response (Conrad et al., 2004; Lovick, 2012). In addition, it has been well documented that stress accelerates brain aging, and that age impacts how the body responds to stress.

3.3.2.2.1 *RELATIONSHIP BETWEEN STRESS AND AGING*

Aging is a process that impacts all organs, including the brain. Many automatically associate aging with memory deficits, especially dementia. Dementia is different than the normal aging process, and age-related cognitive decline, although age-related cognitive decline is a risk factor for developing dementia. Dementia is often associated with neurodegenerative diseases, such as Alzheimer's disease, Parkinson's disease, vascular dementia, etc. And as this problem continues to affect our aging population, people are now looking for ways to prevent age-related decline in hopes that it will reduce the risk for developing subsequent neurodegenerative diseases. Unfortunately, for the last 18

months, the world has had a constant stressor: the COVID-19 pandemic. In addition to the immediate health risks this virus brings, this stress associated with the social response to the crisis likely will have long-term impacts on the population's mental health. In the last several decades, research has shown a relationship between stress (particularly chronic) and aging in the brain (K. C. Chen et al., 2013; Landfield, Blalock, Chen, & Porter, 2007; Porter & Landfield, 1998).

The glucocorticoid cascade hypothesis was introduced in 1986 and suggested that age-related changes in the HPA-axis may cause functional defects and neurotoxicity in the hippocampal neurons, leading to an increase in HPA-axis activity. This process would increase glucocorticoid blood plasma levels, leading to a larger percent of unbound glucocorticoids; some of the glucocorticoids would travel to the brain and cause neurotoxicity. In addition, there would be a decrease in available glucocorticoid receptors, causing attenuation of the negative feedback loop (Bauer, 2005; Garrido et al., 2012; Porter & Landfield, 1998; Sapolsky, Krey, & McEwen, 1986). Aging reduces glucocorticoid receptor's negative feedback, cytoplasmic glucocorticoid receptor levels, and attenuates the transport of the receptor to the nucleus (Mizoguchi et al., 2009). In addition, aged rats have significantly higher levels of glucocorticoids in their hippocampus and prefrontal cortex compared to young rats. However, there is no significant difference in response to restraint stress (Garrido et al., 2012) or they are hypo-responsive (Buechel et al., 2014). This finding indicates that there is a ceiling effect for the stress response in aged animals. Both chronic stress and aging have similar glucocorticoid receptor and neuronal cell loss in the CA3 (Sapolsky, Krey, & McEwen, 1985).

In addition, aging exacerbates the hippocampal microglial responses to immune challenges compared to young adults. This increased activity has been associated with attenuated long-term potentiation (LTP) in the hippocampus, lower levels of brain-derived neurotrophic factor (BDNF- a neurotrophic factor involved in neuronal development, maintenance, survival, and plasticity), and spatial and contextual memory impairments (Barrientos et al., 2015; Murakami, Imbe, Morikawa, Kubo, & Senba, 2005).

3.3.2.2.2 *CHRONIC STRESS*

Chronic stress is often marked by an overactive HPA-axis (Bauer, 2005) and occurs with repeated or long-term stress. Habituation can occur to try to mediate the stress

response associated with chronic stress. This adaptive response decreases the effect of the stressor on the organism and the effects of the stress response. Unsurprisingly, the rate of habituation is based on the severity of the stressor (Herman, 2013). Habituation could be moderated by glucocorticoids, whose consistently high levels act to regulate the excitability of the HPA-axis and limit its responsiveness (Herman, 2013). It could explain why repeated restraint stress gradually loses its impact on the glucocorticoid and mineralocorticoid receptors' mRNA expression in the hippocampus (Girrotti et al., 2006). This process, however, does not cause the organism to return to the pre-stress physiological homeostasis and causes upregulation of CRH, which of course, can lead to HPA-axis activation (Barbaccia et al., 2001; Herman, 2013). Thus, this kind of anticipatory stressor has been modeled in animals has been shown to have similar effects as seen in clinical settings.

Many adverse effects associated with chronic stress are due to the continuous stress response (and its adaptation), but in ordinary circumstances, these responses are beneficial to the health of the organism. However, after chronic stress (21 days), the response does not recover to pre-stress levels (i.e., from the organism's perspective, the stress response has failed to re-establish homeostasis with the environment). A new onset of the stress response with novel stressors creates a unique gene expression profile. Often, the genes affected are epigenetic regulators, which may explain the long-lasting effects of stress exposure (McEwen et al., 2015). For example, as discussed in the previous section, glucocorticoids cause neurons to send negative feedback to the HPA-axis. However, overexposure to glucocorticoids can cause neuronal dysfunction and lead to impaired regulation of the HPA-axis. In addition, BDNF levels and neurogenesis decrease in the hippocampus when exposed to chronic stress (Toth et al., 2008). Chronic stress also changes microglia density and morphology (Hinwood et al., 2013; Tynan et al., 2010).

While chronic stress leads to hippocampal-memory deficits, it does not have the same effect on amygdala-dependent memories. The hippocampal deficits are at least partially due to the CA1, CA3, and dentate gyrus atrophy, and decreased hippocampal neurogenesis (Fensterwald & Alberini, 2014; Jung et al., 2020). However, the same chronic stress exposure appears to strengthen the neuronal activity, synaptic transmission, spine formation, and dendritic growth in the amygdala (Fensterwald & Alberini, 2014), as

if the stress response reduces the capacity for spatial memory encoding, but increases negative emotional capacity.

Like many other systems in the body, stress (both acute and chronic) is sexually dimorphic. In chronic stress, males have impaired spatial memory, females show chronic resilience and potentially enhanced memory (Beck & Luine, 2002; Bisagno et al., 2004; Luine, Gomez, Beck, & Bowman, 2017). In addition, the CA3 neuronal dendrites are not remodeled in females, even though their plasma, stress hormone levels were higher than males (L. A. Galea et al., 1997). Females also appear to have more depressive-like behaviors, bodyweight reduction, and anxiety-like behaviors than in male rats, but the females appear to be more resistant to hippocampal memory deficits (Brummelte & Galea, 2010; McEwen, 2017). At a cellular level, males have a decreased cell survival while females have an increase (Brummelte & Galea, 2010).

3.3.2.2.3 *ACUTE STRESS*

Acute stress has differing effects from chronic. Often, these effects are typically beneficial since the stress response evolved for short-term stressors (e.g., fleeing from predators). There are still acute stress effects that can cause dysfunction in specific processes. One well-documented example is in memory; after acute psychosocial stress, for instance, the rise in glucocorticoids causes deficits in spatial memory retrieval in rodents and humans, and facilitates emotional memory retrieval in humans (Hidalgo, Pulpulos, & Salvador, 2019; Li, Fan, Wang, & Tang, 2012; Olver, Pinney, Maruff, & Norman, 2015; Stillman, Shukitt-Hale, Levy, & Lieberman, 1998; Tollenaar, Elzinga, Spinhoven, & Everaerd, 2008; Yuen et al., 2009). One mechanism acting on this is that acute stress leads to high levels of glucocorticoids and downregulates GABA_A receptors (Barbaccia et al., 2001; Finsterwald & Alberini, 2014). Inhibiting the GABA_A receptors, which provide the negative feedback signal for the HPA-axis, increases the glucocorticoid levels and their downstream effects, prolonging the stress response and causing further memory deficits. In addition, acute stress has been associated with neurodegeneration and attenuation of neurogenesis in the dentate gyrus (Finsterwald & Alberini, 2014).

Unlike chronic stress, acute stressors do not cause long-term changes to a healthy brain. In the hippocampus, there is a decrease in glucocorticoid receptors (Sapolsky et al., 1985) and an increase in BDNF levels (Denhardt, 2018), which are reversible and return to their

pre-stress levels within a week. Similarly, after a severe acute stressor, pro-inflammatory cytokines secretion becomes primed and responds with a greater amplitude and a shorter latency to subsequent challenges, such as peripheral LPS injections, for 24 hours after stress exposure (Frank et al., 2013). While acute stress can disrupt homeostasis, it can show a hormesis-like response, priming the individual to more aggressively combat a subsequent stress exposure.

Glucocorticoids and their receptors influence many functions, such as inflammation, circadian rhythm, and stress response. However, there is still much to uncover regarding the downstream effects of glucocorticoids after the HPA-axis has been activated. At the same time, the primary mechanism of the HPA-axis and glucocorticoids' role in it, the functions of other hormones and proteins, and how they interact with glucocorticoids can be clarified. Another area that is still not well documented is the interaction between glucocorticoids, their receptors, and progesterone. Since acute stress is the basis by which chronic stress acts, several areas need to be investigated, including the less defined female response to acute restraint stress compared to males and progesterone's anti-stress effects and where the stress response occurs. The following chapter describes results from an experiment examining the influence of acute stress and progesterone on RNA integrity, glucocorticoid levels, and molecular signals in the brains of male and female rats to address knowledge gaps in the field.

CHAPTER 4. PROGESTERONE PRETREATMENT ATTENUATES ACUTE STRESS ACTION ON HIPPOCAMPUS WITHOUT THE APPARENT DISRUPTION OF THE HYPOTHALAMIC-PITUITARY-ADRENAL AXIS IN YOUNG ADULT MALE AND FEMALE RATS

4.1 Summary

Behavioral stress is prevalent, sexually dimorphic, and has negative health consequences associated with action in multiple tissues, including the brain. Glucocorticoids are key stress-signaling hormones with enriched hippocampal receptor expression, and stress-driven expression of immediate early genes such as serum- and glucocorticoid kinase 1 (Sgk1) is considered indicative of glucocorticoid receptor-based central action. While glucocorticoids have anti-inflammatory actions, stress exacerbates neuroinflammation, possibly through myelin fragmentation and resulting stimulation of microglia phagocytosis. Previous work has shown that progesterone may ameliorate stress effects, but whether that effect is exerted at the HPA-axis, on downstream targets, or both, remains unclear. To address this knowledge gap, we hypothesize that progesterone pretreatment would reduce acute stress response. Eighty-eight intact adult Sprague-Dawley rats (50 males / 38 females) were trained in the Morris Water Maze. The male and female rats were placed into one of four groups (n = 9-13): 1) control + vehicle; 2) control + progesterone; 3) stressed + vehicle; 4) stressed + progesterone. Oral progesterone-pretreatment (10 mg/ kg) was administered daily for 3 days after each Morris water maze training session. On day 4, a 3-hour restraint was applied immediately prior to the probe trial, and blood and brain were collected within fifteen minutes of probe trial completion. In both sexes, progesterone pretreatment alleviated stress-induced behavioral deficits but did not alter stress-induced corticosterone levels. In males, progesterone also attenuated stress-induced hippocampal Sgk1 mRNA increases, while progesterone, but not stress, increased Iba1 expression in the stratum oriens and Iba1/ Mbp overlap in the alveus. Females showed multiple baseline-level differences compared to males, including increased: maze training path length, blood corticosterone, pyramidal layer Iba1, and reduced Sgk1 mRNA in the hippocampus. Unlike males, female Sgk1 mRNA was unaffected by stress or progesterone, and Iba1 levels in stratum oriens (and Iba1/Mbp overlap in the stratum oriens and pyramidal layer) were increased by both progesterone and stress, but in the stress condition progesterone blunted Iba1 increases. Overall,

although results do not support a myelin-fragment driven effect, results do support sexual dimorphism of stress responses and indicate that progesterone pretreatment blunts stress effect through actions downstream of the HPA-axis activation.

4.2 Introduction

The stress response is essential not only for escaping or surviving threats, but also for adapting to a changing environment. In fact, even ordinarily survivable environmental changes in temperature can have lethal consequences in the absence of an appropriate stress response. However, the body's response to early life severe stress, to traumatic events, or to ongoing unremitting stressors, clearly has negative health consequences, including increased risk of anxiety, post-traumatic stress disorder, adjustment disorder, depression, substance use disorder, cardiovascular disease, type II diabetes, and Alzheimer's disease (Vanitallie, 2002). While stress has always impacted health, experience with the coronavirus pandemic has dramatically increased the number of people experiencing chronic stress in the last 18 months. A recent report by the American Psychological Association found that > 80% of Americans have reported signs of chronic stress, with young adults being of particular concern (Canady, 2021). Mechanistically, chronic stress leads to circadian and sleep disruption, weakened immune function, and limbic and prefrontal cortex volume reductions (Mariotti, 2015). Conceived as an evolutionary answer to conserve the individual in the face of predatory threat, in modern society, the stress response is instead triggered by anticipatory stressors that often are unresolvable by the stress response or by any means of the individual under that stress. While the stress response has been investigated for decades, it has primarily been studied in males. This is problematic because female sex hormones may play a role in moderating the stress response. Females have been shown to have fluctuating stress responses depending on their position in the estrous cycle, and the consequences of stress exposure in females appear to be greater (Conrad et al., 2004; Lovick, 2012; Rosenfeld & Trainor, 2014). Although pharmacologic, counseling, and life-style therapeutics can be effective, many suffer from poor compliance and/or unwanted side effects. Given the likely 'coming storm' of stress related pathologies, further investigation into new therapeutic targets pre- and post-stress are warranted.

The stress response is highly conserved in vertebrates ((Bridgham, Carroll, & Thornton, 2006); reviewed in (Denver, 2009)), and therefore animal models are often used to study its effects (reviewed in (Atrooz et al., 2021)). Further, responses to different stressors/ durations can vary with age, sex, and species (Atrooz et al., 2021; von Dawans et al., 2021). A predominant form of stress affecting people is psychosocial (or anticipatory) stressors such as isolation, disaster displacement, economic uncertainty, divorce, death of a loved one, and restriction of movement (Heinrichs, Baumgartner, Kirschbaum, & Ehlert, 2003; Kajantie & Phillips, 2006). Unlike physiologic stressors, these anticipatory stressors elicit stress responses in the absence of pain or nociceptive pathways activation. Thus, appropriate models in animals also should not cause physical pain (K. Hargis, Buechel, Popovic, & Blalock, 2018; Jansen, Gispens-de Wied, & Kahn, 2000; Kogler et al., 2015). In rodents, restraint (Buechel et al., 2014; Herman & Cullinan, 1997; Yang et al., 2017; Zafir & Banu, 2007) is commonly used to model psychosocial stress as it elicits a stress response in the absence of pain (Buynitsky & Mostofsky, 2009; Herman et al., 2003; Pawlyk, Morrison, Ross, & Brennan, 2008), and recapitulates many aspects of anticipatory stress responses in humans, including elevated adrenaline and glucocorticoid levels, behavioral deficits in hippocampal-dependent tasks, and downstream molecular changes, many of which are driven by stress-associated glucocorticoid secretion (Atrooz et al., 2021; de Quervain et al., 2017).

Adrenaline and glucocorticoid secretion from the adrenal gland are key molecular signals of the hypothalamic-pituitary-adrenal (HPA)- axis in the acute stress response. Acute stress, and its associated increase in glucocorticoids (cortisol in humans and corticosterone in rodents) (Campbell & Ehlert, 2012; Gjerstad et al., 2018) reversibly inhibit memory retrieval (Hidalgo et al., 2019; Li et al., 2012; Olver et al., 2015; Tollenaar et al., 2008; Yuen et al., 2009). Glucocorticoids themselves act through feedback inhibition to terminate the stress response in the brain's amygdala, hippocampus, and paraventricular nucleus (PVN), reducing the PVN's release of corticotropin-releasing hormone onto the anterior pituitary, and also by directly inhibiting adrenocorticotrophic hormone release from the anterior pituitary into the blood (Tasker & Herman, 2011). Glucocorticoids have a broad range of actions; they increase glucose uptake (reviewed in (Jaszczyk & Juszczak, 2021)), inhibit antioxidant enzymatic activity, suppress the immune

system (though it may also promote inflammatory action (MacPherson, Dinkel, & Sapolsky, 2005; Sorrells & Sapolsky, 2007)), and decrease mitochondrial oxygen consumption, neurogenesis and cell survival (Cain & Cidlowski, 2017; Goulding & Guyre, 1993; Jauregui-Huerta et al., 2010; Katyare, Balasubramanian, & Parmar, 2003; McIntosh, Hong, & Sapolsky, 1998; Nicolaides, Kyratzi, Lamprokostopoulou, Chrousos, & Charmandari, 2015; Sorrells & Sapolsky, 2007). Both stress and glucocorticoids are thought to play a role in accelerating brain aging (Cesari, Vellas, & Gambassi, 2013; Garrido, 2011; Kerr, Campbell, Applegate, Brodish, & Landfield, 1991; Landfield, Cadwallader, & Vinsant, 1988; Lavretsky & Newhouse, 2012; Porter & Landfield, 1998; Sapolsky, 1999).

In the brain, glucocorticoids, through glucocorticoid receptor binding, can increase the transcription of target genes, including serum- and glucocorticoid-inducible kinase 1 (Sgk1) (Anacker et al., 2013; Buechel et al., 2014; K. C. Chen et al., 2013; Porter et al., 2012), which has also been linked to aging (Blalock et al., 2003; Blalock et al., 2010; C. Y. Chen et al., 2016; Kadish et al., 2009; Pavlopoulos et al., 2013; Rowe et al., 2007; Stilling et al., 2014; Swanson, Vester, Apanavicius, Kirby, & Schook, 2009; Verbitsky et al., 2004). Originally identified as a cell-volume regulator, Sgk1 has since been described to play a role in a variety of functions by modifying the phosphorylation status of multiple ion channels, transporters, and enzymes (Lang & Shumilina, 2013; Lang et al., 2010). It is present throughout the brain, including recently being identified in oligodendrocytes (Hinds et al., 2017). Sgk1 also plays a role in memory formation (Finsterwald & Alberini, 2014; Lang et al., 2010; Ma, Tsai, Hsu, & Lee, 2006).

In social defeat, acute foot shock, and restraint models of stress, increased microglial inflammatory profiles are seen (Frank, Baratta, Sprunger, Watkins, & Maier, 2007; Tynan et al., 2010; Wohleb et al., 2011). Safaiyan et al. also determined that in aged mice, there is an increase in microglia burdened with myelin debris as subjects age (Safaiyan et al., 2016), and it has been proposed that this may lead to microglial dysfunction in stress and aging (Niraula, Sheridan, & Godbout, 2017; Safaiyan et al., 2016).

Progesterone and its metabolite allopregnanolone have been shown to be neuroprotective and to improve behavioral performance (Guennoun, 2020; Luoma, Stern, & Mermelstein, 2012; Schumacher, Guennoun, Stein, & De Nicola, 2007). In a male

human trial, progesterone decreased behavioral signs of stress (e.g., alertness, arousal, and negative mood) (Childs, Van Dam, & de Wit, 2010). Other studies have also found that progesterone, allopregnanolone, and the enzymes that convert progesterone to allopregnanolone increase after acute stress (Barbaccia et al., 1996; Sanchez, Torres, Gavete, & Ortega, 2008; Sze, Gill, & Brunton, 2018), suggesting an endogenous stress-regulating role for progesterone. However, it is unclear where along the stress response pathway progesterone may be exerting its effects, and whether male and female responses differ.

Here, we address this by investigating progesterone pretreatment's effects on acute stress responses in intact young adult male and female Sprague-Dawley rats. We measured corticosterone blood levels, hippocampus-dependent behavior, hippocampal Sgk1 expression, and Iba1 levels with Western blot to test where, along the pathway from stress perception to stress response, progesterone might be exerting its anti-stress effects, and whether those responses differed between males and females. Overall, our work shows many stress-relevant measures were significantly different at baseline between males and females, and that progesterone ameliorated stress-induced behavioral deficits in both male and female animals but did not alter blood corticosterone levels in either. In males, stress-induced Sgk1 mRNA elevations were reversed by progesterone, but in females, Sgk1 was not altered by any condition or treatment. Taken together, these results demonstrate that the stress response is sexually dimorphic, and that progesterone's protective role appears to occur after the HPA-axis activation and may interfere with glucocorticoid signaling.

4.3 Methods

4.3.1 Animals

Eighty-eight Sprague-Dawley rats aged 2-5 months old were housed in a 12-hour reverse light/dark cycle room (4:30 AM lights off, 4:30 PM lights on) in individual cages with ad libitum access to food and water. Eighty-eight 2-5 months old Sprague-Dawley rats (50 males, 38 females) were obtained, and none died during these experiments. Male (M) and Female (F) animals were randomly divided into 4 groups: vehicle-dosed, control (VC; n = 23, MVC/FVC = 13 / 10), progesterone-dosed, control (PC; n = 21, MPC/FPC = 12 / 9), vehicle-dosed, stress (VS; n = 21, MVS/FVS = 12 / 9), and progesterone-dosed, stress (PS; n = 23, MPS/FPS = 13 / 10). The animals were run in 5 cohorts (n = 20; 11; 19;

19; 19) due to the amount of time to perform water maze during training and on probe trial day. Experiments were performed in accordance with institutional and national guidelines as approved in our IACUC protocol (University of Kentucky #2008-3490).

4.3.2 Oral progesterone

Thirty minutes prior to the animals' light (inactive) phase, half of the animals were given an oral dose of 10 mg/kg of micronized human progesterone mixed in a hazelnut spread (Nutella) on a single piece of dry cereal (Fruit Loops). This treatment was administered each afternoon after spatial cue water maze training (three consecutive days, see below). Vehicle animals received the same treatment, except progesterone was replaced with peanut oil (vehicle).

4.3.3 Water Maze

The Morris Water Maze was performed as previously described (K. Hargis et al., 2018). A circular, black-painted pool (diameter = 180 cm) was enclosed within black curtains. The pool was filled to 45 cm in height, with a hidden, black platform with a 15 cm diameter positioned -1.5 cm below the water. A proximity platform (diameter = 30 cm) was also created within the tracking program, Noldus' EthoVision (XT 14). The temperature was 26.9 ± 1.5 ° C. All training and probe sessions took place during the rats' active period.

4.3.3.1 Visual Cue

In week 1, 3 trials per day for two days of visual cue training were performed to ensure that all animals could learn to swim to a visual cue. On each trial, animals were placed in a different starting quadrant, and the partially submerged platform was indicated by a local cue (a white Styrofoam cup hanging by a thread from the ceiling 12 inches directly above platform). On each trial, the platform and local cue were re-positioned to a new quadrant. The animals were given 60 seconds to find the platform on each trial. If they completed the task before the minute finished, the timer was stopped and they were allowed to remain on the platform; if not, they were gently guided to the platform. After the initial 60s, animals were allowed to remain on the platform for another 60 seconds. Animals were then removed from the pool, dried off with a towel, and placed under a heat lamp in an excelsior bedding 'drying' cage for an inter-trial interval of approximately 90

seconds. This process was repeated until all three trials were complete, and animals were dry, at which point they were placed back into their home cages and returned to the vivarium. By the end of the second day, all animals found the platform in under 30 seconds and continued to the next experiment.

4.3.3.2 Spatial Cue

The following week (week 2), the animals had three spatial training days. Procedures here were the same as during the visual cue, except the platform was left in the same position for all three days, the local “visual cue” was removed, and three distant cues (75 cm x 75 cm; black and white vertical stripes, a black triangle on a white circle, and a black cross on a white square) strategically placed outside the perimeter of the water maze pool were added. The animals entered the pool from the three non-goal quadrants (3 trials per day), and the order of quadrant entry was randomized for each day and each trial. Animals were dosed with vehicle or progesterone (see Oral Progesterone above) at the beginning of their inactive period after each spatial cue day (three times). If animals could not complete the task within 60 seconds in 2 out of 3 trials on the third day, they were considered ‘timed out’ and removed from the experiment.

4.3.3.3 Restraint stress and probe trial

On the final day (day 4) of week 2, half of the animals were restrained as in prior work (Buechel et al., 2011; Buechel et al., 2014; K. Hargis et al., 2018) in their home cages for 3 hours in plastic sleeves (DecapiCones DC-200, Braintree Scientific Inc., MA) secured with paper tape. Restrained animals were continuously monitored during restraint, and the number of times they struggled against the restraints or vocalized was recorded as indicators of stress. The control animals remained in their housing room and home cages.

The platform was removed from the water maze pool and after 3 hours animals were removed from restraint, placed in the goal-opposite quadrant, and allowed to swim for a single 60 s ‘probe’ trial. The number of times the animals passed through the platform’s prior location, total path length, latency and pathlength to the first crossing, and the duration and pathlength within in the proximity platform (the platform areas with an extended diameter of 15 cm) was recorded. After 60 s, animals were removed from the pool, dried off and returned to their home cages.

4.3.3.4 Blood and tissue collection

Immediately after the probe trial, animals were transported to an adjacent necropsy room, anesthetized with isoflurane gas, and decapitated. Trunk blood was collected in BD Vacutainer K2 EDTA 5.4 mg (367856, BD biosciences, NJ), incubated at room temperature for 20 - 60 minutes, and centrifuged at 1200 g for 10 minutes. The serum was collected for corticosterone, progesterone, and testosterone. The brain was removed and hemisected. One hemisphere was post-fixed in 4% paraformaldehyde (PFA) overnight and then cryoprotected in 15% sucrose solution and frozen at -80° C for further use. The other hemisphere was fresh frozen in dry ice, wrapped in parafilm and stored at -80° C until further use.

4.3.4 Immunohistochemistry

Twenty μm sagittal sections containing hippocampus were prepared from post-fixed tissue on a cryotome (Shandon Cryotome FE &FSE, Thermo Electron Corp., PA), mounted on Colorfrost Plus Microscope Slides (Cat. # 12-550-17, Fisher Scientific, PA), and air-dried. They were then washed with TBS and Tris-T before being blocked with Tris-BSA (2% BSA) for one hour. Specimens were then incubated in primary antibodies, anti-Mbp (1:2500- chicken polyclonal, ThermoFisher Cat. # Pa1-10008, Lot # VG3026881; Illinois, USA), and recombinant anti-Iba1 (1:2000- rabbit monoclonal, Abcam Cat. # ab178847, Lot # GR3229566-5) overnight at 4°C. The following morning, the slides were washed with Tris-T before 2-hour secondary incubation in the dark (Goat anti-chicken IgY (H+L), Alexa Fluor 647, ThermoFisher A-21449, Lot # 2010133; Goat anti-rat IgG H&L, Alexa Fluor 488, Abcam ab150077, Lot # GR3313703-1). Specimens were washed again in Tris-T, covered with a VWR micro cover glass (Cat. # 48393-106, VWR, PA), and then entire specimen images were acquired at 20x magnification, tiled and stitched to form a single image for using a Zeiss Axio Scan.Z1 in the University of Kentucky Light Microscopy Core. The fluorescent images used AF488 and AF647, and bright-field images were also acquired.

Once the fluorescent and bright field images were obtained, samples that did not pass quality control (e.g., tears or folds occupying > 50% of a region of interest, low signal-to-noise ratio) were removed. Then, semiquantitative analysis of the signal intensity for both Iba1 and Mbp in four hippocampal regions: alveus, stratum oriens, pyramidal

layer, and stratum radiatum was quantified using FIJI (Java 1.8.0_172 (64-bit);(Schindelin et al., 2012)). First, the signal was split into its AF488 and AF647 channels using the Zen 3.2 lite (blue edition; Zeiss). The images for the two channels were opened in FIJI, and each channel was thresholded to retain the top 15% of signal. The “AND” function from the image calculator was used to combine the thresholded images and quantify overlap. Using a non-thresholded image as a guide, the regions of interest (ROIs) were encircled with the freehand tool. ROIs were then copied and pasted onto the thresholded images. The ROI average of thresholded signal was determined and recorded for Iba1, Mbp, and the overlap.

In order to obtain the images of overlapping expression, the same channel images were opened in FIJI and converted to 8-bit. The “subtract background” function used a 50-pixel rolling radius in order to remove the background noise. Then, brightness was min-max restricted to contain >90% of channel signal for each channel, and the channels were merged (Iba1 green, Mbp red).

4.3.5 Plasma Analysis

Internal standards (corticosterone- d8: Caymen #28524; progesterone-D₉: Millipore Sigma # P-070; 17 β -estradiol-D₅: Millipore Sigma # E-061; testosterone-2,3,4-¹³C₃: Millipore Sigma # T-070) were added into the plasma sample, then the extraction solvent (hexane: MTBE, 75:25, v:v) was added. After mixing and centrifugation, the organic phase was transferred into a glass vial and evaporated under nitrogen at 40°C. The samples were reconstituted in water: methanol (50:50 by volume), and the sample was injected onto the liquid chromatography-tandem mass spectrometry (LC-MS/MS) system. Charcoal stripped rat plasma was used to prepare the calibration curves and QC samples.

LC-MS/MS analysis was performed with an ExionLC™ system coupled to a QTRAP 6500+ mass spectrometer (SCIEX, Framingham, MA, USA) consisting of a binary high-pressure mixing gradient pump with a degasser, a thermostatically controlled autosampler, and a column oven. The chromatographic separation was performed on a Waters ACQUITY BEH C8 column (2.1 × 100 mm, 1.7 μ m) by a gradient elution at a flow rate of 0.25 mL/min using water (mobile phase A) and methanol (mobile phase B). The QTRAP 6500+ mass spectrometer was equipped with an IonDrive™ Turbo V source and was operated in low mass and MRM mode with electrospray ionization. Resulting

values for corticosterone, progesterone, and testosterone were expressed as ng/ml. As noted in the supplemental data for the plasma mass spectrometry analyses, missing values were imputed using the half-minimum (HM) method (reviewed in (Wei et al., 2018)).

4.3.6 Western blot

Roughly one-third of the flash-frozen hippocampi were placed in 0.4 ml of 0.25 M sucrose buffer containing 100 μ l/ 10 ml of Phosphate Inhibitor Set, Cocktail II (Calbiochem-EMD Cat. # 524625, Lot # 3491205; Darmstadt, Germany), 10 μ l of Protease Inhibitor Set, Cocktail III (Calbiochem-EMD Cat. # 539134, Lot # 3596821; Darmstadt; Germany), and 10 mM ALLN (Calbiochem-EMD Cat. # 208719, Lot # 3552708; Darmstadt; Germany) and thawed on ice. Samples were homogenized before adding 2X RIPA buffer (dilute 10X RIPA Lysis Buffer; EMD Millipore Corp. Cat. # 20-188, Lot # 3519189), vortexed, and incubated on ice for 45- 60 minutes. Samples were then centrifuged at 13,600 rpm for 10 minutes before retrieving RIPA supernatant, then stored overnight at -80 ° C.

The following morning, the protein was quantified using a Bradford Protein Assay. Standards were created using Quick Start Bovine Serum Albumin (BSA) Standard (Bio-Rad Cat. # 5000206, Batch # 64411053; California, USA) and diluted in distilled water (volume = 800 μ l). The 3 μ l of the sample was diluted in distilled water. 200 μ l of Quick Start Bradford 1x Dye Reagent was added (Bio-Rad Cat. # 5000205, Batch # 64406046; California, USA). The absorption was measured with a Molecular Devices SpectraMax M2^c Microplate Reader and SoftMax Pro 5.4.5 (Molecular Devices; California, USA) and used to determine protein concentration.

Samples were standardized to 50 μ g in 50 μ l with 1 M dithiothreitol (DTT; Thermo Scientific Cat. # R0861, Assembling Lot # 01075524, Filling Lot # 01068117; Vilnius, Lithuania), 4X Laemmli Sample Buffer (LSB; Bio-Rad Cat. # 1610747, Lot # 64295860), and a 1:1 mixture of 2X RIPA and sucrose buffer. The protein solution was heated at 65° C for 25 minutes before being stored at - 20° C. Criterion TGX Precast Gels (4-20%, 26-well comb; Bio-Rad Cat. # 5671095; California, USA) were placed in running buffer (a Tris-glycine solution), and 13 μ l of the sample was loaded along with 10 μ l of Precision Plus Protein Dual Color Standards (Bio-Rad Cat. #

1610374, Batch # 64389512). The gels were run for 45 minutes at a constant voltage (150 V) using a PowerPac Basic Power Supply (Bio-Rad Cat. # 1645050).

Immobilon-FL PVDF membranes (EMD Millipore Cat. # IPFL00010, Lot # R1CB59664; Carrigtwohill County, Ireland) were wetted in methanol before being placed transfer buffer. The Criterion blotter Filter paper (Bio-Rad Cat. # 1704085; California, USA) was also pre-wet in the transfer buffer. Once the transfer sandwiches were prepared, the transfer occurred for the next 16 hours and 40 minutes with a constant 70 mA current applied.

The following morning, the membranes were transferred into and washed with 1X PBS before being blocked with Intercept Protein-Free Blocking Buffer (Li-Cor Cat. # 927-90001, Lot # D10201-05; Nebraska, USA) for approximately 6 hours. The primaries were added to a 1:1 solution of blocking buffer and PBS/ 0.4% Tween before being added to the membrane to incubate at 4° C overnight. Each incubation included two primaries: 1) recombinant anti-Iba1 (1:2000- rabbit monoclonal, Abcam Cat. # ab178847, Lot # GR3229566) and anti-alpha 1 sodium potassium ATPase (1:3000- mouse monoclonal, Abcam Cat. # ab7671, Lot # GR3294995); 2) anti-Sgk1 (1:750- rabbit polyclonal, Abcam Cat. # ab59337, Lot # GR3296662) and anti-alpha 1 sodium potassium ATPase (1:3000); or 3) anti- Mbp (1:10,000- chicken polyclonal, ThermoFisher Cat. # Pa1-10008, Lot # VG3026881; Illinois, USA) and recombinant anti-sodium potassium ATPase (1:10,000- rabbit monoclonal, Abcam Cat. # ab76020, Lot # GR3237646-4). The membranes were washed in PBS/ 0.4% Tween the next morning before incubating in secondaries for 2 hours. The Iba1 and Sgk1 membranes were incubated in IRDye 680RD goat anti-rabbit (1:10,000- Li-Cor Cat. # 926-68071, Lot # C90827-25; Nebraska, USA) and IRDye 800CW donkey anti-mouse (1:10,000- Li-Cor Cat. # C90805-13, Lot # C90805-13; Nebraska, USA). The Mbp membrane was incubated in IRDye 680RD goat anti-rabbit (1:10,000- Li-Cor Cat. # 926-68071, Lot # C90827-25; Nebraska, USA) and IRDye 800 CW donkey anti-chicken (1:10,000- Li-Cor Cat. # 926-32218, Lot # D01105-05; Nebraska, USA). Then the membranes were washed in PBS, 0.4% Tween, and PBS.

The membranes were then imaged using an Odyssey imaging system (Li-Cor; Nebraska, USA) and Image Studio (Li-Cor; Nebraska, USA). The files were then analyzed using Image Studio Lite v. 5.2 (Li-Cor; Nebraska, USA). The signal intensity for the

proteins of interest (Iba1, Mbp, and Sgk1) and the control (sodium potassium ATPase) were determined, and the ratio between the protein of interest and control was calculated. Samples with protein concentration $< 1.5 \mu\text{g}/\mu\text{l}$ or no visible signal on the Western blot were removed from the analysis.

4.3.7 Real Time- qPCR: RIPA Extract and cDNA Synthesis

One-third of the hippocampus was placed in *RNAlater* (Invitrogen Cat. # AM7024, Lot # 00881774; Vilnius, Lithuania) before being stored at -80°C . RNA was extracted using the Maxwell RSC simplyRNA Tissue Kit (Promega Cat. # AS1340, Lot # 118514; Wisconsin, USA). The 1-Thioglycerol/ Homogenization solution and DNase I solution were prepared according to the manufacture's protocol. The 1-Thioglycerol/ Homogenization and two autoclaved metal beads were placed into a tube on ice on a metal block, and then fresh frozen hippocampus was added. The tissue was then homogenized at 1250 RPM for 1 minute using a Geno/ Grinder 2010 (SPEX Sample Prep; New Jersey, USA). The homogenized samples and the lysis buffer from the RNA extraction kit were then combined and vortexed before being placed in the RSC Cartridge. The DNase I solution was placed 3 wells away from the sample in the cartridge. The plunger and Elution tubes were on the opposite side of the cartridge. The nuclease-free water was then added to the Elution Tubes. The RNA was purified using the Maxwell RSC Instrument (Promega Cat. # AS4500; Wisconsin, USA). RNA was aliquoted to determine RNA integrity numbers (RINs), which were determined using the Agilent Technology standards by the University of Kentucky Genomics Laboratory Core (Mueller et al., 2004). The RNA was then stored at -80°C . Improperly stored samples were not analyzed for RIN or RT-PCT.

The remaining RNA was placed on ice to thaw. Two microliters were used to determine the sample RNA concentration using NanoDrop (Thermo Scientific) for cDNA synthesis. The nuclease-free water, qScript cDNA SuperMix (QuantaBio Cat. # 84035, Lot # 66182308; Massachusetts, USA), and RNA were combined in TempAssure 0.2 mL PCR 8-Tube Strips (USA Scientific, Cat. # 1402-3900, Lot # 19453; USA). The samples were then loaded into the thermocycler (iCycler, Bio- Rad Cat. # 170-8740; California, USA) using the cDNA program. The cDNA was then diluted at a 1:10 ratio in nuclease-free water before being stored at -20°C .

The cDNA was then combined with a master mix. This master mix consisted of PerfeCTa SYBR Green Fast Mix (Quanta Bio Cat. # 95072, Lot # 121719A; Massachusetts, USA), nuclease-free water, and primers (GAPDH forward: 5'-GCCAAAAGGGTCATCATCTC-3', reverse: 5'-GGCCATCCACAGTCTTCT-3', Eurofins; Sgk1 forward: 5'-TGGGTCCATCCTCAAATCC-3', reverse 5'-CGCCAAACCCTCTGACTTCCACTTC-3', Eurofins). The samples were then placed into the CFX96 Real-Time System (Bio-Rad Cat. # 1845097) and C1000 Touch Thermal Cycler (Bio-Rad Cat. # 1851196). They were annealed at 60° C and cycled 37 times.

4.3.8 Statistical analysis

The data was first separated into male and female groups. Within each sex, each treatment group had outliers removed (≥ 2 * standard deviations of the group mean; the complete dataset, including outliers, is provided in Supplemental Data 1). Because animals were run in 5 cohorts, cohort effects were also tested within each sex by one-way ANOVA. As noted in the results, if a significant cohort effect was detected for an outcome measure, then data was standardized within each sex within each cohort before analysis. In these normalized conditions, statistical testing of males vs. females would be inappropriate, so the non-normalized data was used to test for sex differences, acknowledging that cohort effects may impact the analysis. Heteroscedastic t-tests, two-way ANOVAs, and two-way ANOVAs with repeated measures were calculated (SigmaPlot 14.0.3.192, as described in Results).

4.4 Results

Eighty-three intact 2-5 month old Sprague-Dawley rats (48 males (M), 35 females (F)) were assigned to one of 4 groups: vehicle-dosed, control (VC; n =22, MVC/FVC = 13 / 9), progesterone-dosed, control (PC; n = 18, MPC/FPC = 11 / 7), vehicle-dosed, stress (VS; n = 20, MVS/FVS = 12 / 8), and progesterone-dosed, stress (PS; n = 23, MPS/FPS= 13 / 10).

4.4.1 Morris Water Maze

4.4.1.1 Spatial Cue

Males showed significantly shorter path lengths than females as training progressed on days 1-3, but both males and females showed significant improvement over

training (Figure 4.1; two-way ANOVA female $p = 0.017$; male $p = 1.71E-14$).

Progesterone had no detectable effect on either latency or path length measures. (5 animals timed out: 1 FVS; 1 MPC; 2 FPC; and 1 MVC.)

4.4.1.2 Struggles during restraint stress

On day 4, 3 hours before the probe trial, half of the animals were taken to a procedure room and restrained in their home cages for 3 hours (see Methods). A staggered entry design was used with a 10-minute spacing between the animals to ensure each animal spent 3 hours in restraint and had approximately the same time gap between restraint ending and water maze probe trial beginning. During restraint, the number of struggles and vocalizations were counted. While there was no difference in the number of struggles between vehicle and progesterone (two-way ANOVA $p = 0.657$), there was a significant increase in the number of struggles in the males compared to females ($p = 0.003$; Figure 4.2).

4.4.1.3 Probe trials

Within 10 minutes of being removed from restraint, animals underwent water maze probe trial testing. Both male and female stressed animals swam faster than control animals (two-way ANOVA female $p = 0.016$; male $p = 0.003$; Figure 4.3A), and this effect was not significantly altered by progesterone pretreatment. We also found a cohort effect on velocity in both sexes (one-way ANOVA female $p = 0.001$; male $p = 0.013$). Therefore, we normalized the data by cohort (see Methods) to remove the cohort effects. The normalized data showed similar findings to the raw data, significantly increased velocity with stress (two-way ANOVA female $p = 0.003$; male $p = 1.80E-4$; Figure 4.3B).

Because velocity was significantly increased by stress, pathlengths rather than latencies were used for subsequent analyses. If an animal never crossed the platform area, the total pathlength was used to represent 'first crossing', and pathlength within the proximity platform area was left at '0'. While there were no significant differences in the path to first crossing between the sexes or the females in any treatment group, the males given progesterone traveled significantly shorter distances than those given the vehicle (two-way ANOVA $p = 0.017$; Figure 4.4A). In addition, the percent of the total pathway spent in the proximity platform location (PP%) was significantly higher in males than

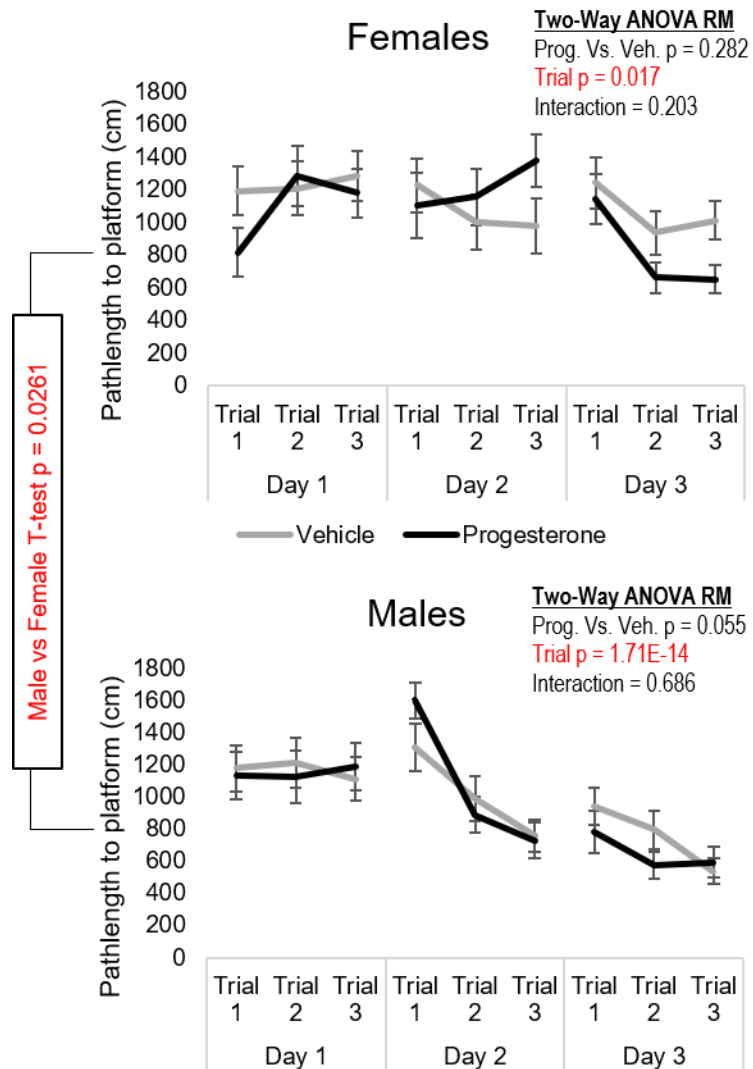


Figure 4.1. Spatial Cue.

Rats were trained in spatial cue with 3 trials each of 3 days prior to probe. The males and females were analyzed separately using a two-way ANOVA with repeated measures. Red values represent significant results, $p \leq 0.05$. The ANOVA results are shown in the top right corner for both sexes. The box to the left of the graphs shows the heteroscedastic T-test results between the males and females. Progesterone (Prog.); vehicle (Veh.).

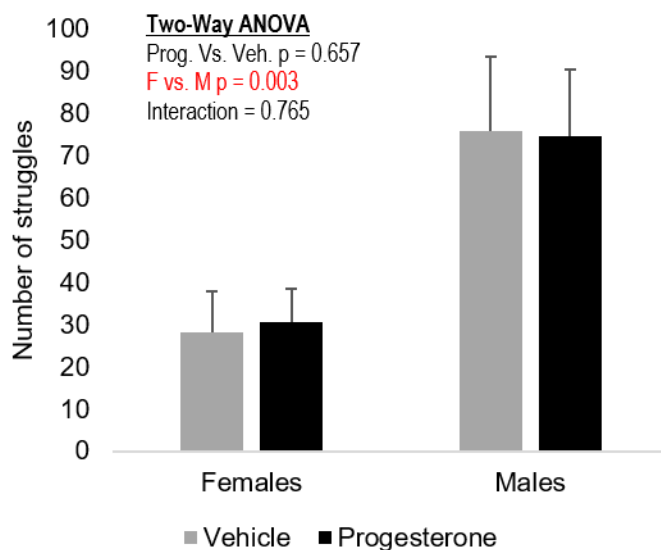


Figure 4.2. Number of struggles during restraint stress.

During restraint, the number of times the rats struggled or vocalized was recorded to indicate their stress level. The males struggled significantly more than the females, though progesterone did not have an effect. Vehicle (Veh); progesterone (Prog); female (F); male (M); red is used for significant values.

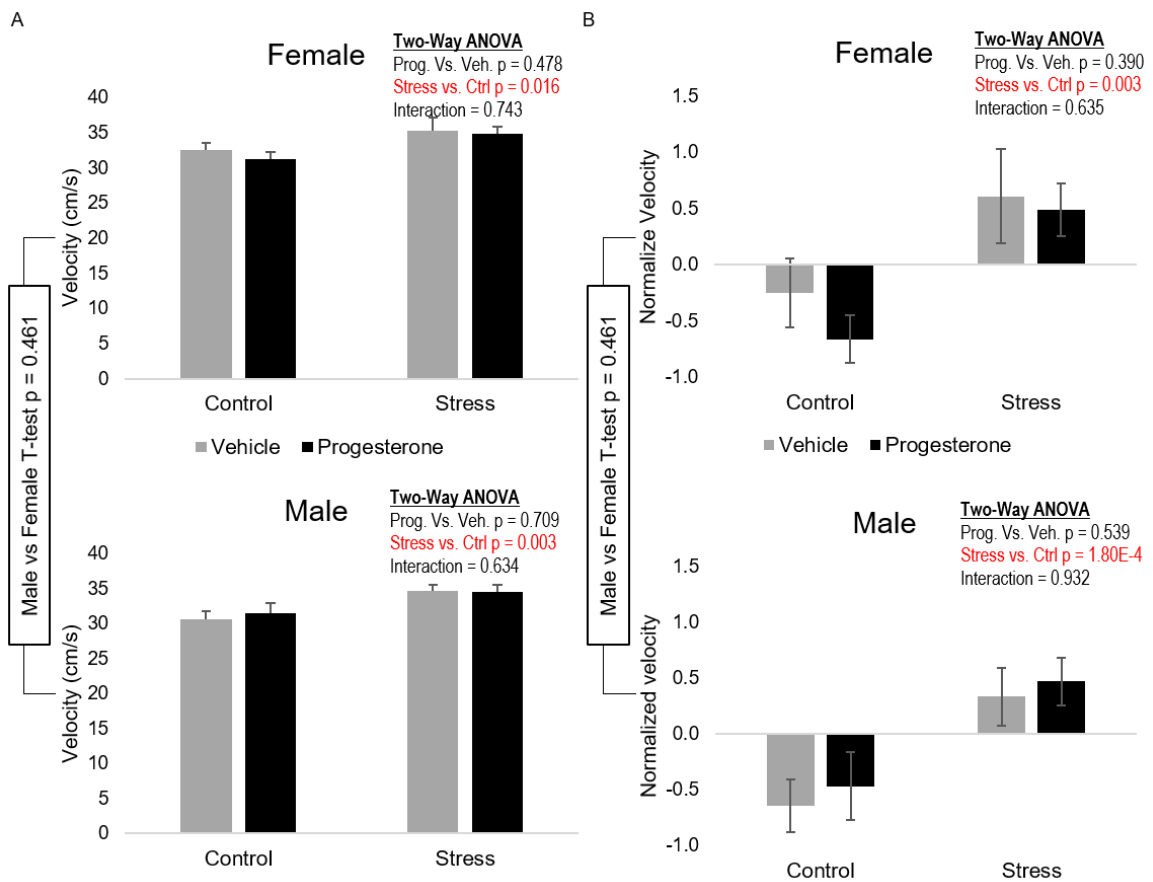


Figure 4.3. Normalized velocity during probe trial.

The raw data (A) and the standardized data (B) for velocity. The data was normalized due to a cohort effect; this does not remove effects, only ensures that any cohort differences do not influence the findings between the treatment groups. Error bars are standard error. The box to the left of the graphs shows the heteroscedastic T-test results between the males and females. Red values represent significance. Progesterone (Prog.); vehicle (Veh.); control (Ctrl); * ≤ 0.05 ; ** ≤ 0.001 .

females (t-test $p = 0.0323$). The FPS spent a significantly higher PP% compared to the FVS (Bonferroni $p = 9.256E-5$) and FPC (Bonferroni $p = 0.012$) groups (Figure 4.4B). The progesterone-dosed males also had a larger PP% compared to the vehicle-dosed males (two-way ANOVA $p = 0.049$), and stressed males had significantly lower PP% than controls (two-way ANOVA $p = 0.031$; Figure 4.4B).

4.4.2 Trunk Plasma Hormones Levels

Immediately after the probe trial, animals were anesthetized, trunk blood and brains were collected. Corticosterone, progesterone, and testosterone in blood were measured using liquid chromatography-tandem mass spectrometry (LC-MS/MS). The corticosterone analysis showed a significant increase in the stressed animals compared to the control animals in both males (two-way ANOVA $p = 1.87E-6$) and females (two-way ANOVA $p = 6.79E-6$). In all treatments, females had a significantly and nearly two-fold higher corticosterone level than males (t-test $p = 2.88E-8$; Figure 4.5A), in agreement with prior work showing elevated levels in females (L. A. Galea et al., 1997). Progesterone did not significantly influence plasma corticosterone levels.

Testosterone was significantly lower in males that had been stressed (two-way ANOVA $p = 0.011$; Figure 4.5B). Testosterone was borderline undetectable in females and there was no difference in the treatment groups in the females. As expected, the males had significantly higher levels of testosterone than females (t-test $p = 4.74E-8$), and progesterone had no effect in any treatment group or sex.

Progesterone was not significantly different in any male treatment group (Figure 4.5C). Further, in females, progesterone pre-treatment resulted in a significant decrease in the progesterone concentration (Two-way ANOVA $p = 0.046$), while stress significantly increased progesterone levels (two-way ANOVA $p = 0.0011$). As expected, the females had significantly higher progesterone levels than the males (t-test $p = 2.42E-10$).

Progesterone levels return to baseline approximately 12 hours after micronized progesterone is orally ingested in humans (de Lignieres, 1999). Our animals were given their last dose of progesterone approximately 22 hours before the probe trials began, and therefore the reduction in progesterone levels may represent a feedback inhibition response of endogenous production in response to exogenous administration (Dagklis, Ravanos, Makedou, Kourtis, & Rousso, 2015).

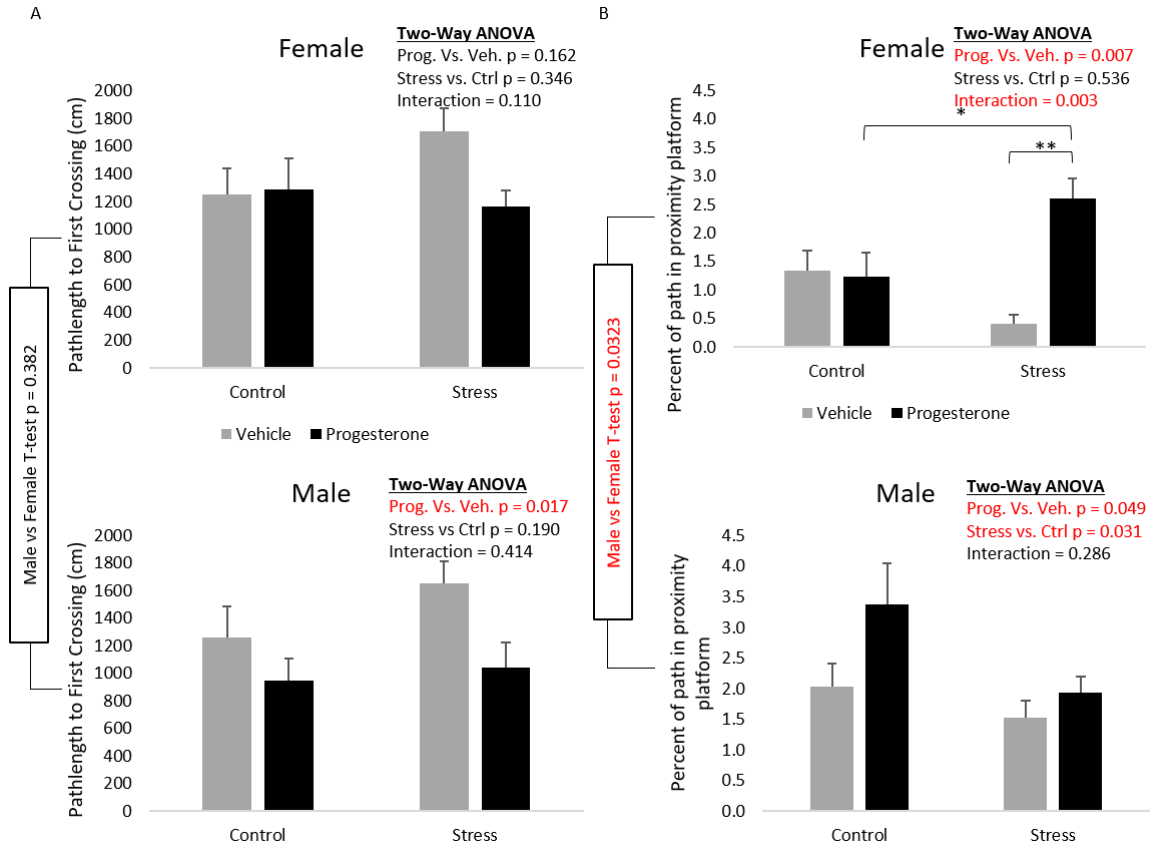


Figure 4.4. Distance during probe trial.

Distance traveled to first crossing (A). The males dosed with progesterone had a significantly shorter pathlength than those given the vehicle. The percent of distance traveled in proximity platform (B). This indicated that both males and females given progesterone travelled more in the proximity platform area than the vehicle in the stress condition. Within females, this was seen mostly with progesterone-dosed, stressed animals. In males, stress significantly reduced, and progesterone significantly increased, percent of path in the proximity platform area. Error bars are standard error. The box to the left of the graphs shows the heteroscedastic T-test results between the males and females. Red values represent significance. Progesterone (Prog.); vehicle (Veh.); control (Ctrl).

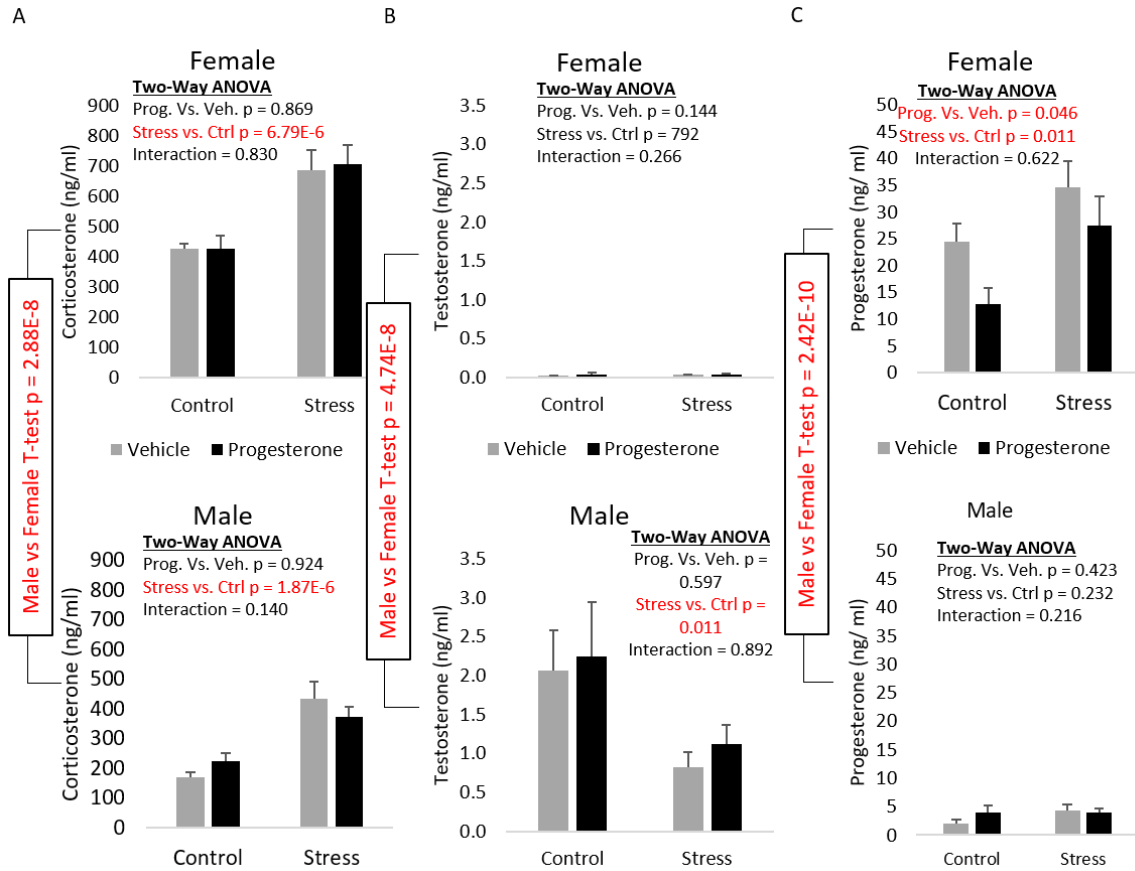


Figure 4.5. Hormone concentrations from trunk plasma.

LC-MS/MS found the trunk plasma concentrations of corticosterone (A); testosterone (B); and progesterone (C). Vehicle (Veh); progesterone (Prog.); control (Ctrl). Red text represents significance.

4.4.3 Immunohistochemistry

Sagittal sections containing the hippocampus from post-fixed rat brain hemispheres were examined immunohistochemically for Iba1 and Mbp expression. Some subjects were removed due to poor tissue quality (29 animals were removed: 7 MPS, 3 FPS, 2 MVS, 4 FVS, 4 MPC, 1 FPC, 5 MVC, 3 FVC). These are indicated in Supplemental data 1. Using a semiquantitative analysis, the average signal intensity of Iba1 (microglia marker), Mbp (myelin marker), and their overlap in the alveus, stratum oriens, pyramidal layer, and stratum radiatum of hippocampal CA1 (Figure 4.6- example of regions of interest) were determined.

Iba1 thresholded signal in the stratum oriens was not different between males and females. In males, progesterone pre-treatment significantly increased Iba1 signal ($p = 0.007$; two-way ANOVA) and stress had no significant effect (Figure 4.7; Table 4.1). Within the females, there was a significant interaction between progesterone and stress (two-way ANOVA interaction $p = 0.021$) with both stress and progesterone increasing Iba1, while in the presence of stress, progesterone appeared to suppress Iba1 signal. The differences in Iba1 expression can be seen visually in the females (Figure 4.7B; left: vehicle-dosed, stress; right: progesterone-dosed, stress) and males (Figure 4.7C; left: vehicle-dosed, control; right: progesterone-dosed, control).

While the Mbp did not show any effects based on the treatment groups (Table 4.1), we did find a significant difference between the sexes in stratum oriens (t-test $p = 0.0179$), pyramidal layer (t-test $p = 0.0170$), and the stratum radiatum (t-test $p = 0.0157$), with the females consistently having higher levels.

Finally, we also examined the thresholded signal for the overlap of myelin and microglia during immunohistochemistry. While no differences were found in the stratum radiatum, the other 3 regions showed significant changes. In the alveus, there was no effect in the females, but there was a significant increase in the overlap in the male, progesterone-dosed animals compared (Figure 4.8D) to vehicle (Figure 4.8E) counterparts (two-way ANOVA $p = 0.049$; Figure 4.8A). In the stratum oriens, the females showed significantly increased overlap with either stress (Bonferroni $p = 0.046$; Figure 4.8B) or progesterone (Bonferroni $p = 0.029$), but in the presence of stress, progesterone appeared to reduce this response. In the pyramidal layer, females showed significantly higher

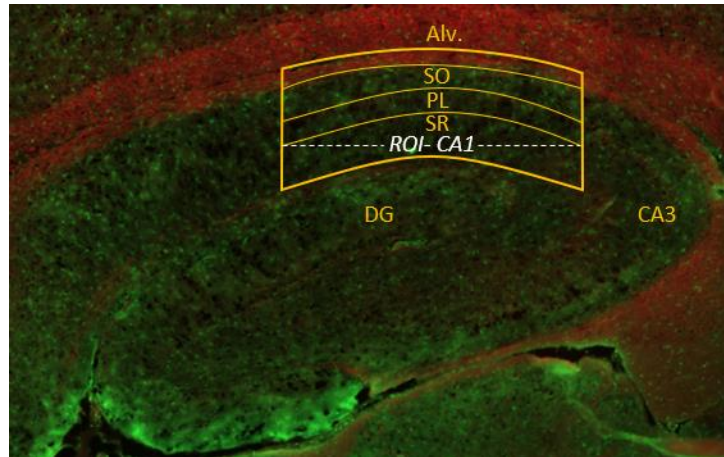


Figure 4.6. Example of hippocampal section used for IHC.

Immunohistochemistry section of the hippocampus stained for myelin basic protein (Mbp- red) and ionized calcium binding adaptor molecule 1 (Iba1- green). The different areas measured are surrounded in gold and includes alveus (Alv), stratum oriens (SO), pyramidal layer (PL), and the stratum radiatum (SR).

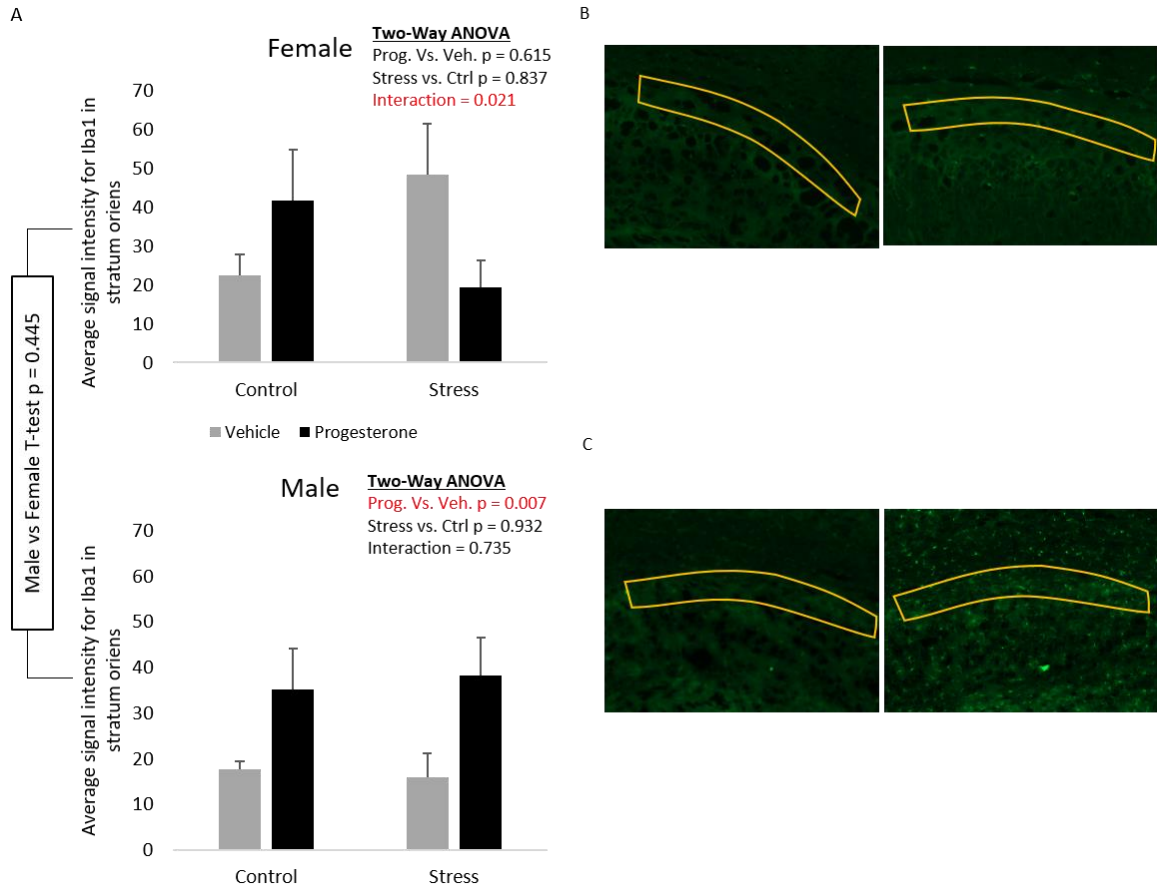


Figure 4.7. Iba1 expression changes in stratum oriens.

Iba1 expression was measured in the stratum oriens. The significant changes are shown in A. Two representative female stratum oriens; vehicle-stressed female (left); progesterone-stressed (right; B). Two representative male stratum oriens; vehicle-control (left); progesterone-control (right; C). Vehicle (Veh); progesterone (Prog.); control (Ctrl). Red text represents significance.

Table 4.1. ANOVA values for IHC Analysis

The males and females were analyzed separately. The alveus, stratum oriens, pyramidal layer, and stratum radiatum were analyzed for the average signal intensity of Iba1 and Mbp after thresholding, and the overlap of these signals. Two-way ANOVAs were used for drug treatment (progesterone [Prog.] and vehicle [Veh.]) and stress condition (stress or control [Ctrl]), and p-value for these results and their interaction are recorded. The final column shows the results for a heteroscedastic t-test between males and females. Red values are used for significant p-values.

	ANOVA p	Female			Male			Male vs. Female
		Prog. vs Veh.	Stress vs. Ctrl	Intrxn	Prog. vs Veh.	Stress vs. Ctrl	Intrxn	T-Test
Iba1	Alveus	0.983	0.297	0.444	0.075	0.998	0.128	0.129
	Stratum Oriens	<i>See Fig. 7</i>						
	Pyramidal Layer	0.648	0.413	0.132	0.085	0.7	0.842	0.0387
	Stratum Radiatum	0.443	0.129	0.272	0.078	0.340	0.320	0.681
Mbp	Alveus	0.189	0.571	0.708	0.157	0.564	0.236	0.417
	Stratum Oriens	0.991	0.268	0.057	0.335	0.509	0.154	0.0179
	Pyramidal Layer	0.341	0.839	0.059	0.132	0.226	0.533	0.0170
	Stratum Radiatum	0.879	0.204	0.407	0.412	0.594	0.708	0.0157
Overlap	Alveus	<i>See Fig. 8A</i>						
	Stratum Oriens	<i>See Fig. 8B</i>						
	Pyramidal Layer	<i>See Fig. 8C</i>						
	Stratum Radiatum	0.700	0.444	0.188	0.901	0.307	0.475	0.0522

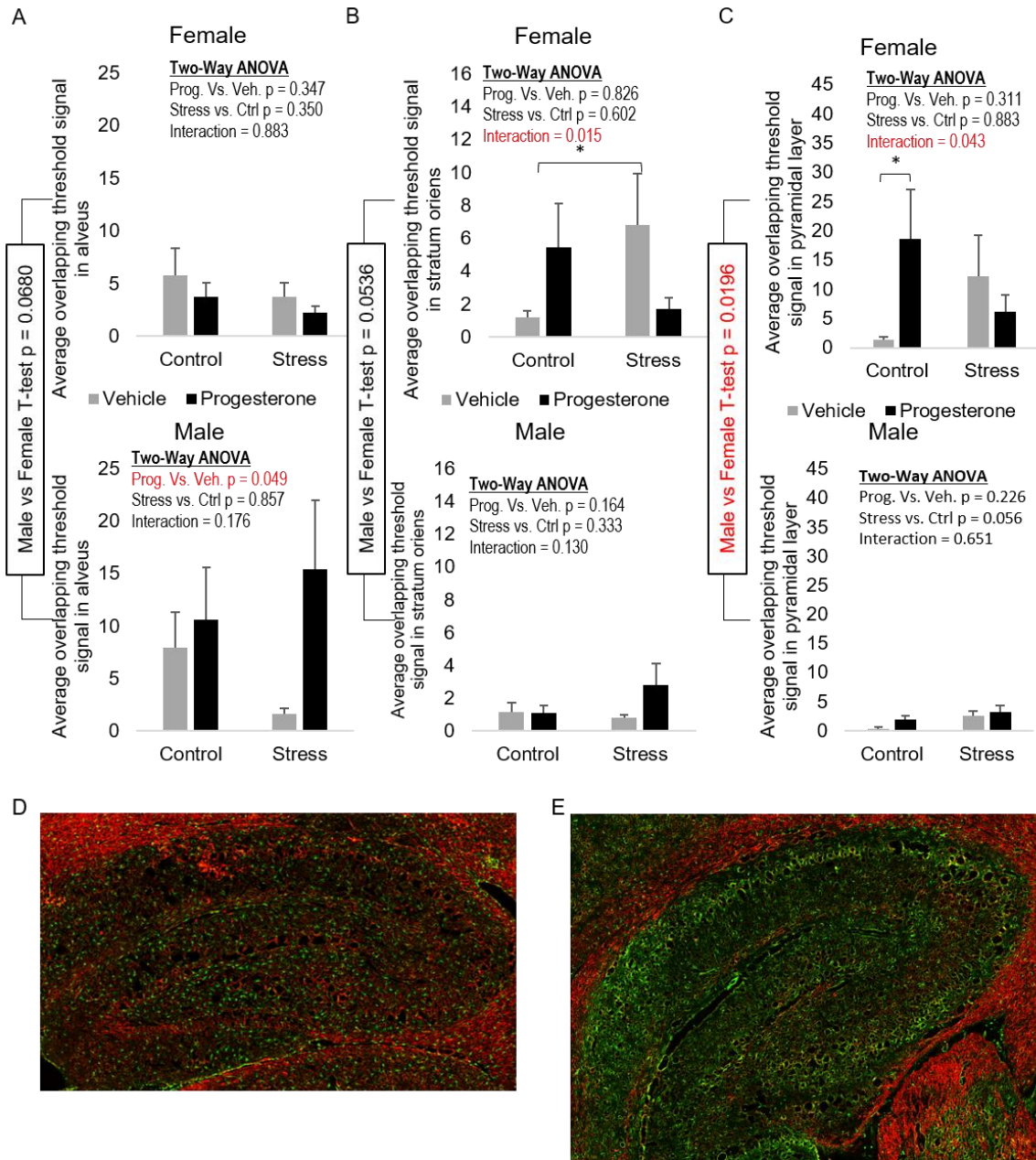


Figure 4.8. Mean signal for overlapping Iba1 and Mbp.

The overlapping signal for Iba1 and Mbp were determined and analyzed for the alveus (A), stratum oriens (B), and the pyramidal layer (C). Representative IHC showing Iba1 (green) Mbp (red) staining, and the overlap appearing as yellow; progesterone-stress male (left); vehicle-stress male (right). Vehicle (Veh); progesterone (Prog.); control (Ctrl). Red text represents significance.

overlap than males (t-test $p = 0.0196$; Figure 4.8C), and in the control condition, progesterone significantly increased that overlap.

4.4.4 Western Blot

Approximately 1/3 of the hippocampus from the frozen brain hemispheres of the 83 animals were homogenized and standardized to equal protein concentration. Sixteen of these samples had protein concentrations too low to meet the $1.5 \mu\text{g}/\mu\text{l}$ concentration and were not processed further (Iba1- 17 samples removed: 5 MPS, 3 MVS, 1 FVS, 3 MPC, 1 FPC, 4 MVC; Mbp- 15 samples: 5 MPS, 3 MVS, 1 FVS, 3 MPC, 3MVC; Sgk1- 21 samples: 5 MPS, 1 FPS, 3 MVS, 2 FVS, 3 MPC, 2 FPV, 3MVC, 2 FVC). The remaining samples were prepared for Western blots. Iba1 (Figure 4.9B), Mbp (Figure 4.9D), and Sgk1 (normalized to address significant cohort effect, Figure 4.9F) were all normalized with the housekeeping protein, Sodium-Potassium ATPase (NKA). Iba1 was significantly higher in females (t-test $p = 0.0197$), but not significantly affected by any treatment in females. In males, there was a significant decrease with progesterone in the control condition (Bonferroni $p = 2.43\text{E-}3$), and a significant increase in Iba1 with progesterone in the stress condition (Bonferroni $p = 0.006$). There was also a significant increase in Iba1 in males between the control and stress conditions (Bonferroni $p = 0.015$; Figure 4.9A). The Mbp (Figure 4.9C) and Sgk1 (normalized; Figure 4.9E) showed no significant differences with sex, progesterone, or stress.

4.4.5 Real Time-PCR

Twenty animals were removed from the Sgk1 mRNA analysis because their hippocampi were improperly stored (18 samples removed: 6 MPS, 4 MVS, 3 MPC, 5 MVC; Supplemental Data 4.1). Using the Genomics Core Laboratory at the University of Kentucky, the remaining RNA samples' quality was determined using the RNA integrity numbers (RINs) (Table 4.2; Supplementary Table 4.1). While there was no significant sex- or group- effect, there was a cohort effect (one-way ANOVA female $p = 6.45\text{e-}11$; male $p = 2.98\text{E-}8$) for both sexes. However, because there was no significant correlation between RIN and the RT-PCR's $\Delta\Delta\text{-CT}$, we did not correct the cohort effect.

Using the comparative method of qRT-PCR, we compared the amount of serum and glucocorticoid-regulated kinase (Sgk1) to GAPDH. After removing the samples that did not have Sgk1 expression (1 MVS, 1 MPC, 1 MVC), $N = 65$ samples (7 MPS, 10 FPS,

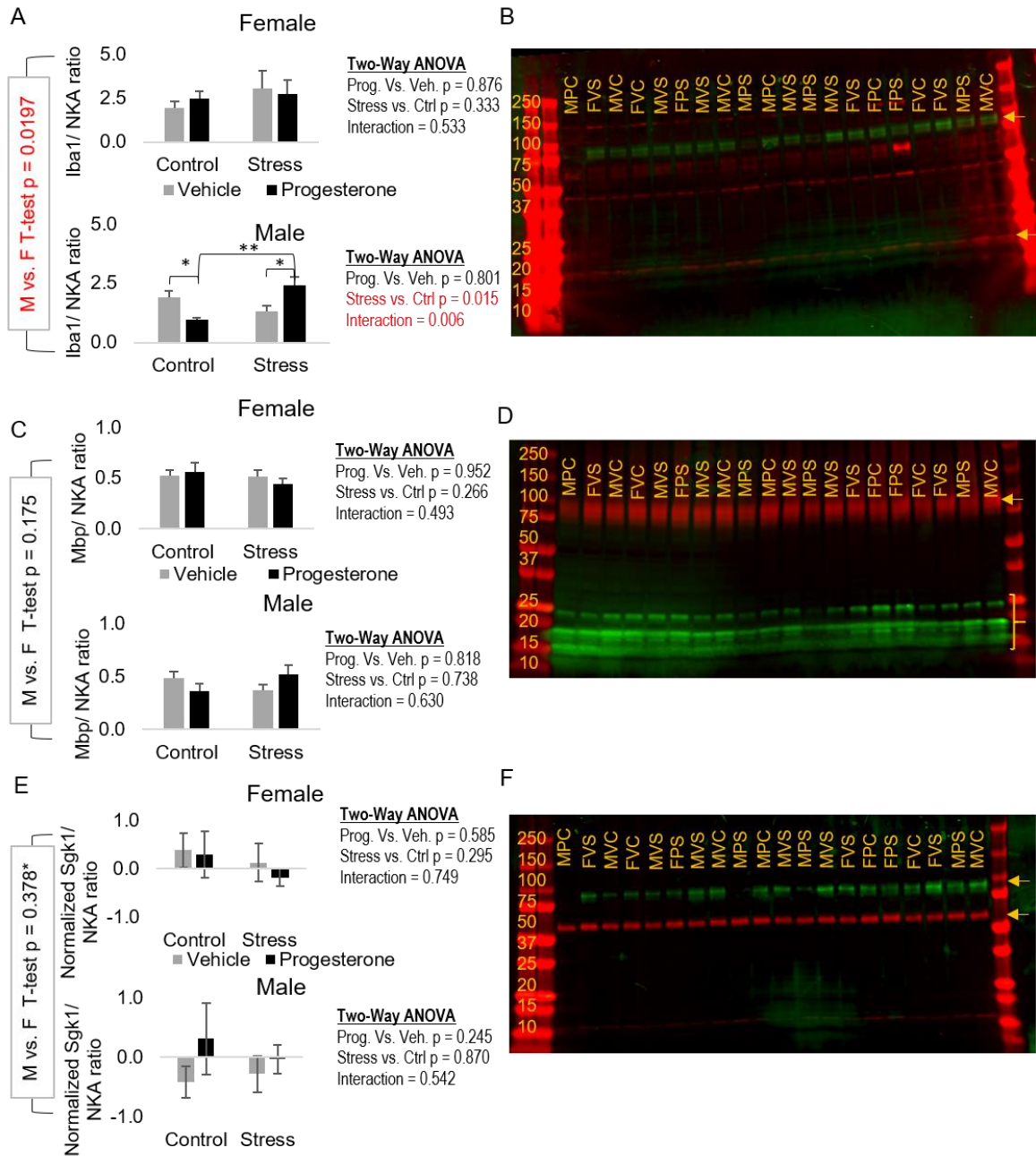


Figure 4.9. Western blot analysis.

The ratio between the protein of interest (Iba1 [A], Mbp [C], and Sgk1 [E]) and sodium-potassium ATPase (NKA) were measured and analyzed. The corresponding Western blots show samples and their brightness. Iba1 appears in red (17 kDa) and NKA in green (predicted: 113 kDa; appear ~ 80 kDa) (B); Mbp appears in green (21.5, 18.5, 17, and 14 kDa) and NKA in red (D); Sgk1 appears in red (55 kDa) and NKA in green (F). Red text represents significance. Male (M); female (F); vehicle (Veh, V); progesterone (Prog., P); control (Ctrl, C); stress (S).

Table 4.2. RIN values by sex and group

Columns: Sex- Male or female; Group- The treatment group; RIN Avg. (\pm SEM)- the average RIN and standard deviation for each group; RIN range- range of RINs for each group. Progesterone-stressed (PS); vehicle-stressed (VS); progesterone-control (PC); and vehicle-control (VC).

Sex	Group	RIN Avg. (\pm SEM)	RIN Range
Male	PS	9.61 \pm 0.14	9.1 – 10.0
	VS	9.61 \pm 0.15	9.3 – 10.0
	PU	9.64 \pm 0.12	8.9 – 10.0
	VU	9.59 \pm 0.15	9.1 – 10.0
Female	PS	9.75 \pm 0.11	9.2 – 10.0
	VS	9.62 \pm 0.15	9.0 – 10.0
	PU	9.68 \pm 0.11	9.2 – 10.0
	VU	9.72 \pm 0.12	9.1 – 10.0

8 MVS, 8 FVS, 8 MPC, 7 FPC, 7 MVC, 10 FVC) were analyzed. The $\Delta\Delta$ -cycle threshold (CT), which is equivalent to a \log_2 fold change (L2FC), was calculated. There was a significant increase in Sgk1 in males (t-test $p = 0.0439$) and males showed a stress-induced increase in Sgk1 (Bonferroni $p = 4.96E-4$; Figure 4.10) that was reduced by progesterone pre-treatment (Bonferroni $p = 0.001$). In females, there was no significant effect of stress or progesterone treatment on Sgk1 mRNA levels.

4.5 Discussion

In this paper, we examine differences between male and female subjects exposed to an acute stress and hypothesized that progesterone pretreatment would blunt stress effects. Prior work has shown that progesterone can disrupt glucocorticoid signaling (Brinton et al., 2008; Cadepond, Ulmann, & Baulieu, 1997; Graham & Clarke, 1997; Irwin et al., 2015; M. Singh & Su, 2013; Wang, Johnston, Ball, & Brinton, 2005) and stress (Childs et al., 2010; Kalil, Leite, Carvalho-Lima, & Anselmo-Franci, 2013; Sanchez et al., 2008), although whether progesterone could work as a pretreatment, and whether action involves suppression of the HPA-axis, remains unclear. We measured for a potential influence at four canonical ‘decision’ points along the stress pathway in males and females: 1) the perception of stress (quantified by struggles during restraint); 2) the glucocorticoid secretion in response to stress (quantified with blood corticosterone assays); 3) the behavioral consequences of stress (quantified by Morris Water Maze); and 4) the molecular response to stress-induced glucocorticoid exposure (quantified by measuring the mRNA for immediate early gene serum-and-glucocorticoid kinase 1 [Sgk1]). Finally, we also quantified the degree of overlap between myelin basic protein (Mbp- a marker of myelin and myelin fragments) and ionized calcium binding adapter protein 1 (Iba1- a marker for macrophages including microglia) expression in hippocampal subregions, as aging-related changes in the degree of overlap between these two have been reported, but whether acute stress can induce similar changes remains unclear.

Overall, we found multiple baseline differences between male and female, including performance in MWM training and probe trials, number of struggles, blood hormone levels, Sgk1 mRNA expression, and Iba1 protein expression. Thus, highlighting the importance of including female subjects in research on these fundamental measures. In both male and female animals, progesterone did not influence pre-stress water maze

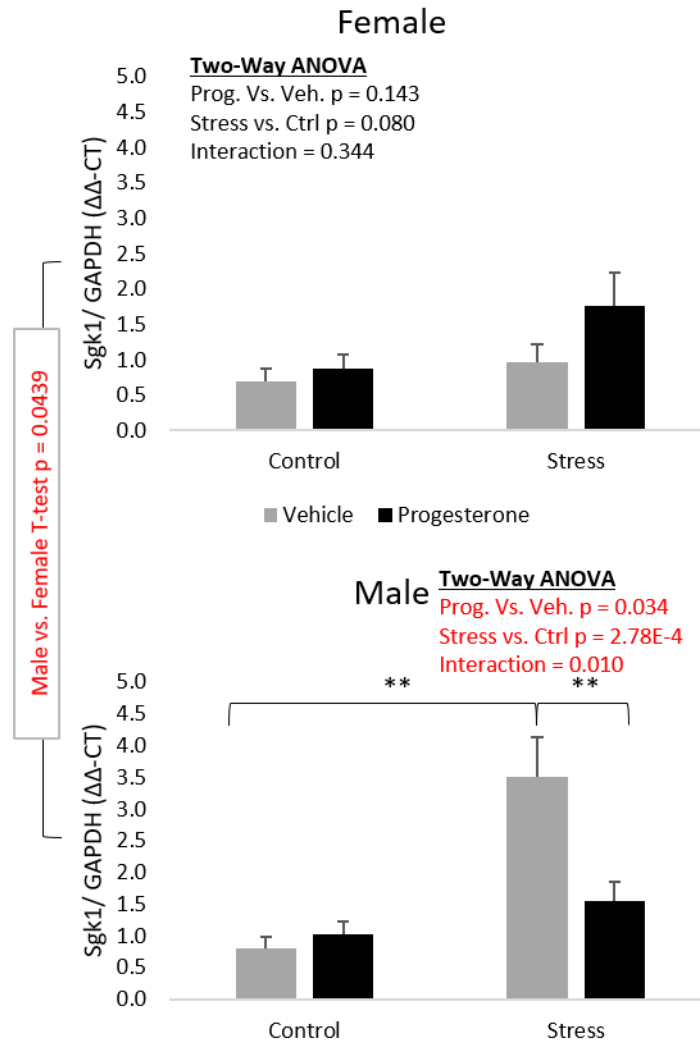


Figure 4.10. Sgk1 mRNA expression

Using RT-PCT, the expression level of Sgk1 and GAPDH (housekeeping gene) were quantified, and the $\Delta\Delta$ -cycle threshold (CT) was calculated. Vehicle (Veh); progesterone (Prog); control (Ctrl); ** $p \leq 0.001$.

training (Figure 4.1), number of struggles during restraint (the perception of stress- Figure 4.2), stress-induced swim speed increase (Figure 4.3), or stress-induced corticosterone secretion increase (Figure 4.5A). However, in both males and females, progesterone improved water maze probe trial performance (Figure 4.4), suggesting that progesterone's actions are downstream of stress perception and the resulting HPA-axis activation. In males, the well-recognized stress-induced *Sgk1* mRNA elevations were significantly attenuated by progesterone pretreatment. However, in females, there was a markedly different profile- *Sgk1* levels were not increased by stress or progesterone, and this may indicate that the significantly higher endogenous progesterone levels in females (Figure 4.5C) could natively disrupt this well-characterized response.

Progesterone treatment had no effect on water maze training in male or female animals (Figure 4.1). Although female learning curves were significantly less-steep than those in males, both males and females showed significant improvement over training as in prior work (Beiko, Lander, Hampson, Boon, & Cain, 2004). During the three-hour restraint, females struggled significantly less than male animals, while progesterone pretreatment had no effect (Figure 4.2) on the number of struggles. Both male and female animals that had been restrained showed increased swim velocities during the probe trial compared to the controls (Figure 4.3). This was not influenced by progesterone pretreatment, but increased swim speed after stress did provide rationale for using the pathlengths rather than latencies for water maze analysis.

In the probe trial, males showed a significantly higher proportional occupancy based on pathlength of the goal area than females (Figure 4.4B), as seen previously (Beiko et al., 2004). In both males and females, restraint resulted in a significant behavioral deficit (Diamond, Park, Heman, & Rose, 1999; Gaikwad et al., 2011; C. R. Park, Zoladz, Conrad, Fleshner, & Diamond, 2008; Sandi et al., 2005; Snihur, Hampson, & Cain, 2008; Wong et al., 2007). However, there have been reports of improved performance after stress in females (Conrad et al., 2004; Lipatova, Campolattaro, Dixon, & Durak, 2018). This difference might be explained by the differences in restraint duration (one hour, and 30 minutes respectively compared to the three hours used in this study), as well as in the behavioral assessment (spontaneous Y maze alterations, and open field tower maze, respectively, compared to the Morris water maze used here). Position in the estrous cycle

was not assessed here but is reported to influence the stress response in female rats (Conrad et al., 2004; Lovick, 2012). Additionally, the magnitude of the stress effect on behavior appeared greater in females (Figure 4.4B), in keeping with prior reports of sexual dimorphism in the acute stress response (reviewed in (Rosenfeld & Trainor, 2014)). In males, progesterone pretreatment significantly increased platform area occupancy for both control and stress groups, while in females, progesterone was associated with significant improvement selective in female stress group only.

Corticosterone levels were significantly higher in females than males (Figure 4.5A), as in prior work (L. A. Galea et al., 1997; Roof & Stein, 1999). In both males and females, restraint induced significant increases (Campbell & Ehlert, 2012; Gjerstad et al., 2018) that were unaffected by progesterone pretreatment. Although glucocorticoids were originally named for their role in promoting circulating glucose levels, they have since been determined to have key roles in inflammation, development, fluid homeostasis, arousal, and cognition (Baschant & Tuckermann, 2010; Erickson, Drevets, & Schulkin, 2003; Kuo, McQueen, Chen, & Wang, 2015; Oitzl, Champagne, van der Veen, & de Kloet, 2010; Tasker, 2006). The severity of acute stress exposure is positively correlated with blood glucocorticoid concentration (Keim & Sigg, 1976) and the corticosterone levels reported here for males (~400 ng/ml) are consistent with a moderate-high-stress (Kalil et al., 2013), while the female levels in both control and stress conditions were nearly twice that of the males.

In male subjects, Sgk1 mRNA (Figure 4.10), but not protein (Figure 4.9E), was significantly increased by acute restraint, and this response was significantly reduced in males pretreated with progesterone. However, in females, there was no significant effect of stress or progesterone on Sgk1 protein or mRNA levels. The mRNA versus protein effect in males is entirely consistent with prior studies on immediate early genes such as Sgk1, whose mRNA transcription is upregulated much earlier than the protein is translated (Anacker et al., 2013). At the molecular level, serum-and-glucocorticoid-kinase-1 (Sgk1) is well established as an immediate early gene whose mRNA levels increase rapidly in response to glucocorticoid signaling, and can be considered a molecular marker of glucocorticoid action (Buechel et al., 2014; C. Y. Chen et al., 2016; Porter et al., 2012). It is important to note that in normal physiologic conditions, hippocampal Sgk1 is positively

correlated with spatial memory (J. C. Park et al., 2021), suggesting that complete blockade of Sgk1 would be deleterious to normal function, and a recent study found when Sgk1 levels are overexpressed in female APP/PS1 mice, it led to increased spatial memory and inhibited protein markers of Alzheimer's disease (Lian et al., 2020). Further, prior work reported stress-induced Sgk1 mRNA upregulation in females (Roszkowski et al., 2016), although that work was done in mice and used shorter stress durations (30 min restraint). Here, the progesterone associated reduction of Sgk1 mRNA without altering stress-induced glucocorticoid levels suggests that progesterone disrupts stress-driven gene expression. Finally, Sgk1 mRNA has been shown to increase not only with stress, but also aging (Blalock et al., 2003; Blalock et al., 2010; Buechel et al., 2014; K. C. Chen et al., 2013; Hinds et al., 2017; Kadish et al., 2009; Porter et al., 2012; Rowe et al., 2007), similar to other studies that have found compelling parallels between the brain's response to stress and its response to aging (Cesari et al., 2013; Garrido, 2011; Landfield et al., 2007; Lavretsky & Newhouse, 2012; Porter & Landfield, 1998; Sapolsky, 1999)

Iba1/ Mbp immunohistochemical staining (Figure 4.8) showed significant increases with stress in the stratum oriens (but not stratum radiatum or the pyramidal layer) in female and no effect in the males. Recent work has shown that aging impacts the levels of Iba1 and Mbp, with their overlap indicating increased myelin fragment uptake by microglia with age (Safaiyan et al., 2016). Further, Western blot analysis did not indicate a difference in female Iba1 levels (Figure 4.9A, B), suggesting that microglia/ macrophages may have migrated to the area, rather than increased synthesis or reduced degradation of extant protein. Thus, stress may recapitulate an aging-like microglial myelin fragment burden, albeit restricted to a female hippocampal subregion. Interestingly, in the male alveus and the female pyramidal layer, progesterone itself increased this Iba1/ Mbp overlap (Figure 4.8). Western blots (Figure 4.9) showed no changes in Mbp expression in any sex or treatment condition. In males, Iba1 expression was lower than in females and progesterone showed opposing effects, increasing Iba1 expression in stressed animals and reducing it in controls. Females also struggled significantly less than males during restraint (Figure 4.2) yet showed higher corticosterone levels and a more dramatic stress-induced water maze deficit. Taken together, these findings indicate that females may more

be more vulnerable to the objective helplessness of this experimental design (Maier & Seligman, 2016).

Progesterone alleviated male and female stress-induced spatial memory deficits, supporting previously findings (DIAZ-BRUIKE et al., 2010), although, as in prior work, it does not enhance spatial memory on its own in both sexes (Harburger, Pechenino, Saadi, & Frick, 2008). Our work suggests that progesterone's anti-stress effects appear downstream of stress perception and HPA-activation and may involve disruption of glucocorticoid signaling. Candidate mechanisms may include: antagonized glucocorticoid receptor binding, inhibited 11 β -hydroxysteroid dehydrogenase 1 (which converts glucocorticoids from their inactive to active form) activity (Chapman, Holmes, & Seckl, 2013); specific action at individual GC target genes, and action through progesterone's own signaling cascade. In addition, progesterone is an antagonist at the mineralocorticoid receptors, and could disrupt glucocorticoids' basal mineralocorticoid occupancy. Both glucocorticoids and progesterone have similar affinities for the receptor (Baker & Katsu, 2020).

The increased progesterone levels found in females (L. A. Galea et al., 1997) may also result in elevated levels of its metabolite, allopregnanolone, which has anxiolytic properties and is increased with psychological stress (Purdy, Morrow, Moore, & Paul, 1991; Wirth, 2011). However, anxiolytic agents are classically associated with suppression of HPA-axis corticosterone secretion (Urban, Van de Kar, Lorens, & Bethea, 1986), females had higher corticosterone levels, and progesterone pretreatment did not influence that level. Further, the half-lives of progesterone (3.32 ± 1.35 hours in humans) (McAuley, Kroboth, & Kroboth, 1996) and allopregnanolone (4 hours in rodents) (Irwin et al., 2015) suggest neither exogenous progesterone nor its potential exogenously-derived active metabolite were on-board during restraint, while the lowered progesterone levels in progesterone-treated animals were likely due to negative feedback at the hypothalamus-pituitary-gonadal (HPG)-axis (Dagklis et al., 2015). In males, a similar HPG-axis feedback via corticosterone may also explain stress-induced testosterone decreases (Figure 4.5B) (Whirledge & Cidlowski, 2010). Finally, glucocorticoid blood levels particularly in stressed female subjects, were reflective of levels seen during severe stress, a condition in which glucocorticoids can become neurotoxic with chronic exposure (Uno et al., 1994),

with concomitant decay of RNA quality. Further, recent work has determined that the glucocorticoid receptor-mediated decay (GMD) pathway (Cho et al., 2015; O. H. Park et al., 2016) can promote the degradation of select mRNA targets. In our hands, RNA integrity from hippocampal tissue of these subjects was unaffected by acute stress or progesterone in either sex (Table 4.2), although future studies on chronic stress or long-term glucocorticoid exposure should include assays of RNA quality.

Regarding possible mechanisms, while progesterone is known to be protective against the stress response (Childs et al., 2010; Kalil et al., 2013; Sanchez et al., 2008), our data indicates this effect is not exerted at the level of the HPA-axis. This also suggests that a mechanism whereby allopregnanolone, progesterone's anxiolytic metabolite, acts upon the GABA_A receptors to inhibit the hypothalamus from releasing the corticotrophin-releasing hormone (Wirth, 2011) may also be unlikely. Additionally, because exogenous progesterone was metabolically cleared prior to stress exposure, proposed mechanisms in which progesterone disrupts signaling via contemporaneous mechanisms (e.g., receptor antagonism) are less likely. Instead, mechanisms where progesterone pretreatment alters elements of the glucocorticoid response pathway, for instance by downregulating glucocorticoid receptors (McDonnell, Shahbaz, Vegeto, & Goldman, 1994; Wen, Xu, Mais, Goldman, & McDonnell, 1994) or promoting the synthesis, availability or stability of the molecular 'gatekeepers' of glucocorticoid signaling (Timmermans et al., 2019), seems more feasible.

It is important to keep in mind that the rats were euthanized within 15 minutes of being released from restraint, and therefore measurements taken reflect a fairly acute state, and some effects, particularly at the protein level, may not have had sufficient time to develop. Further work examining longer time frames post stress may be useful. Additionally, despite *Sgk1*'s reputation as a glucocorticoid-responsive gene, it is also upregulated by other factors, and prior work has shown that, although glucocorticoids may be necessary for its rapid induction, they are not sufficient, and the response also requires adrenaline action through the beta-adrenergic pathway (Roszkowski et al., 2016). Finally, it may also be translationally relevant to examine the influence of progesterone treatment concomitant with, or after, stress exposure. It should be noted that the stress response is not simply sexually dimorphic, but also may be more variable in females depending on

their position in the estrous cycle (Lovick, 2012; ter Horst, Kentrop, de Kloet, & Oitzl, 2013; Wagenmaker & Moenter, 2017), and future work assessing female cycle status may also be an important consideration (L. A. M. Galea, Choleris, Albert, McCarthy, & Sohrabji, 2020; L. R. Miller et al., 2017).

In conclusion, this work strongly supports prior work that stress responses are sexually dimorphic, and this should be considered in developing intervention targets. To our knowledge, this is the first experiment to look at how progesterone pretreatment impacts the hippocampal expression of *Sgk1* after acute restraint stress, and whether myelin fragment burden in microglia is increased as a result. As in prior work, male rats showed behavioral deficits, increased corticosterone (Ishikawa, Hara, Ohdo, & Ogawa, 1992; Whirledge & Cidlowski, 2010) and increased hippocampal *Sgk1* mRNA (Hinds et al., 2017). Stress-induced behavioral and *Sgk1* changes, but not blood corticosterone levels, were blunted by progesterone pretreatment. The resistance to stress effects engendered by progesterone pretreatment is supported by prior work (DIAZ-BRUIKE et al., 2010; Harburger et al., 2008), and suggests that progesterone's actions are downstream of the HPA-axis. Although *Sgk1* is a reliable marker of glucocorticoid action in male hippocampus, this did not appear to be the case in female subjects, suggesting that the behavioral impact of stress in both sexes can either proceed through molecularly distinct pathways. Changes in *Mbp*/*Iba1* overlap measured by immunohistochemistry, combined with relative lack of protein-level changes in these molecules by Western blot, suggest redistribution of extant protein (e.g., through microglial migration and/or myelin fragment phagocytosis), rather than a change in synthesis. Finally, we determined that RNA quality is not significantly impacted by acute restraint stress.

CHAPTER 5. DISSERTATION DISCUSSIONS

5.1 Introduction

Both studies presented here investigate areas that have been overlooked historically. In transcriptional profiling studies, the sample's RNA can be impacted by various sources, which can negatively influence the measured gene expression. To prevent wasteful spending and use of time, determining RNA integrity numbers (RINs) can be determined for the samples to remove poor quality samples that would give erroneous transcriptional profiling results. While a few journals require disambiguated RINs to be published along with the data, most do not, and therefore most published data does not include individual RINs (Copoio et al., 2007; Gallego Romero et al., 2014; Jaffe et al., 2017; Opitz et al., 2010). Instead, often a range or average is given in their report. This is problematic because, as shown in Chapter 2, RINs impact the measured gene expression, even in control tissue, just as other commonly reported metavariabiles.

Meanwhile, there has been significantly less work on the female stress response and how the female hormone, progesterone, impacts both males' and females' behavioral and molecular responses. While the male stress response is well-defined (Anacker et al., 2013; Campbell & Ehlert, 2012; Diamond et al., 1999; Gaikwad et al., 2011; Gjerstad et al., 2018; Hinds et al., 2017; C. R. Park et al., 2008; Sandi et al., 2005), we found that there are sexually dimorphic characteristics in these responses using our stress model. In addition, our RIN study found a sex and age difference in the number of genes associated with RNA integrity. Specifically, aged male subjects appeared to have significantly more RIN-sensitive genes. This could indicate that older subjects are more likely to have a longer agonal state, and illness can be a physiological stressor. Therefore, stress could be exacerbating the effects of a disease on vulnerable pathways (note that although our control subjects had no evident neuropathology, other chronic diseases were not identified for all subjects and were likely present among subjects). To our knowledge, no one has investigated whether hormones play a role in the gene expression changes associated with poor RNA quality. This is of particular note since recent studies have found a glucocorticoid receptor-mediated decay (GMD) pathway (Cho et al., 2015; O. H. Park et al., 2016). While no one has investigated the prevalence of the GMD pathway in the brain, with the high levels of glucocorticoids and glucocorticoid receptors, it would be surprising

if glucocorticoids did not degrade RNA in the brain either through the GM or neurodegeneration associated with prolonged exposure. While RNase activity is primarily responsible for rRNA degradation, there has been no research into GMD's impact on rRNA.

Furthermore, even if GMD does not impact RIN scores, it likely still causes gene-specific degradation. The GMD relies on ligand binding to the glucocorticoid receptor before decay begins, indicating that any regulator of the HPA-axis or of glucocorticoids and their receptors may impact RNA degradation. While we showed that progesterone is not acting on the HPA-axis, that does not exclude the possibility of influencing glucocorticoid signaling. Though it is outside the scope of the current studies, the GMD pathway and its impact on RNA integrity would be an exciting topic for future research.

5.2 Declining RNA integrity in control autopsy brain tissue is robustly and asymmetrically associated with selective neuronal mRNA signal loss

5.2.1 Implications

Our study on the effects of RNA quality on microarray gene expression found that specific genes and pathways are more sensitive to RNA quality and that there is usually an exponential or sigmoidal shape describing the relationship between RIN and gene expression. We also propose a neuron-selective RNA degradation in control tissue that is consistent with selective mRNA damage primarily in the synapses; this effect shares characteristics with Alzheimer's disease (AD). In addition, we found that age and sex interact to influence gene sensitivity to RNA degradation. Each of these findings should motivate careful consideration of the way RINs are used, both as to quality control and as normalizing variables, in transcriptional profiling.

Relatively few studies have investigated the association between RNA quality and genes expression (Gallego Romero et al., 2014; Opitz et al., 2010), and RIN-associated genes appear to be tissue-dependent. Ours was the first study to determine specific genes and pathways in human, control prefrontal cortex (PFC) that are significantly impacted by RNA quality. This finding gives researchers particular genes that can be used as biomarkers for poor RNA quality, even when disambiguated RINs are not reported within the PFC. It also indicates that variations in RNA quality impact gene levels in the absence of any reported pathology. In addition, since these RIN-sensitive genes and their

associated pathways are more sensitive to RNA degradation, procedures that correct RIN in transcriptional datasets should use ‘gene-at-a-time’ rather than ‘sample-at-a-time’ correction strategies.

Current normalizing approaches for RIN, even if they use a ‘gene-at-a-time’ strategy to normalize gene expression based on RIN, also rely on narrow linear relationships. However, we discovered that many genes have an exponential or sigmoidal-shaped relationship with RNA quality during the study, which has several implications. The first is that if a gene is in a sample outside of the linear RIN range, a linear correction method improperly adjusts the mRNA’s value, leading to inaccurate data. Thus, a ceiling (and possibly a floor) effect on the relationship between RNA quality and gene expression exists. Second, the linear assumption regarding the relationship between gene expression and RIN does not appear to hold, and the data support an exponential or sigmoidal relationship. Third, this would result in the under-correction of gene expression in the linear range and over-correction of values outside the range. Essentially, if RINs are above 8.6 (in our hands), RIN has no statistically detectable effect. On the other end of the spectrum, at lower RINs, there reaches a point where RNA is so degraded that any additional damage does not appear to further impact gene expression measures and a RIN correction procedure would likely obfuscate an unreliable reading rather than rescue it.

Within the PFC, these RIN-sensitive genes mapped back to processes and cellular compartments associated with neuronal synapses. Synapses are an essential part of brain function; they are the primary points of electrochemical communication between neurons and are thought to represent the majority of the information processing power in the brain. Further, mRNA, ribosomes, and mitochondria are subcellularly localized to synapses. If these mRNA species are more sensitive to RNA degradation, then when triggered, RNA degradation would affect neurons more quickly than glial cells. This finding is significant since many of these genes are also downregulated in AD. Our data indicate the effects of AD exacerbate the effects found with RNA degradation or vice versa. Prior work found that when the RIN effect is controlled for, in control versus AD transcriptional profiling, the entire set of downregulated AD genes that have been robustly reported in multiple prior studies become non-significant (J. A. Miller et al., 2017). The authors observed that RINs were significantly lower in AD than control samples and concluded that it was due

to other influences, instead of *in vivo* RNA degradation. RIN may be confounded with AD in this situation, and normalization should be omitted (or performed within rather than across conditions). Based on the lack of correlation between RIN and post-mortem interval in the present work, RNA degradation may occur *in vivo*, not only post-mortem. In addition, if RNA degradation is more likely to impact neurons' synapses, which is exacerbated by AD, neurons could be more vulnerable because their synapse-selective mRNA degradation results in neuronal dysfunction that increases the risk of cell death.

Interestingly, there were not any consistent correlations between the RINs and other metavariation measurements. While it is commonly assumed that there is a significant correlation between RNA quality and the post-mortem interval (PMI), we along with others have not found such a connection (Birdsill et al., 2011; Ervin et al., 2007; Johnson et al., 1986; Stan et al., 2006) at the post-mortem intervals tested. However, a study from the University of Maryland found that brain RNA's quality does not significantly drop until after 36 hours post-mortem (White et al., 2018). Since most of our subjects had PMIs less than 36 hours, it could be that the post-mortem intervals here were not sufficient to show a detectable response. When we correlated age to RIN scores, we also did not find any consistently significant association. It was not until we investigated the number of RIN-sensitive genes with sex or age that we found a significant difference between the metavariation measurements. When tested at estimated statistically equivalent power, there was a trend that females had more RIN-sensitive genes than males. Fascinatingly, it was when we split the groups into young (16 – 50 years old) and aged (> 50 years old) that we found a surprising difference in the number of significant genes in males and females. Young females appeared more sensitive to RNA degradation than their aged counterparts, while aged males were more sensitive than young males. This sex difference suggests that there may be hormonal cause for both of these. In women, sex hormones dramatically decrease during menopause, and men decrease testosterone with age (Moffat, 2005). Thus, testosterone may be protective, while estrogen or progesterone may confer vulnerability. These hormones and their downstream effects may be regulating aspects of the RNA degradation pathways, though no relationship has been established in the literature. In addition, having sexually dimorphic RIN-sensitivity may indicate that RIN correction measures need to be corrected separately, depending on the subjects' ages and the

correction technique being implemented. Again, this points to the importance of reporting disambiguated meta-variables when possible, although patient anonymity must also be maintained in human studies.

These findings could have impacts on the way that brain tissue transcriptional profiling, extending further than microarray analysis into RNA-seq. RNA-seq relies on the alignment of counted RNA to identify and quantify mRNA species and has a broader dynamic range and thus may be more sensitive to RNA degradation. Since transcriptional profiling is a standard tool used to quantify relative gene expression, our work suggests reasonable thresholds above which RIN correction is not necessary, calls into question the appropriateness of regression techniques, and suggests that employing corrections when the factor upon which the corrections are based is confounded with treatment conditions under study should be avoided.

5.2.2 Future Directions

While our study was able to determine exciting findings, our work brought to light several more. For one, using a metadata analysis study limited us to already published work and its data. Because of this, we could not answer some questions, such as what additional information can be found with profiles spanning the entire RIN scale, how the rate of RNA degradation differs among specific genes and pathways, and what pre-mortem conditions may be contributing to variability in RIN. Other questions for future work include investigating the mechanism of age's impact on RIN-sensitivity and determining if different known causes of declining RIN (heat, time, pH, oxidation) result in similar pathways of transcriptional effect.

Our study relied on others' published works, which meant we were restricted to their published RIN scores. Poor RIN scores were probably not included in most datasets since RINs are typically used to establish a cutoff value before running a profile. Our data indicated that RINs of 6.7 – 7 represented a lower range below which gene expression reached a minimum and was no longer correlated with RIN (therefore could not be rescued with a RIN-based correction). However, scores from throughout the entire RIN range (1 - 10) would be needed to fully understand the dynamics of RIN's relationship to gene expression. Ideally, instead of using published data, this experiment would be done by a single lab to control tissue collection handling and storage conditions impacting RINs

(Gallego Romero et al., 2014; Jia et al., 2021), compared to variation collected by sampling from a large brain bank such as that at Sanders-Brown Center on Aging. By encompassing as much of the RIN in similarly handled, stored, and prepared tissue, one could see a more complete picture of the relationship between gene expression and RIN. In addition, it would clarify when most RINs were too low to be saved with correction. The range in which genes are too degraded to be saved by correction may depend on the gene. There is evidence that different pathways impacting mRNA quality are affected at different rates in post-mortem mice and zebrafish (Pozhitkov et al., 2017). If this is the case, there could be a cascading effect, which would also explain the different templates associated with the genes and RIN scores.

RNA-Seq is still relatively new, and its bioinformatic pipeline has not been standardized yet (Simoneau et al., 2021). Because of this, a retrospective analysis of RNA-seq data was not feasible, and our study focused instead on the effects of RNA-degradation in the older and more standardized microarray technology. However, since RNA-seq is not limited by low detection thresholds or saturation, it can more reliably find splice variants and mutations (Sirbu et al., 2012; van der Kloet et al., 2020). RNA-Seq is becoming more popular. Since this technology depends on counting the number of mRNA species sequenced by synthesis (compared to oligonucleotide microarrays used for this study), we hypothesize that RNA-seq based mRNA species quantification would be more sensitive to RIN numbers.

Other microarray technologies may have different sensitivities to RINs. While Affymetrix uses the oligonucleotide microarrays, Illumina Inc. uses bead-based fiber optic microarrays and Agilent Technologies microfabricated arrays using ink-jet pumps (Blanchard et al., 1996; Walt, 2000). Our study did not include datasets across platforms because we wanted to reduce platform-based variability. Affymetrix-type arrays use a highly standardized protocol, and data is shared publicly at a sufficiently ‘raw’ level that researchers can reprocess that raw data (as done in Chapter 2) to ensure that the resulting data is as homogeneously handled as possible. However, differences in procedures prior to RNA extraction could impact results. If so, then this would increase variability and reduce agreement among independent data sets. Thus, the common set of RIN-sensitive genes among multiple independent datasets may be higher than that found in this work.

Another area that needs to be investigated is the impact of age and sex on RIN-sensitive genes. While neither age nor sex appeared to correlate with RIN, when the number of RIN-sensitive genes was analyzed between young and aged males and females, the females had more RIN-sensitive genes in the young, while the males had more in the aged group (Figure 2.4). Currently, it is unknown if aging consistently causes this effect, and if so, by what mechanism. The results appear sexually dimorphic, given the opposite findings in males and females. This could indicate that sex hormones are playing a role, but further investigation is required.

Overall, this paper has some significant findings that transcriptional profiling analysis, such as: determining specific genes and pathways that are RIN-sensitive; the relationship between RIN and gene expression is exponential instead of linear; the ranges of RIN that do not need correction (> 8.6), can be corrected ($6.7-8.6$), and are too degraded to produce accurate results (< 6.7); the interaction between age and sex on RIN-sensitivity; and that RNA degradation effects in normal control tissue share characteristics with those seen in neurodegenerative disease. This study was the first step in understanding that there is a robust, synaptically targeted effect of RNA degradation on brain tissue analyzed using transcriptional profiling methods.

5.3 Progesterone pretreatment attenuates acute stress action on hippocampus without the apparent disruption of the hypothalamic-pituitary-adrenal axis in young adult male and female rats

5.3.1 Implications

This experiment on acute restraint stress in male and female Sprague-Dawley rats tested for progesterone pretreatment's ability to attenuate these responses. The work confirmed prior findings showing that rats, like humans, have a sexually dimorphic response to stress and extended prior observations that progesterone reduces this response by showing that it appeared downstream of the hypothalamus-pituitary-adrenal (HPA)-axis.

While there are studies involving females, most of our understanding of the HPA-axis and the downstream consequences of its activation comes from males. Several studies that have compared male and female memory after acute stress, including our own, have found that the behavior changes are significantly greater in females than males (Rosenfeld

& Trainor, 2014). In addition, our data supported prior work (C. R. Park et al., 2008; Snihur et al., 2008) that restraint causes a deficit in memory after acute stress. However, other studies have found that acute stress increases memory performance in females (Conrad et al., 2004; Lipatova et al., 2018). While these findings might be explained by shorter stress duration or types of behavioral tests, the fact remains that acute stress-associated deficits in memory in females do not follow the canonical stress response that has been established over decades of research in primarily male subjects.

In addition, serum-and-glucocorticoid serum kinase 1 is a well-studied immediate-early gene associated with the glucocorticoid receptor (Buechel et al., 2014; C. Y. Chen et al., 2016; Porter et al., 2012). However, our study found that this well-established association in acute stress is present in males but not females (Figure 4.10). Recent studies have shown that Sgk1 mRNA increases with acute stress (Anacker et al., 2013; Hinds et al., 2017); however, much of this research has been done in males and cell lines. Therefore, findings made in males regarding the downstream actions of the stress response need to be measured in females to determine which effects are canonical for both sexes and which may be sexually dimorphic.

This work was also the first study investigating progesterone pretreatments to alleviate the stress response in intact male and female rats. Elucidating the mechanism of progesterone's effects could lead to a novel anti-stress therapeutic target. Because of the time between the progesterone pretreatment and the stressor (~20 hours), it is unlikely allopregnanolone, which is a known anxiolytic, is exerting its effects in this case. Progesterone and allopregnanolone both have too short of half-lives (3.32 ± 1.35 in humans and 4 hours in rodents, respectively (Irwin et al., 2015; McAuley et al., 1996)) to be onboard during the assessment. In addition, progesterone levels were lower in progesterone-treated females, and there was no significant effect of progesterone pretreatment on blood progesterone levels in males.

We can also conclude that this effect is not occurring at the HPA-axis but further downstream. Progesterone did not impact glucocorticoid levels or the stress-induced glucocorticoid elevation in either sex, which indicates that any attenuation is less likely to be via the hypothalamus, pituitary, or adrenal glands. It should be noted that stress increased glucocorticoids in both sexes and decreased hormones associated with sex

(testosterone in the males, progesterone in the female). The latter implies that the HPA-axis and the hypothalamus-pituitary-gonadal (HPG)-axis are connected. Future work should investigate progesterone's potential mechanism acting upon the stress response. We propose three potential mechanisms: 1) reduction in glucocorticoid receptor expression; 2) inhibited 11 β -hydroxysteroid dehydrogenase; and 3) action through progesterone's signal cascade to reduce the GC-GR complex access to DNA.

5.3.2 Future Directions

As previously discussed, the progesterone pretreatment mechanism is yet to be determined. It appears to be working downstream of the HPA response, and the current study suggests that whatever the mechanism may be, it is effective as pretreatment, and the progesterone does not need to be 'onboard' to exert its effects. By determining where progesterone pretreatment is acting in the stress response, new pharmacological interventions can be determined. This new target would be sensitive to progesterone and its metabolites. Therefore, it would be essential to know the effects of long-term progesterone treatments because some medications already include them. In addition, there is a high likelihood that females would experience these effects at a higher level than males due to the increased endogenous progesterone. Further, because cognition does not appear to be impaired, such a pretreatment, given as a prophylactic, could reduce stress responses without impairing normal cognitive function. In addition, it would be necessary to see how long-term pretreatments could impact chronic stress to ensure that there are no detrimental long-term effects or interaction with the stress response.

Another aspect needing further investigation is how progesterone (and possibly allopregnanolone) treatments during the hormone's half-life impact the stress response. Progesterone is known to have neuroprotective effects after brain injury (J. Cai et al., 2015; W. Cai et al., 2008) as well as having positive effects against deficits caused by both acute and chronic stress (Childs et al., 2010; DIAZ-BRUIKE et al., 2010). These effects are often explained by allopregnanolone, an anxiolytic that works by altering GABA_A receptor subunit composition, resulting in a more easily activated inhibitory network (Guennoun, 2020; Guennoun et al., 2015; Melcangi & Panzica, 2014; Sayeed, Parvez, Wali, Siemen, & Stein, 2009); in addition, allopregnanolone rescues hippocampal learning and memory in AD model mice (C. Singh et al., 2012). However, to our knowledge, there

have been no studies investigating the long-term effects of progesterone treatment on chronic stress that include measurements taken from the brain. It is also likely that progesterone and allopregnanolone actions are not restricted to the hippocampus but also impact the stress response in other brain areas such as the amygdala, hippocampus, and prefrontal cortex. Therefore, to fully understand the effects of progesterone and its metabolites on the stress response (both acute and chronic), pretreatments as seen in this study, and treatments given during the stressor, and critically, after the stressor to rescue function, need to be investigated further.

An additional area that needs further investigation is the relationship between Iba1/Mbp overlap with stress. Our findings indicated that increased Iba1/Mbp overlap occurred in different regions of the CA1 and was impacted by both stress and progesterone in a sex and region-specific manner. This may be due to several reasons. For one, the measurements were taken from tissue prepared ~15 minutes after stress exposure, and additional time may have allowed fuller development of the response. Another (and probably more prominent) potential factor is that stress and progesterone pretreatments may need to occur in a more chronic time frame. The myelin burden on the microglia occurs with age (Safaiyan et al., 2016), which shares characteristics with chronic (K. C. Chen et al., 2013; Landfield et al., 2007; Porter & Landfield, 1998), not acute stress. While this study found some Iba1/Mbp overlap using immunohistochemistry, chronic stress may lead to more region- and sex-specific findings. Therefore, the rate of myelin burdened microglia needs to be determined in chronic stress.

RNA integrity numbers (RINs) are impacted by pre-and post-mortem factors (Durrenberger et al., 2010). This study investigated whether acute stress was one of these factors and found no effect. However, acute stress has fewer negative consequences compared to chronic stress. In addition, the duration of a subject's agonal state also can play a role in decreasing RNA quality, typically by acidosis. The longer a subject suffers before death, the lower their RIN (Chevyreva, Faull, Green, & Nicholson, 2008). It seems probable that, like the agonal state, stress' effects on RIN, if they exist, may also be time-dependent. Therefore, it will be essential to evaluate RIN in chronic stress settings. In addition, since there is now an identified mRNA degradation pathway regulated by glucocorticoids, glucocorticoid receptor-mediated decay (GMD) (Cho et al., 2015; O. H.

Park et al., 2016) may play a role. Although it is not known to affect rRNA (the primary source of material evaluated by RIN), it may coincide with that degradation and explain some of the targeted mRNA reductions seen with RIN. Therefore, future studies measuring mRNA involving chronic stress should also include disambiguated RINs.

5.4 Concluding remarks

The “Declining RNA integrity in control autopsy brain tissue is robustly and asymmetrically associated with selective neuronal mRNA signal loss” study found several aspects that may have been overlooked or incorrectly assumed in prior work. The first is that RIN values do not have a consistently linear relationship with gene expression but instead an exponential (and possibly sigmoidal) one. Our analysis suggests a low range where RNA quality no longer impacts gene expression, a middle range in which there is a linear relationship between RIN values and gene expression, and an upper range where variations in RIN do not detectably impact gene expression. In addition, we found that in the PFC, synaptic genes are robustly RIN-sensitive. This finding supports prior work that RNA degradation impacts specific genes and pathways at a greater rate (Gallego Romero et al., 2014; Opitz et al., 2010). Even though the work was restricted to control brain tissue, RIN-sensitive genes in the brain were significantly similar to those downregulated in Alzheimer’s disease (AD). Therefore, researchers need to be careful when removing the effects of RIN from data, especially if the RIN itself is significantly different between control and neurodegenerative disease cases because RINs would be confounded with disease status, and normalization could obscure potentially effects.

The “Progesterone pretreatment attenuates acute stress action on hippocampus without the apparent disruption of the hypothalamic-pituitary-adrenal axis in young adult male, and female rats” experiment found that progesterone attenuates memory deficits caused by acute stress. However, the acute stress response is sexually dimorphic, with females having a greater stress response, though there was no impact on female immediate-early gene *Sgk1*’s mRNA expression, in contrast to prior work in males (and confirmed in our work). The different *Sgk1* expression levels indicate that different mechanisms may be triggered by stress in males and females. Furthermore, while progesterone alleviated the behavioral response to increased stress in both sexes and the increase in *Sgk1* mRNA in males, the mechanism is unclear. It is less likely that this effect

was directly caused by progesterone or its anxiolytic metabolite (allopregnanolone) acting on the HPA-axis since both had already been metabolized, and pretreatment did not change blood corticosterone response to stress in either sex. However, stress and progesterone appeared to independently influence the Iba1/ Mbp overlap in the hippocampus, indicating an increased myelin burden on the microglia. This study confirms that the stress response is behaviorally and molecularly sexually dimorphic and that progesterone exerts its action downstream of the HPA-axis.

REFERENCES

- Almawi, W. Y., & Melemedjian, O. K. (2002). Negative regulation of nuclear factor-kappaB activation and function by glucocorticoids. *J Mol Endocrinol*, *28*(2), 69-78. doi:10.1677/jme.0.0280069
- Anacker, C., Cattaneo, A., Musaelyan, K., Zunszain, P. A., Horowitz, M., Molteni, R., . . . Pariante, C. M. (2013). Role for the kinase SGK1 in stress, depression, and glucocorticoid effects on hippocampal neurogenesis. *Proc Natl Acad Sci U S A*, *110*(21), 8708-8713. doi:10.1073/pnas.1300886110
- Ansorge, W. J. (2009). Next-generation DNA sequencing techniques. *N Biotechnol*, *25*(4), 195-203. doi:10.1016/j.nbt.2008.12.009
- Ashburner, M., Ball, C. A., Blake, J. A., Botstein, D., Butler, H., Cherry, J. M., . . . Sherlock, G. (2000). Gene ontology: tool for the unification of biology. The Gene Ontology Consortium. *Nat Genet*, *25*(1), 25-29. doi:10.1038/75556
- Atrooz, F., Alkadhi, K. A., & Salim, S. (2021). Understanding stress: Insights from rodent models. *Current Research in Neurobiology*, 100013.
- Atz, M., Walsh, D., Cartagena, P., Li, J., Evans, S., Choudary, P., . . . Pritzker Neuropsychiatric Disorders Research, C. (2007). Methodological considerations for gene expression profiling of human brain. *J Neurosci Methods*, *163*(2), 295-309. doi:10.1016/j.jneumeth.2007.03.022
- Baker, M. E., & Katsu, Y. (2020). Progesterone: An enigmatic ligand for the mineralocorticoid receptor. *Biochem Pharmacol*, *177*, 113976. doi:10.1016/j.bcp.2020.113976
- Barbaccia, M. L., Roscetti, G., Trabucchi, M., Mostallino, M. C., Concas, A., Purdy, R. H., & Biggio, G. (1996). Time-dependent changes in rat brain neuroactive steroid concentrations and GABAA receptor function after acute stress. *Neuroendocrinology*, *63*(2), 166-172. doi:10.1159/000126953
- Barbaccia, M. L., Serra, M., Purdy, R. H., & Biggio, G. (2001). Stress and neuroactive steroids. *Int Rev Neurobiol*, *46*, 243-272. doi:10.1016/s0074-7742(01)46065-x
- Barmada, S. J., Ju, S., Arjun, A., Batarse, A., Archbold, H. C., Peisach, D., . . . Finkbeiner, S. (2015). Amelioration of toxicity in neuronal models of amyotrophic lateral sclerosis by hUPF1. *Proc Natl Acad Sci U S A*, *112*(25), 7821-7826. doi:10.1073/pnas.1509744112
- Barrett, T., Wilhite, S. E., Ledoux, P., Evangelista, C., Kim, I. F., Tomashevsky, M., . . . Soboleva, A. (2013). NCBI GEO: archive for functional genomics data sets--update. *Nucleic Acids Res*, *41*(Database issue), D991-995. doi:10.1093/nar/gks1193
- Barrientos, R. M., Thompson, V. M., Kitt, M. M., Amat, J., Hale, M. W., Frank, M. G., . . . Maier, S. F. (2015). Greater glucocorticoid receptor activation in hippocampus of aged rats sensitizes microglia. *Neurobiol Aging*, *36*(3), 1483-1495. doi:10.1016/j.neurobiolaging.2014.12.003
- Baschant, U., & Tuckermann, J. (2010). The role of the glucocorticoid receptor in inflammation and immunity. *J Steroid Biochem Mol Biol*, *120*(2-3), 69-75. doi:10.1016/j.jsbmb.2010.03.058
- Bauer, M. E. (2005). Stress, glucocorticoids and ageing of the immune system. *Stress*, *8*(1), 69-83. doi:10.1080/10253890500100240

- Beck, K. D., & Luine, V. N. (2002). Sex differences in behavioral and neurochemical profiles after chronic stress: role of housing conditions. *Physiol Behav*, *75*(5), 661-673. doi:10.1016/s0031-9384(02)00670-4
- Beiko, J., Lander, R., Hampson, E., Boon, F., & Cain, D. P. (2004). Contribution of sex differences in the acute stress response to sex differences in water maze performance in the rat. *Behav Brain Res*, *151*(1-2), 239-253. doi:10.1016/j.bbr.2003.08.019
- Benjamini, Y., & Hochberg, Y. (1995). Controlling the false discovery rate: a practical and powerful approach to multiple testing. *Journal of the Royal statistical society: series B (Methodological)*, *57*(1), 289-300.
- Berchtold, N. C., Coleman, P. D., Cribbs, D. H., Rogers, J., Gillen, D. L., & Cotman, C. W. (2013). Synaptic genes are extensively downregulated across multiple brain regions in normal human aging and Alzheimer's disease. *Neurobiol Aging*, *34*(6), 1653-1661. doi:10.1016/j.neurobiolaging.2012.11.024
- Berchtold, N. C., Cribbs, D. H., Coleman, P. D., Rogers, J., Head, E., Kim, R., . . . Cotman, C. W. (2008). Gene expression changes in the course of normal brain aging are sexually dimorphic. *Proc Natl Acad Sci U S A*, *105*(40), 15605-15610. doi:10.1073/pnas.0806883105
- Birdsill, A. C., Walker, D. G., Lue, L., Sue, L. I., & Beach, T. G. (2011). Postmortem interval effect on RNA and gene expression in human brain tissue. *Cell Tissue Bank*, *12*(4), 311-318. doi:10.1007/s10561-010-9210-8
- Bisagno, V., Grillo, C. A., Piroli, G. G., Giraldo, P., McEwen, B., & Luine, V. N. (2004). Chronic stress alters amphetamine effects on behavior and synaptophysin levels in female rats. *Pharmacol Biochem Behav*, *78*(3), 541-550. doi:10.1016/j.pbb.2004.04.023
- Blalock, E. M., Chen, K. C., Sharrow, K., Herman, J. P., Porter, N. M., Foster, T. C., & Landfield, P. W. (2003). Gene microarrays in hippocampal aging: statistical profiling identifies novel processes correlated with cognitive impairment. *J Neurosci*, *23*(9), 3807-3819.
- Blalock, E. M., Grondin, R., Chen, K. C., Thibault, O., Thibault, V., Pandya, J. D., . . . Landfield, P. W. (2010). Aging-related gene expression in hippocampus proper compared with dentate gyrus is selectively associated with metabolic syndrome variables in rhesus monkeys. *J Neurosci*, *30*(17), 6058-6071. doi:10.1523/JNEUROSCI.3956-09.2010
- Blanchard, A., Kaiser, R., & Hood, L. (1996). High-density oligonucleotide arrays. *Biosensors and bioelectronics*, *11*(6-7), 687-690.
- Bolshakov, A. P., Tret'yakova, L. V., Kvichansky, A. A., & Gulyaeva, N. V. (2021). Glucocorticoids: Dr. Jekyll and Mr. Hyde of Hippocampal Neuroinflammation. *Biochemistry (Mosc)*, *86*(2), 156-167. doi:10.1134/S0006297921020048
- Bolstad, B. M., Irizarry, R. A., Astrand, M., & Speed, T. P. (2003). A comparison of normalization methods for high density oligonucleotide array data based on variance and bias. *Bioinformatics*, *19*(2), 185-193. doi:10.1093/bioinformatics/19.2.185
- Borbolis, F., & Syntichaki, P. (2015). Cytoplasmic mRNA turnover and ageing. *Mech Ageing Dev*, *152*, 32-42. doi:10.1016/j.mad.2015.09.006

- Bridgham, J. T., Carroll, S. M., & Thornton, J. W. (2006). Evolution of hormone-receptor complexity by molecular exploitation. *Science*, *312*(5770), 97-101. doi:10.1126/science.1123348
- Brinton, R. D., Thompson, R. F., Foy, M. R., Baudry, M., Wang, J., Finch, C. E., . . . Nilsen, J. (2008). Progesterone receptors: form and function in brain. *Front Neuroendocrinol*, *29*(2), 313-339. doi:10.1016/j.yfrne.2008.02.001
- Brummelte, S., & Galea, L. A. (2010). Chronic high corticosterone reduces neurogenesis in the dentate gyrus of adult male and female rats. *Neuroscience*, *168*(3), 680-690. doi:10.1016/j.neuroscience.2010.04.023
- Buechel, H. M., Popovic, J., Searcy, J. L., Porter, N. M., Thibault, O., & Blalock, E. M. (2011). Deep sleep and parietal cortex gene expression changes are related to cognitive deficits with age. *PLoS One*, *6*(4), e18387. doi:10.1371/journal.pone.0018387
- Buechel, H. M., Popovic, J., Staggs, K., Anderson, K. L., Thibault, O., & Blalock, E. M. (2014). Aged rats are hypo-responsive to acute restraint: implications for psychosocial stress in aging. *Front Aging Neurosci*, *6*, 13. doi:10.3389/fnagi.2014.00013
- Bullitt, E. (1990). Expression of c-fos-like protein as a marker for neuronal activity following noxious stimulation in the rat. *J Comp Neurol*, *296*(4), 517-530. doi:10.1002/cne.902960402
- Bumgarner, R. (2013). Overview of DNA microarrays: types, applications, and their future. *Curr Protoc Mol Biol*, Chapter 22, Unit 22 21. doi:10.1002/0471142727.mb2201s101
- Buynitsky, T., & Mostofsky, D. I. (2009). Restraint stress in biobehavioral research: Recent developments. *Neurosci Biobehav Rev*, *33*(7), 1089-1098. doi:10.1016/j.neubiorev.2009.05.004
- Cadepond, F., Ulmann, A., & Baulieu, E. E. (1997). RU486 (mifepristone): mechanisms of action and clinical uses. *Annu Rev Med*, *48*, 129-156. doi:10.1146/annurev.med.48.1.129
- Cai, J., Cao, S., Chen, J., Yan, F., Chen, G., & Dai, Y. (2015). Progesterone alleviates acute brain injury via reducing apoptosis and oxidative stress in a rat experimental subarachnoid hemorrhage model. *Neurosci Lett*, *600*, 238-243. doi:10.1016/j.neulet.2015.06.023
- Cai, W., Zhu, Y., Furuya, K., Li, Z., Sokabe, M., & Chen, L. (2008). Two different molecular mechanisms underlying progesterone neuroprotection against ischemic brain damage. *Neuropharmacology*, *55*(2), 127-138. doi:10.1016/j.neuropharm.2008.04.023
- Cain, D. W., & Cidlowski, J. A. (2017). Immune regulation by glucocorticoids. *Nat Rev Immunol*, *17*(4), 233-247. doi:10.1038/nri.2017.1
- Campbell, J., & Ehlert, U. (2012). Acute psychosocial stress: does the emotional stress response correspond with physiological responses? *Psychoneuroendocrinology*, *37*(8), 1111-1134. doi:10.1016/j.psyneuen.2011.12.010
- Canady, V. A. (2021). APA survey: Majority of Americans reporting prolonged stress. In (Vol. 31, pp. 6). *Mental Health Weekly*: Wiley Periodicals, Inc.

- Carvalho, B. S., & Irizarry, R. A. (2010). A framework for oligonucleotide microarray preprocessing. *Bioinformatics*, *26*(19), 2363-2367. doi:10.1093/bioinformatics/btq431
- Caudal, D., Jay, T. M., & Godsil, B. P. (2014). Behavioral stress induces regionally-distinct shifts of brain mineralocorticoid and glucocorticoid receptor levels. *Front Behav Neurosci*, *8*, 19. doi:10.3389/fnbeh.2014.00019
- Cesari, M., Vellas, B., & Gambassi, G. (2013). The stress of aging. *Exp Gerontol*, *48*(4), 451-456. doi:10.1016/j.exger.2012.10.004
- Chai, Z., Alheim, K., Lundkvist, J., Gatti, S., & Bartfai, T. (1996). Subchronic glucocorticoid pretreatment reversibly attenuates IL-beta induced fever in rats; IL-6 mRNA is elevated while IL-1 alpha and IL-1 beta mRNAs are suppressed, in the CNS. *Cytokine*, *8*(3), 227-237. doi:10.1006/cyto.1996.0032
- Chandramohan, Y., Droste, S. K., Arthur, J. S., & Reul, J. M. (2008). The forced swimming-induced behavioural immobility response involves histone H3 phosphoacetylation and c-Fos induction in dentate gyrus granule neurons via activation of the N-methyl-D-aspartate/extracellular signal-regulated kinase/mitogen- and stress-activated kinase signalling pathway. *Eur J Neurosci*, *27*(10), 2701-2713. doi:10.1111/j.1460-9568.2008.06230.x
- Chapman, K., Holmes, M., & Seckl, J. (2013). 11beta-hydroxysteroid dehydrogenases: intracellular gate-keepers of tissue glucocorticoid action. *Physiol Rev*, *93*(3), 1139-1206. doi:10.1152/physrev.00020.2012
- Chen, C. Y., Logan, R. W., Ma, T., Lewis, D. A., Tseng, G. C., Sibille, E., & McClung, C. A. (2016). Effects of aging on circadian patterns of gene expression in the human prefrontal cortex. *Proc Natl Acad Sci U S A*, *113*(1), 206-211. doi:10.1073/pnas.1508249112
- Chen, K. C., Blalock, E. M., Curran-Rauhut, M. A., Kadish, I., Blalock, S. J., Brewer, L., . . . Landfield, P. W. (2013). Glucocorticoid-dependent hippocampal transcriptome in male rats: pathway-specific alterations with aging. *Endocrinology*, *154*(8), 2807-2820. doi:10.1210/en.2013-1139
- Chevyreva, I., Faull, R. L., Green, C. R., & Nicholson, L. F. (2008). Assessing RNA quality in postmortem human brain tissue. *Exp Mol Pathol*, *84*(1), 71-77. doi:10.1016/j.yexmp.2007.08.019
- Childs, E., Van Dam, N. T., & de Wit, H. (2010). Effects of acute progesterone administration upon responses to acute psychosocial stress in men. *Exp Clin Psychopharmacol*, *18*(1), 78-86. doi:10.1037/a0018060
- Cho, H., Park, O. H., Park, J., Ryu, I., Kim, J., Ko, J., & Kim, Y. K. (2015). Glucocorticoid receptor interacts with PNRC2 in a ligand-dependent manner to recruit UPF1 for rapid mRNA degradation. *Proc Natl Acad Sci U S A*, *112*(13), E1540-1549. doi:10.1073/pnas.1409612112
- Chung, S., Son, G. H., & Kim, K. (2011). Circadian rhythm of adrenal glucocorticoid: its regulation and clinical implications. *Biochim Biophys Acta*, *1812*(5), 581-591. doi:10.1016/j.bbadis.2011.02.003
- Conrad, C. D., Jackson, J. L., Wiczorek, L., Baran, S. E., Harman, J. S., Wright, R. L., & Korol, D. L. (2004). Acute stress impairs spatial memory in male but not female rats: influence of estrous cycle. *Pharmacol Biochem Behav*, *78*(3), 569-579. doi:10.1016/j.pbb.2004.04.025

- Consortium, G. T. (2013). The Genotype-Tissue Expression (GTEx) project. *Nat Genet*, *45*(6), 580-585. doi:10.1038/ng.2653
- Copois, V., Bibeau, F., Bascoul-Mollevis, C., Salvetat, N., Chalbos, P., Bareil, C., . . . Del Rio, M. (2007). Impact of RNA degradation on gene expression profiles: assessment of different methods to reliably determine RNA quality. *J Biotechnol*, *127*(4), 549-559. doi:10.1016/j.jbiotec.2006.07.032
- Costa-Silva, J., Domingues, D., & Lopes, F. M. (2017). RNA-Seq differential expression analysis: An extended review and a software tool. *PLoS One*, *12*(12), e0190152. doi:10.1371/journal.pone.0190152
- Courtney, E., Kornfeld, S., Janitz, K., & Janitz, M. (2010). Transcriptome profiling in neurodegenerative disease. *J Neurosci Methods*, *193*(2), 189-202. doi:10.1016/j.jneumeth.2010.08.018
- Crossley, B. M., Bai, J., Glaser, A., Maes, R., Porter, E., Killian, M. L., . . . Toohey-Kurth, K. (2020). Guidelines for Sanger sequencing and molecular assay monitoring. *J Vet Diagn Invest*, *32*(6), 767-775. doi:10.1177/1040638720905833
- Dagklis, T., Ravanos, K., Makedou, K., Kourtis, A., & Rousso, D. (2015). Common features and differences of the hypothalamic-pituitary-gonadal axis in male and female. *Gynecol Endocrinol*, *31*(1), 14-17. doi:10.3109/09513590.2014.959917
- Datson, N. A., van der Perk, J., de Kloet, E. R., & Vreugdenhil, E. (2001). Identification of corticosteroid-responsive genes in rat hippocampus using serial analysis of gene expression. *Eur J Neurosci*, *14*(4), 675-689. doi:10.1046/j.0953-816x.2001.01685.x
- De Bosscher, K., Vanden Berghe, W., & Haegeman, G. (2003). The interplay between the glucocorticoid receptor and nuclear factor-kappaB or activator protein-1: molecular mechanisms for gene repression. *Endocr Rev*, *24*(4), 488-522. doi:10.1210/er.2002-0006
- de Lignieres, B. (1999). Oral micronized progesterone. *Clin Ther*, *21*(1), 41-60; discussion 41-42. doi:10.1016/S0149-2918(00)88267-3
- de Quervain, D., Schwabe, L., & Roozendaal, B. (2017). Stress, glucocorticoids and memory: implications for treating fear-related disorders. *Nat Rev Neurosci*, *18*(1), 7-19. doi:10.1038/nrn.2016.155
- Decker, C. J., & Parker, R. (2012). P-bodies and stress granules: possible roles in the control of translation and mRNA degradation. *Cold Spring Harb Perspect Biol*, *4*(9), a012286. doi:10.1101/cshperspect.a012286
- Denhardt, D. T. (2018). Effect of stress on human biology: Epigenetics, adaptation, inheritance, and social significance. *J Cell Physiol*, *233*(3), 1975-1984. doi:10.1002/jcp.25837
- Denver, R. J. (2009). Structural and functional evolution of vertebrate neuroendocrine stress systems. *Ann N Y Acad Sci*, *1163*, 1-16. doi:10.1111/j.1749-6632.2009.04433.x
- Diamond, D. M., Park, C. R., Heman, K. L., & Rose, G. M. (1999). Exposing rats to a predator impairs spatial working memory in the radial arm water maze. *Hippocampus*, *9*(5), 542-552. doi:10.1002/(SICI)1098-1063(1999)9:5<542::AID-HIPO8>3.0.CO;2-N
- DIAZ-BRUIKE, Y., Gonzalez-Sandoval, C. E., Valencia-Alfonso, C. E., Huerta, M., Trujillo, X., Diaz, L., . . . Luquín, S. (2010). Progesterone regulates corticosterone

- elevation and alterations in spatial memory and exploratory behavior induced by stress in Wistar rats. *Universitas Psychologica*, 9(3), 627-640.
- Die, J. V., Obrero, Á., González-Verdejo, C. I., & Román, B. (2011). Characterization of the 3':5' ratio for reliable determination of RNA quality. *Anal Biochem*, 419(2), 336-338. doi:10.1016/j.ab.2011.08.012
- Dinkel, K., MacPherson, A., & Sapolsky, R. M. (2003). Novel glucocorticoid effects on acute inflammation in the CNS. *J Neurochem*, 84(4), 705-716. doi:10.1046/j.1471-4159.2003.01604.x
- Dundas, C. M., Demonte, D., & Park, S. (2013). Streptavidin-biotin technology: improvements and innovations in chemical and biological applications. *Appl Microbiol Biotechnol*, 97(21), 9343-9353. doi:10.1007/s00253-013-5232-z
- Durrenberger, P. F., Fernando, S., Kashefi, S. N., Ferrer, I., Hauw, J. J., Seilhean, D., . . . Reynolds, R. (2010). Effects of antemortem and postmortem variables on human brain mRNA quality: a BrainNet Europe study. *J Neuropathol Exp Neurol*, 69(1), 70-81. doi:10.1097/NEN.0b013e3181c7e32f
- Erickson, K., Drevets, W., & Schulkin, J. (2003). Glucocorticoid regulation of diverse cognitive functions in normal and pathological emotional states. *Neurosci Biobehav Rev*, 27(3), 233-246. doi:10.1016/s0149-7634(03)00033-2
- Ervin, J. F., Heinzen, E. L., Cronin, K. D., Goldstein, D., Szymanski, M. H., Burke, J. R., . . . Hulette, C. M. (2007). Postmortem delay has minimal effect on brain RNA integrity. *J Neuropathol Exp Neurol*, 66(12), 1093-1099. doi:10.1097/nen.0b013e31815c196a
- Fenger-Gron, M., Fillman, C., Norrild, B., & Lykke-Andersen, J. (2005). Multiple processing body factors and the ARE binding protein TTP activate mRNA decapping. *Mol Cell*, 20(6), 905-915. doi:10.1016/j.molcel.2005.10.031
- Ferreira, P. G., Munoz-Aguirre, M., Reverter, F., Sa Godinho, C. P., Sousa, A., Amadoz, A., . . . Guigo, R. (2018). The effects of death and post-mortem cold ischemia on human tissue transcriptomes. *Nat Commun*, 9(1), 490. doi:10.1038/s41467-017-02772-x
- Feyzi, E., Sundheim, O., Westbye, M. P., Aas, P. A., Vagbo, C. B., Otterlei, M., . . . Krokan, H. E. (2007). RNA base damage and repair. *Curr Pharm Biotechnol*, 8(6), 326-331. doi:10.2174/138920107783018363
- Finsterwald, C., & Alberini, C. M. (2014). Stress and glucocorticoid receptor-dependent mechanisms in long-term memory: from adaptive responses to psychopathologies. *Neurobiol Learn Mem*, 112, 17-29. doi:10.1016/j.nlm.2013.09.017
- Fleige, S., & Pfaffl, M. W. (2006). RNA integrity and the effect on the real-time qRT-PCR performance. *Mol Aspects Med*, 27(2-3), 126-139. doi:10.1016/j.mam.2005.12.003
- Flint, M. S., Baum, A., Chambers, W. H., & Jenkins, F. J. (2007). Induction of DNA damage, alteration of DNA repair and transcriptional activation by stress hormones. *Psychoneuroendocrinology*, 32(5), 470-479. doi:10.1016/j.psyneuen.2007.02.013
- Fodor, S. P., Read, J. L., Pirrung, M. C., Stryer, L., Lu, A. T., & Solas, D. (1991). Light-directed, spatially addressable parallel chemical synthesis. *Science*, 251(4995), 767-773. doi:10.1126/science.1990438

- Frank, M. G., Baratta, M. V., Sprunger, D. B., Watkins, L. R., & Maier, S. F. (2007). Microglia serve as a neuroimmune substrate for stress-induced potentiation of CNS pro-inflammatory cytokine responses. *Brain Behav Immun*, *21*(1), 47-59. doi:10.1016/j.bbi.2006.03.005
- Frank, M. G., Watkins, L. R., & Maier, S. F. (2013). Stress-induced glucocorticoids as a neuroendocrine alarm signal of danger. *Brain Behav Immun*, *33*, 1-6. doi:10.1016/j.bbi.2013.02.004
- Frazier, H. N., Ghoweri, A. O., Sudkamp, E., Johnson, E. S., Anderson, K. L., Fox, G., . . . Thibault, O. (2020). Long-Term Intranasal Insulin Aspart: A Profile of Gene Expression, Memory, and Insulin Receptors in Aged F344 Rats. *J Gerontol A Biol Sci Med Sci*, *75*(6), 1021-1030. doi:10.1093/gerona/glz105
- Gadek-Michalska, A., Spyрка, J., Rachwalska, P., Tadeusz, J., & Bugajski, J. (2013). Influence of chronic stress on brain corticosteroid receptors and HPA axis activity. *Pharmacol Rep*, *65*(5), 1163-1175.
- Gaikwad, S., Stewart, A., Hart, P., Wong, K., Piet, V., Cachat, J., & Kalueff, A. V. (2011). Acute stress disrupts performance of zebrafish in the cued and spatial memory tests: the utility of fish models to study stress-memory interplay. *Behav Processes*, *87*(2), 224-230. doi:10.1016/j.beproc.2011.04.004
- Galea, L. A., McEwen, B. S., Tanapat, P., Deak, T., Spencer, R. L., & Dhabhar, F. S. (1997). Sex differences in dendritic atrophy of CA3 pyramidal neurons in response to chronic restraint stress. *Neuroscience*, *81*(3), 689-697. doi:10.1016/s0306-4522(97)00233-9
- Galea, L. A. M., Choleris, E., Albert, A. Y. K., McCarthy, M. M., & Sohrabji, F. (2020). The promises and pitfalls of sex difference research. *Front Neuroendocrinol*, *56*, 100817. doi:10.1016/j.yfrne.2019.100817
- Gallego Romero, I., Pai, A. A., Tung, J., & Gilad, Y. (2014). RNA-seq: impact of RNA degradation on transcript quantification. *BMC Biol*, *12*, 42. doi:10.1186/1741-7007-12-42
- Gant, J. C., Blalock, E. M., Chen, K. C., Kadish, I., Thibault, O., Porter, N. M., & Landfield, P. W. (2018). FK506-Binding Protein 12.6/1b, a Negative Regulator of [Ca²⁺], Rescues Memory and Restores Genomic Regulation in the Hippocampus of Aging Rats. *J Neurosci*, *38*(4), 1030-1041. doi:10.1523/JNEUROSCI.2234-17.2017
- Ganter, S., Northoff, H., Mannel, D., & Gebicke-Harter, P. J. (1992). Growth control of cultured microglia. *J Neurosci Res*, *33*(2), 218-230. doi:10.1002/jnr.490330205
- Garabedian, M. J., Harris, C. A., & Jeanneteau, F. (2017). Glucocorticoid receptor action in metabolic and neuronal function. *F1000Res*, *6*, 1208. doi:10.12688/f1000research.11375.1
- Garrido, P. (2011). Aging and stress: past hypotheses, present approaches and perspectives. *Aging Dis*, *2*(1), 80-99.
- Garrido, P., de Blas, M., Del Arco, A., Segovia, G., & Mora, F. (2012). Aging increases basal but not stress-induced levels of corticosterone in the brain of the awake rat. *Neurobiol Aging*, *33*(2), 375-382. doi:10.1016/j.neurobiolaging.2010.02.015
- Gautier, L., Cope, L., Bolstad, B. M., & Irizarry, R. A. (2004). affy--analysis of Affymetrix GeneChip data at the probe level. *Bioinformatics*, *20*(3), 307-315. doi:10.1093/bioinformatics/btg405

- Gene Ontology, C. (2021). The Gene Ontology resource: enriching a GOLD mine. *Nucleic Acids Res*, 49(D1), D325-D334. doi:10.1093/nar/gkaa1113
- Gentleman, R. C., Carey, V. J., Bates, D. M., Bolstad, B., Dettling, M., Dudoit, S., . . . Zhang, J. (2004). Bioconductor: open software development for computational biology and bioinformatics. *Genome Biol*, 5(10), R80. doi:10.1186/gb-2004-5-10-r80
- Gergen, J. P., Stern, R. H., & Wensink, P. C. (1979). Filter replicas and permanent collections of recombinant DNA plasmids. *Nucleic Acids Res*, 7(8), 2115-2136. doi:10.1093/nar/7.8.2115
- Girotti, M., Pace, T. W., Gaylord, R. I., Rubin, B. A., Herman, J. P., & Spencer, R. L. (2006). Habituation to repeated restraint stress is associated with lack of stress-induced c-fos expression in primary sensory processing areas of the rat brain. *Neuroscience*, 138(4), 1067-1081. doi:10.1016/j.neuroscience.2005.12.002
- Gjerstad, J. K., Lightman, S. L., & Spiga, F. (2018). Role of glucocorticoid negative feedback in the regulation of HPA axis pulsatility. *Stress*, 21(5), 403-416. doi:10.1080/10253890.2018.1470238
- Goujon, E., Parnet, P., Laye, S., Combe, C., Kelley, K. W., & Dantzer, R. (1995). Stress downregulates lipopolysaccharide-induced expression of proinflammatory cytokines in the spleen, pituitary, and brain of mice. *Brain Behav Immun*, 9(4), 292-303. doi:10.1006/brbi.1995.1028
- Goulding, N. J., & Guyre, P. M. (1993). Glucocorticoids, lipocortins and the immune response. *Curr Opin Immunol*, 5(1), 108-113. doi:10.1016/0952-7915(93)90089-b
- Graham, J. D., & Clarke, C. L. (1997). Physiological action of progesterone in target tissues. *Endocr Rev*, 18(4), 502-519. doi:10.1210/edrv.18.4.0308
- Grunstein, M., & Hogness, D. S. (1975). Colony hybridization: a method for the isolation of cloned DNAs that contain a specific gene. *Proc Natl Acad Sci U S A*, 72(10), 3961-3965. doi:10.1073/pnas.72.10.3961
- Guennoun, R. (2020). Progesterone in the Brain: Hormone, Neurosteroid and Neuroprotectant. *Int J Mol Sci*, 21(15). doi:10.3390/ijms21155271
- Guennoun, R., Labombarda, F., Gonzalez Deniselle, M. C., Liere, P., De Nicola, A. F., & Schumacher, M. (2015). Progesterone and allopregnanolone in the central nervous system: response to injury and implication for neuroprotection. *J Steroid Biochem Mol Biol*, 146, 48-61. doi:10.1016/j.jsbmb.2014.09.001
- Harburger, L. L., Pechenino, A. S., Saadi, A., & Frick, K. M. (2008). Post-training progesterone dose-dependently enhances object, but not spatial, memory consolidation. *Behav Brain Res*, 194(2), 174-180. doi:10.1016/j.bbr.2008.07.014
- Hargis, K., Buechel, H. M., Popovic, J., & Blalock, E. M. (2018). Acute psychosocial stress in mid-aged male rats causes hyperthermia, cognitive decline, and increased deep sleep power, but does not alter deep sleep duration. *Neurobiol Aging*, 70, 78-85. doi:10.1016/j.neurobiolaging.2018.06.009
- Hargis, K. E., & Blalock, E. M. (2017). Transcriptional signatures of brain aging and Alzheimer's disease: What are our rodent models telling us? *Behav Brain Res*, 322(Pt B), 311-328. doi:10.1016/j.bbr.2016.05.007
- Heinrichs, M., Baumgartner, T., Kirschbaum, C., & Ehlert, U. (2003). Social support and oxytocin interact to suppress cortisol and subjective responses to psychosocial stress. *Biol Psychiatry*, 54(12), 1389-1398. doi:10.1016/s0006-3223(03)00465-7

- Heitzer, M. D., Wolf, I. M., Sanchez, E. R., Witchel, S. F., & DeFranco, D. B. (2007). Glucocorticoid receptor physiology. *Rev Endocr Metab Disord*, 8(4), 321-330. doi:10.1007/s11154-007-9059-8
- Herman, J. P. (2013). Neural control of chronic stress adaptation. *Front Behav Neurosci*, 7, 61. doi:10.3389/fnbeh.2013.00061
- Herman, J. P., & Cullinan, W. E. (1997). Neurocircuitry of stress: central control of the hypothalamo-pituitary-adrenocortical axis. *Trends Neurosci*, 20(2), 78-84. doi:10.1016/s0166-2236(96)10069-2
- Herman, J. P., Figueiredo, H., Mueller, N. K., Ulrich-Lai, Y., Ostrander, M. M., Choi, D. C., & Cullinan, W. E. (2003). Central mechanisms of stress integration: hierarchical circuitry controlling hypothalamo-pituitary-adrenocortical responsiveness. *Front Neuroendocrinol*, 24(3), 151-180. doi:10.1016/j.yfrne.2003.07.001
- Hidalgo, V., Pulopulos, M. M., & Salvador, A. (2019). Acute psychosocial stress effects on memory performance: Relevance of age and sex. *Neurobiol Learn Mem*, 157, 48-60. doi:10.1016/j.nlm.2018.11.013
- Hinds, L. R., Chun, L. E., Woodruff, E. R., Christensen, J. A., Hartsock, M. J., & Spencer, R. L. (2017). Dynamic glucocorticoid-dependent regulation of Sgk1 expression in oligodendrocytes of adult male rat brain by acute stress and time of day. *PLoS One*, 12(4), e0175075. doi:10.1371/journal.pone.0175075
- Hinwood, M., Tynan, R. J., Charnley, J. L., Beynon, S. B., Day, T. A., & Walker, F. R. (2013). Chronic stress induced remodeling of the prefrontal cortex: structural reorganization of microglia and the inhibitory effect of minocycline. *Cereb Cortex*, 23(8), 1784-1797. doi:10.1093/cercor/bhs151
- Hrdlickova, R., Toloue, M., & Tian, B. (2017). RNA-Seq methods for transcriptome analysis. *Wiley Interdiscip Rev RNA*, 8(1). doi:10.1002/wrna.1364
- Huber, W., Carey, V. J., Gentleman, R., Anders, S., Carlson, M., Carvalho, B. S., . . . Morgan, M. (2015). Orchestrating high-throughput genomic analysis with Bioconductor. *Nat Methods*, 12(2), 115-121. doi:10.1038/nmeth.3252
- Illumina, I. (Producer). (2016). Illumina Sequencing by Synthesis. [Video]
- Illumina, I. (2017). An introduction to Next-Generation Sequencing Technology. In Irizarry, R. A., Hobbs, B., Collin, F., Beazer-Barclay, Y. D., Antonellis, K. J., Scherf, U., & Speed, T. P. (2003). Exploration, normalization, and summaries of high density oligonucleotide array probe level data. *Biostatistics*, 4(2), 249-264. doi:10.1093/biostatistics/4.2.249
- Irwin, R. W., Solinsky, C. M., Loya, C. M., Salituro, F. G., Rodgers, K. E., Bauer, G., . . . Brinton, R. D. (2015). Allopregnanolone preclinical acute pharmacokinetic and pharmacodynamic studies to predict tolerability and efficacy for Alzheimer's disease. *PLoS One*, 10(6), e0128313. doi:10.1371/journal.pone.0128313
- Ishikawa, M., Hara, C., Ohdo, S., & Ogawa, N. (1992). Plasma corticosterone response of rats with sociopsychological stress in the communication box. *Physiol Behav*, 52(3), 475-480. doi:10.1016/0031-9384(92)90333-w
- Ismaili, N., & Garabedian, M. J. (2004). Modulation of glucocorticoid receptor function via phosphorylation. *Ann N Y Acad Sci*, 1024, 86-101. doi:10.1196/annals.1321.007

- Jaffe, A. E., Tao, R., Norris, A. L., Kealhofer, M., Nellore, A., Shin, J. H., . . . Weinberger, D. R. (2017). qSVA framework for RNA quality correction in differential expression analysis. *Proc Natl Acad Sci U S A*, *114*(27), 7130-7135. doi:10.1073/pnas.1617384114
- Jaksik, R., Iwanaszko, M., Rzeszowska-Wolny, J., & Kimmel, M. (2015). Microarray experiments and factors which affect their reliability. *Biol Direct*, *10*, 46. doi:10.1186/s13062-015-0077-2
- Jansen, L. M., Gispen-de Wied, C. C., & Kahn, R. S. (2000). Selective impairments in the stress response in schizophrenic patients. *Psychopharmacology (Berl)*, *149*(3), 319-325. doi:10.1007/s002130000381
- Jaszczak, A., & Juszcak, G. R. (2021). Glucocorticoids, metabolism and brain activity. *Neurosci Biobehav Rev*, *126*, 113-145. doi:10.1016/j.neubiorev.2021.03.007
- Jauregui-Huerta, F., Ruvalcaba-Delgadillo, Y., Gonzalez-Castaneda, R., Garcia-Estrada, J., Gonzalez-Perez, O., & Luquin, S. (2010). Responses of glial cells to stress and glucocorticoids. *Curr Immunol Rev*, *6*(3), 195-204. doi:10.2174/157339510791823790
- Jia, E., Zhou, Y., Shi, H., Pan, M., Zhao, X., & Ge, Q. (2021). Effects of brain tissue section processing and storage time on gene expression. *Anal Chim Acta*, *1142*, 38-47. doi:10.1016/j.aca.2020.10.046
- Johnson, S. A., Morgan, D. G., & Finch, C. E. (1986). Extensive postmortem stability of RNA from rat and human brain. *J Neurosci Res*, *16*(1), 267-280. doi:10.1002/jnr.490160123
- Jung, S., Choe, S., Woo, H., Jeong, H., An, H. K., Moon, H., . . . Yu, S. W. (2020). Autophagic death of neural stem cells mediates chronic stress-induced decline of adult hippocampal neurogenesis and cognitive deficits. *Autophagy*, *16*(3), 512-530. doi:10.1080/15548627.2019.1630222
- Kadish, I., Thibault, O., Blalock, E. M., Chen, K. C., Gant, J. C., Porter, N. M., & Landfield, P. W. (2009). Hippocampal and cognitive aging across the lifespan: a bioenergetic shift precedes and increased cholesterol trafficking parallels memory impairment. *J Neurosci*, *29*(6), 1805-1816. doi:10.1523/JNEUROSCI.4599-08.2009
- Kajantie, E., & Phillips, D. I. (2006). The effects of sex and hormonal status on the physiological response to acute psychosocial stress. *Psychoneuroendocrinology*, *31*(2), 151-178. doi:10.1016/j.psyneuen.2005.07.002
- Kalil, B., Leite, C. M., Carvalho-Lima, M., & Anselmo-Franci, J. A. (2013). Role of sex steroids in progesterone and corticosterone response to acute restraint stress in rats: sex differences. *Stress*, *16*(4), 452-460. doi:10.3109/10253890.2013.777832
- Kang, H. J., Kawasawa, Y. I., Cheng, F., Zhu, Y., Xu, X., Li, M., . . . Sestan, N. (2011). Spatio-temporal transcriptome of the human brain. *Nature*, *478*(7370), 483-489. doi:10.1038/nature10523
- Katyare, S. S., Balasubramanian, S., & Parmar, D. V. (2003). Effect of corticosterone treatment on mitochondrial oxidative energy metabolism in developing rat brain. *Exp Neurol*, *183*(1), 241-248. doi:10.1016/s0014-4886(03)00176-6
- Keim, K. L., & Sigg, E. B. (1976). Physiological and biochemical concomitants of restraint stress in rats. *Pharmacol Biochem Behav*, *4*(3), 289-297. doi:10.1016/0091-3057(76)90244-6

- Kerr, D. S., Campbell, L. W., Applegate, M. D., Brodish, A., & Landfield, P. W. (1991). Chronic stress-induced acceleration of electrophysiologic and morphometric biomarkers of hippocampal aging. *J Neurosci*, *11*(5), 1316-1324.
- Kim, Y. K., & Maquat, L. E. (2019). UPF1 in RNA decay: UPF1 in nonsense-mediated mRNA decay and beyond. *RNA*, *25*(4), 407-422. doi:10.1261/rna.070136.118
- Kitchen, R. R., Sabine, V. S., Simen, A. A., Dixon, J. M., Bartlett, J. M., & Sims, A. H. (2011). Relative impact of key sources of systematic noise in Affymetrix and Illumina gene-expression microarray experiments. *BMC Genomics*, *12*, 589. doi:10.1186/1471-2164-12-589
- Kogler, L., Muller, V. I., Chang, A., Eickhoff, S. B., Fox, P. T., Gur, R. C., & Derntl, B. (2015). Psychosocial versus physiological stress - Meta-analyses on deactivations and activations of the neural correlates of stress reactions. *Neuroimage*, *119*, 235-251. doi:10.1016/j.neuroimage.2015.06.059
- Korsunsky, I., Millard, N., Fan, J., Slowikowski, K., Zhang, F., Wei, K., . . . Raychaudhuri, S. (2019). Fast, sensitive and accurate integration of single-cell data with Harmony. *Nat Methods*, *16*(12), 1289-1296. doi:10.1038/s41592-019-0619-0
- Kuo, T., McQueen, A., Chen, T. C., & Wang, J. C. (2015). Regulation of Glucose Homeostasis by Glucocorticoids. *Adv Exp Med Biol*, *872*, 99-126. doi:10.1007/978-1-4939-2895-8_5
- Labno, A., Tomecki, R., & Dziembowski, A. (2016). Cytoplasmic RNA decay pathways - Enzymes and mechanisms. *Biochim Biophys Acta*, *1863*(12), 3125-3147. doi:10.1016/j.bbamcr.2016.09.023
- Ladisich, W. (1975). Influence of stress on regional brain serotonin metabolism after progesterone treatment and upon plasma progesterone in the rat. *J Neural Transm*, *36*(1), 33-42. doi:10.1007/BF01243435
- Lakatos, A., Goldberg, N. R., & Blurton-Jones, M. (2017). Integrated analysis of genetic, behavioral, and biochemical data implicates neural stem cell-induced changes in immunity, neurotransmission and mitochondrial function in Dementia with Lewy Body mice. *Acta Neuropathol Commun*, *5*(1), 21. doi:10.1186/s40478-017-0421-0
- Landfield, P. W., Blalock, E. M., Chen, K. C., & Porter, N. M. (2007). A new glucocorticoid hypothesis of brain aging: implications for Alzheimer's disease. *Curr Alzheimer Res*, *4*(2), 205-212. doi:10.2174/156720507780362083
- Landfield, P. W., Cadwallader, L. B., & Vinsant, S. (1988). Quantitative changes in hippocampal structure following long-term exposure to delta 9-tetrahydrocannabinol: possible mediation by glucocorticoid systems. *Brain Res*, *443*(1-2), 47-62. doi:10.1016/0006-8993(88)91597-1
- Lang, F., & Shumilina, E. (2013). Regulation of ion channels by the serum- and glucocorticoid-inducible kinase SGK1. *FASEB J*, *27*(1), 3-12. doi:10.1096/fj.12-218230
- Lang, F., Strutz-Seebohm, N., Seebohm, G., & Lang, U. E. (2010). Significance of SGK1 in the regulation of neuronal function. *J Physiol*, *588*(Pt 18), 3349-3354. doi:10.1113/jphysiol.2010.190926
- Lanz, T. A., Joshi, J. J., Reinhart, V., Johnson, K., Grantham, L. E., 2nd, & Volfson, D. (2015). STEP levels are unchanged in pre-frontal cortex and associative striatum in post-mortem human brain samples from subjects with schizophrenia, bipolar

- disorder and major depressive disorder. *PLoS One*, *10*(3), e0121744.
doi:10.1371/journal.pone.0121744
- Lavretsky, H., & Newhouse, P. A. (2012). Stress, inflammation, and aging. *Am J Geriatr Psychiatry*, *20*(9), 729-733. doi:10.1097/JGP.0b013e31826573cf
- Le Mevel, J. C., Abitbol, S., Beraud, G., & Maniey, J. (1978). Dynamic changes in plasma adrenocorticotrophin after neurotropic stress in male and female rats. *J Endocrinol*, *76*(2), 359-360. doi:10.1677/joe.0.0760359
- Lenoir, T., & Giannella, E. (2006). The emergence and diffusion of DNA microarray technology. *J Biomed Discov Collab*, *1*, 11. doi:10.1186/1747-5333-1-11
- Li, S., Fan, Y. X., Wang, W., & Tang, Y. Y. (2012). Effects of acute restraint stress on different components of memory as assessed by object-recognition and object-location tasks in mice. *Behav Brain Res*, *227*(1), 199-207.
doi:10.1016/j.bbr.2011.10.007
- Lian, B., Liu, M., Lan, Z., Sun, T., Meng, Z., Chang, Q., . . . Zhao, C. (2020). Hippocampal overexpression of SGK1 ameliorates spatial memory, rescues Abeta pathology and actin cytoskeleton polymerization in middle-aged APP/PS1 mice. *Behav Brain Res*, *383*, 112503. doi:10.1016/j.bbr.2020.112503
- Liao, Y., Wang, J., Jaehnig, E. J., Shi, Z., & Zhang, B. (2019). WebGestalt 2019: gene set analysis toolkit with revamped UIs and APIs. *Nucleic Acids Res*, *47*(W1), W199-W205. doi:10.1093/nar/gkz401
- Lipatova, O., Campolattaro, M. M., Dixon, D. C., & Durak, A. (2018). Sex differences and the role of acute stress in the open-field tower maze. *Physiol Behav*, *189*, 16-25. doi:10.1016/j.physbeh.2018.02.046
- Liu, H., Rodgers, N. D., Jiao, X., & Kiledjian, M. (2002). The scavenger mRNA decapping enzyme DcpS is a member of the HIT family of pyrophosphatases. *EMBO J*, *21*(17), 4699-4708. doi:10.1093/emboj/cdf448
- Lockhart, D. J., Dong, H., Byrne, M. C., Follettie, M. T., Gallo, M. V., Chee, M. S., . . . Brown, E. L. (1996). Expression monitoring by hybridization to high-density oligonucleotide arrays. *Nat Biotechnol*, *14*(13), 1675-1680. doi:10.1038/nbt1296-1675
- Lovick, T. A. (2012). Estrous cycle and stress: influence of progesterone on the female brain. *Braz J Med Biol Res*, *45*(4), 314-320. doi:10.1590/s0100-879x2012007500044
- Luine, V., Gomez, J., Beck, K., & Bowman, R. (2017). Sex differences in chronic stress effects on cognition in rodents. *Pharmacol Biochem Behav*, *152*, 13-19.
doi:10.1016/j.pbb.2016.08.005
- Luoma, J. I., Stern, C. M., & Mermelstein, P. G. (2012). Progesterone inhibition of neuronal calcium signaling underlies aspects of progesterone-mediated neuroprotection. *J Steroid Biochem Mol Biol*, *131*(1-2), 30-36.
doi:10.1016/j.jsbmb.2011.11.002
- Ma, Y. L., Tsai, M. C., Hsu, W. L., & Lee, E. H. (2006). SGK protein kinase facilitates the expression of long-term potentiation in hippocampal neurons. *Learn Mem*, *13*(2), 114-118. doi:10.1101/lm.179206
- MacPherson, A., Dinkel, K., & Sapolsky, R. (2005). Glucocorticoids worsen excitotoxin-induced expression of pro-inflammatory cytokines in hippocampal cultures. *Exp Neurol*, *194*(2), 376-383. doi:10.1016/j.expneurol.2005.02.021

- Maier, S. F., & Seligman, M. E. (2016). Learned helplessness at fifty: Insights from neuroscience. *Psychol Rev*, *123*(4), 349-367. doi:10.1037/rev0000033
- Mardis, E. R. (2008). Next-generation DNA sequencing methods. *Annu Rev Genomics Hum Genet*, *9*, 387-402. doi:10.1146/annurev.genom.9.081307.164359
- Mariotti, A. (2015). The effects of chronic stress on health: new insights into the molecular mechanisms of brain-body communication. *Future Sci OA*, *1*(3), FSO23. doi:10.4155/fso.15.21
- McAuley, J. W., Kroboth, F. J., & Kroboth, P. D. (1996). Oral administration of micronized progesterone: a review and more experience. *Pharmacotherapy*, *16*(3), 453-457.
- McDermaid, A., Monier, B., Zhao, J., Liu, B., & Ma, Q. (2019). Interpretation of differential gene expression results of RNA-seq data: review and integration. *Brief Bioinform*, *20*(6), 2044-2054. doi:10.1093/bib/bby067
- McDonnell, D. P., Shahbaz, M. M., Vegeto, E., & Goldman, M. E. (1994). The human progesterone receptor A-form functions as a transcriptional modulator of mineralocorticoid receptor transcriptional activity. *J Steroid Biochem Mol Biol*, *48*(5-6), 425-432. doi:10.1016/0960-0760(94)90190-2
- McEwen, B. S. (2017). Neurobiological and Systemic Effects of Chronic Stress. *Chronic Stress (Thousand Oaks)*, *1*. doi:10.1177/2470547017692328
- McEwen, B. S., Bowles, N. P., Gray, J. D., Hill, M. N., Hunter, R. G., Karatsoreos, I. N., & Nasca, C. (2015). Mechanisms of stress in the brain. *Nat Neurosci*, *18*(10), 1353-1363. doi:10.1038/nn.4086
- McIntosh, L. J., Hong, K. E., & Sapolsky, R. M. (1998). Glucocorticoids may alter antioxidant enzyme capacity in the brain: baseline studies. *Brain Res*, *791*(1-2), 209-214. doi:10.1016/s0006-8993(98)00115-2
- Melcangi, R. C., & Panzica, G. C. (2014). Allopregnanolone: state of the art. *Prog Neurobiol*, *113*, 1-5. doi:10.1016/j.pneurobio.2013.09.005
- Metzker, M. L. (2010). Sequencing technologies - the next generation. *Nat Rev Genet*, *11*(1), 31-46. doi:10.1038/nrg2626
- Meyer, S., Temme, C., & Wahle, E. (2004). Messenger RNA turnover in eukaryotes: pathways and enzymes. *Crit Rev Biochem Mol Biol*, *39*(4), 197-216. doi:10.1080/10409230490513991
- Mifsud, K. R., & Reul, J. (2018). Mineralocorticoid and glucocorticoid receptor-mediated control of genomic responses to stress in the brain. *Stress*, *21*(5), 389-402. doi:10.1080/10253890.2018.1456526
- Miller, A. H., Spencer, R. L., Pulera, M., Kang, S., McEwen, B. S., & Stein, M. (1992). Adrenal steroid receptor activation in rat brain and pituitary following dexamethasone: implications for the dexamethasone suppression test. *Biol Psychiatry*, *32*(10), 850-869. doi:10.1016/0006-3223(92)90175-y
- Miller, J. A., Guillozet-Bongaarts, A., Gibbons, L. E., Postupna, N., Renz, A., Beller, A. E., . . . Lein, E. (2017). Neuropathological and transcriptomic characteristics of the aged brain. *Elife*, *6*. doi:10.7554/eLife.31126
- Miller, L. R., Marks, C., Becker, J. B., Hurn, P. D., Chen, W. J., Woodruff, T., . . . Clayton, J. A. (2017). Considering sex as a biological variable in preclinical research. *FASEB J*, *31*(1), 29-34. doi:10.1096/fj.201600781R

- Miller, M. B., & Tang, Y. W. (2009). Basic concepts of microarrays and potential applications in clinical microbiology. *Clin Microbiol Rev*, 22(4), 611-633. doi:10.1128/CMR.00019-09
- Mistry, M., & Pavlidis, P. (2010). A cross-laboratory comparison of expression profiling data from normal human postmortem brain. *Neuroscience*, 167(2), 384-395. doi:10.1016/j.neuroscience.2010.01.016
- Mizoguchi, K., Ikeda, R., Shoji, H., Tanaka, Y., Maruyama, W., & Tabira, T. (2009). Aging attenuates glucocorticoid negative feedback in rat brain. *Neuroscience*, 159(1), 259-270. doi:10.1016/j.neuroscience.2008.12.020
- Moffat, S. D. (2005). Effects of testosterone on cognitive and brain aging in elderly men. *Ann N Y Acad Sci*, 1055, 80-92. doi:10.1196/annals.1323.014
- Mueller, O., Lightfoot, S., & Schroeder, A. (2004). RNA integrity number (RIN)—standardization of RNA quality control. *Agilent application note, publication, 1*, 1-8.
- Munck, A., & Naray-Fejes-Toth, A. (1994). Glucocorticoids and stress: permissive and suppressive actions. *Ann N Y Acad Sci*, 746, 115-130; discussion 131-113. doi:10.1111/j.1749-6632.1994.tb39221.x
- Murakami, S., Imbe, H., Morikawa, Y., Kubo, C., & Senba, E. (2005). Chronic stress, as well as acute stress, reduces BDNF mRNA expression in the rat hippocampus but less robustly. *Neurosci Res*, 53(2), 129-139. doi:10.1016/j.neures.2005.06.008
- Nagy, A. (2000). Cre recombinase: the universal reagent for genome tailoring. *Genesis*, 26(2), 99-109.
- Nam, D. K., Lee, S., Zhou, G., Cao, X., Wang, C., Clark, T., . . . Wang, S. M. (2002). Oligo(dT) primer generates a high frequency of truncated cDNAs through internal poly(A) priming during reverse transcription. *Proc Natl Acad Sci U S A*, 99(9), 6152-6156. doi:10.1073/pnas.092140899
- Nicolaidis, N. C., Kyratzi, E., Lamprokostopoulou, A., Chrousos, G. P., & Charmandari, E. (2015). Stress, the stress system and the role of glucocorticoids. *Neuroimmunomodulation*, 22(1-2), 6-19. doi:10.1159/000362736
- Niraula, A., Sheridan, J. F., & Godbout, J. P. (2017). Microglia Priming with Aging and Stress. *Neuropsychopharmacology*, 42(1), 318-333. doi:10.1038/npp.2016.185
- Oakley, R. H., & Cidlowski, J. A. (2013). The biology of the glucocorticoid receptor: new signaling mechanisms in health and disease. *J Allergy Clin Immunol*, 132(5), 1033-1044. doi:10.1016/j.jaci.2013.09.007
- Oitzl, M. S., Champagne, D. L., van der Veen, R., & de Kloet, E. R. (2010). Brain development under stress: hypotheses of glucocorticoid actions revisited. *Neurosci Biobehav Rev*, 34(6), 853-866. doi:10.1016/j.neubiorev.2009.07.006
- Olver, J. S., Pinney, M., Maruff, P., & Norman, T. R. (2015). Impairments of spatial working memory and attention following acute psychosocial stress. *Stress and Health*, 31(2), 115-123.
- Opitz, L., Salinas-Riester, G., Grade, M., Jung, K., Jo, P., Emons, G., . . . Gaedcke, J. (2010). Impact of RNA degradation on gene expression profiling. *BMC Med Genomics*, 3, 36. doi:10.1186/1755-8794-3-36
- Park, C. R., Zoladz, P. R., Conrad, C. D., Fleshner, M., & Diamond, D. M. (2008). Acute predator stress impairs the consolidation and retrieval of hippocampus-dependent

- memory in male and female rats. *Learn Mem*, 15(4), 271-280.
doi:10.1101/lm.721108
- Park, J. C., Jeon, Y. J., Jang, Y. S., Cho, J., Choi, D. H., & Han, J. S. (2021). SGK1 knockdown in the medial prefrontal cortex reduces resistance to stress-induced memory impairment. *Eur Neuropsychopharmacol*, 45, 29-34.
doi:10.1016/j.euroneuro.2021.02.012
- Park, O. H., Park, J., Yu, M., An, H. T., Ko, J., & Kim, Y. K. (2016). Identification and molecular characterization of cellular factors required for glucocorticoid receptor-mediated mRNA decay. *Genes Dev*, 30(18), 2093-2105.
doi:10.1101/gad.286484.116
- Parsana, P., Ruberman, C., Jaffe, A. E., Schatz, M. C., Battle, A., & Leek, J. T. (2019). Addressing confounding artifacts in reconstruction of gene co-expression networks. *Genome Biol*, 20(1), 94. doi:10.1186/s13059-019-1700-9
- Pasricha, N., Joels, M., & Karst, H. (2011). Rapid effects of corticosterone in the mouse dentate gyrus via a nongenomic pathway. *J Neuroendocrinol*, 23(2), 143-147.
doi:10.1111/j.1365-2826.2010.02091.x
- Pavlopoulos, E., Jones, S., Kosmidis, S., Close, M., Kim, C., Kovalerchik, O., . . . Kandel, E. R. (2013). Molecular mechanism for age-related memory loss: the histone-binding protein RbAp48. *Sci Transl Med*, 5(200), 200ra115.
doi:10.1126/scitranslmed.3006373
- Pawitan, Y., Michiels, S., Koscielny, S., Gusnanto, A., & Ploner, A. (2005). False discovery rate, sensitivity and sample size for microarray studies. *Bioinformatics*, 21(13), 3017-3024. doi:10.1093/bioinformatics/bti448
- Pawlyk, A. C., Morrison, A. R., Ross, R. J., & Brennan, F. X. (2008). Stress-induced changes in sleep in rodents: models and mechanisms. *Neurosci Biobehav Rev*, 32(1), 99-117. doi:10.1016/j.neubiorev.2007.06.001
- Pluchino, N., Luisi, M., Lenzi, E., Centofanti, M., Begliuomini, S., Freschi, L., . . . Genazzani, A. R. (2006). Progesterone and progestins: effects on brain, allopregnanolone and beta-endorphin. *J Steroid Biochem Mol Biol*, 102(1-5), 205-213. doi:10.1016/j.jsbmb.2006.09.023
- Porter, N. M., Bohannon, J. H., Curran-Rauhut, M., Buechel, H. M., Dowling, A. L., Brewer, L. D., . . . Blalock, E. M. (2012). Hippocampal CA1 transcriptional profile of sleep deprivation: relation to aging and stress. *PLoS One*, 7(7), e40128.
doi:10.1371/journal.pone.0040128
- Porter, N. M., & Landfield, P. W. (1998). Stress hormones and brain aging: adding injury to insult? *Nat Neurosci*, 1(1), 3-4. doi:10.1038/196
- Pozhitkov, A. E., Neme, R., Domazet-Loso, T., Leroux, B. G., Soni, S., Tautz, D., & Noble, P. A. (2017). Tracing the dynamics of gene transcripts after organismal death. *Open Biol*, 7(1). doi:10.1098/rsob.160267
- Preece, P., & Cairns, N. J. (2003). Quantifying mRNA in postmortem human brain: influence of gender, age at death, postmortem interval, brain pH, agonal state and inter-lobe mRNA variance. *Brain Res Mol Brain Res*, 118(1-2), 60-71.
doi:10.1016/s0169-328x(03)00337-1
- Purdy, R. H., Morrow, A. L., Moore, P. H., Jr., & Paul, S. M. (1991). Stress-induced elevations of gamma-aminobutyric acid type A receptor-active steroids in the rat brain. *Proc Natl Acad Sci U S A*, 88(10), 4553-4557.

- Roof, R. L., & Stein, D. G. (1999). Gender differences in Morris water maze performance depend on task parameters. *Physiol Behav*, *68*(1-2), 81-86. doi:10.1016/s0031-9384(99)00162-6
- Rosenfeld, C. S., & Trainor, B. C. (2014). Environmental Health Factors and Sexually Dimorphic Differences in Behavioral Disruptions. *Curr Environ Health Rep*, *1*(4), 287-301. doi:10.1007/s40572-014-0027-7
- Roszkowski, M., Manuella, F., von Ziegler, L., Duran-Pacheco, G., Moreau, J. L., Mansuy, I. M., & Bohacek, J. (2016). Rapid stress-induced transcriptomic changes in the brain depend on beta-adrenergic signaling. *Neuropharmacology*, *107*, 329-338. doi:10.1016/j.neuropharm.2016.03.046
- Rowe, W. B., Blalock, E. M., Chen, K. C., Kadish, I., Wang, D., Barrett, J. E., . . . Landfield, P. W. (2007). Hippocampal expression analyses reveal selective association of immediate-early, neuroenergetic, and myelinogenic pathways with cognitive impairment in aged rats. *J Neurosci*, *27*(12), 3098-3110. doi:10.1523/JNEUROSCI.4163-06.2007
- Safaiyan, S., Kannaiyan, N., Snaidero, N., Brioschi, S., Biber, K., Yona, S., . . . Simons, M. (2016). Age-related myelin degradation burdens the clearance function of microglia during aging. *Nat Neurosci*, *19*(8), 995-998. doi:10.1038/nn.4325
- Sampaio-Silva, F., Magalhaes, T., Carvalho, F., Dinis-Oliveira, R. J., & Silvestre, R. (2013). Profiling of RNA degradation for estimation of post mortem [corrected] interval. *PLoS One*, *8*(2), e56507. doi:10.1371/journal.pone.0056507
- Sanchez, P., Torres, J. M., Gavete, P., & Ortega, E. (2008). Effects of swim stress on mRNA and protein levels of steroid 5alpha-reductase isozymes in prefrontal cortex of adult male rats. *Neurochem Int*, *52*(3), 426-431. doi:10.1016/j.neuint.2007.07.019
- Sandi, C., Woodson, J. C., Haynes, V. F., Park, C. R., Touyarot, K., Lopez-Fernandez, M. A., . . . Diamond, D. M. (2005). Acute stress-induced impairment of spatial memory is associated with decreased expression of neural cell adhesion molecule in the hippocampus and prefrontal cortex. *Biol Psychiatry*, *57*(8), 856-864. doi:10.1016/j.biopsych.2004.12.034
- Sanger, F., Nicklen, S., & Coulson, A. R. (1977). DNA sequencing with chain-terminating inhibitors. *Proc Natl Acad Sci U S A*, *74*(12), 5463-5467. doi:10.1073/pnas.74.12.5463
- Sapolsky, R. M. (1999). Glucocorticoids, stress, and their adverse neurological effects: relevance to aging. *Exp Gerontol*, *34*(6), 721-732. doi:10.1016/s0531-5565(99)00047-9
- Sapolsky, R. M., Krey, L. C., & McEwen, B. S. (1985). Prolonged glucocorticoid exposure reduces hippocampal neuron number: implications for aging. *J Neurosci*, *5*(5), 1222-1227.
- Sapolsky, R. M., Krey, L. C., & McEwen, B. S. (1986). The neuroendocrinology of stress and aging: the glucocorticoid cascade hypothesis. *Endocr Rev*, *7*(3), 284-301. doi:10.1210/edrv-7-3-284
- Satija, R., Farrell, J. A., Gennert, D., Schier, A. F., & Regev, A. (2015). Spatial reconstruction of single-cell gene expression data. *Nat Biotechnol*, *33*(5), 495-502. doi:10.1038/nbt.3192

- Sauer, B., & Henderson, N. (1988). Site-specific DNA recombination in mammalian cells by the Cre recombinase of bacteriophage P1. *Proc Natl Acad Sci U S A*, 85(14), 5166-5170. doi:10.1073/pnas.85.14.5166
- Sayed, I., Parvez, S., Wali, B., Siemen, D., & Stein, D. G. (2009). Direct inhibition of the mitochondrial permeability transition pore: a possible mechanism for better neuroprotective effects of allopregnanolone over progesterone. *Brain Res*, 1263, 165-173. doi:10.1016/j.brainres.2009.01.045
- Scarpa, J. R., Jiang, P., Gao, V. D., Fitzpatrick, K., Millstein, J., Olker, C., . . . Vitaterna, M. H. (2018). Cross-species systems analysis identifies gene networks differentially altered by sleep loss and depression. *Sci Adv*, 4(7), eaat1294. doi:10.1126/sciadv.aat1294
- Schena, M., Shalon, D., Davis, R. W., & Brown, P. O. (1995). Quantitative monitoring of gene expression patterns with a complementary DNA microarray. *Science*, 270(5235), 467-470.
- Schindelin, J., Arganda-Carreras, I., Frise, E., Kaynig, V., Longair, M., Pietzsch, T., . . . Cardona, A. (2012). Fiji: an open-source platform for biological-image analysis. *Nat Methods*, 9(7), 676-682. doi:10.1038/nmeth.2019
- Schoenberg, D. R., & Maquat, L. E. (2012). Regulation of cytoplasmic mRNA decay. *Nat Rev Genet*, 13(4), 246-259. doi:10.1038/nrg3160
- Schroeder, A., Mueller, O., Stocker, S., Salowsky, R., Leiber, M., Gassmann, M., . . . Ragg, T. (2006). The RIN: an RNA integrity number for assigning integrity values to RNA measurements. *BMC Mol Biol*, 7, 3. doi:10.1186/1471-2199-7-3
- Schumacher, M., Guennoun, R., Stein, D. G., & De Nicola, A. F. (2007). Progesterone: therapeutic opportunities for neuroprotection and myelin repair. *Pharmacol Ther*, 116(1), 77-106. doi:10.1016/j.pharmthera.2007.06.001
- Simoneau, J., Dumontier, S., Gosselin, R., & Scott, M. S. (2021). Current RNA-seq methodology reporting limits reproducibility. *Brief Bioinform*, 22(1), 140-145. doi:10.1093/bib/bbz124
- Singh, C., Liu, L., Wang, J. M., Irwin, R. W., Yao, J., Chen, S., . . . Brinton, R. D. (2012). Allopregnanolone restores hippocampal-dependent learning and memory and neural progenitor survival in aging 3xTgAD and nonTg mice. *Neurobiol Aging*, 33(8), 1493-1506. doi:10.1016/j.neurobiolaging.2011.06.008
- Singh, M., & Su, C. (2013). Progesterone and neuroprotection. *Horm Behav*, 63(2), 284-290. doi:10.1016/j.yhbeh.2012.06.003
- Sirbu, A., Kerr, G., Crane, M., & Ruskin, H. J. (2012). RNA-Seq vs dual- and single-channel microarray data: sensitivity analysis for differential expression and clustering. *PLoS One*, 7(12), e50986. doi:10.1371/journal.pone.0050986
- Smoak, K. A., & Cidlowski, J. A. (2004). Mechanisms of glucocorticoid receptor signaling during inflammation. *Mech Ageing Dev*, 125(10-11), 697-706. doi:10.1016/j.mad.2004.06.010
- Snihur, A. W., Hampson, E., & Cain, D. P. (2008). Estradiol and corticosterone independently impair spatial navigation in the Morris water maze in adult female rats. *Behav Brain Res*, 187(1), 56-66. doi:10.1016/j.bbr.2007.08.023
- Somel, M., Liu, X., Tang, L., Yan, Z., Hu, H., Guo, S., . . . Khaitovich, P. (2011). MicroRNA-driven developmental remodeling in the brain distinguishes humans

- from other primates. *PLoS Biol*, 9(12), e1001214.
doi:10.1371/journal.pbio.1001214
- Sonntag, K. C., Tejada, G., Subburaju, S., Berretta, S., Benes, F. M., & Woo, T. U. (2016). Limited predictability of postmortem human brain tissue quality by RNA integrity numbers. *J Neurochem*, 138(1), 53-59. doi:10.1111/jnc.13637
- Soreq, L., Consortium, U. K. B. E., North American Brain Expression, C., Rose, J., Soreq, E., Hardy, J., . . . Ule, J. (2017). Major Shifts in Glial Regional Identity Are a Transcriptional Hallmark of Human Brain Aging. *Cell Rep*, 18(2), 557-570. doi:10.1016/j.celrep.2016.12.011
- Sorrells, S. F., Caso, J. R., Munhoz, C. D., & Sapolsky, R. M. (2009). The stressed CNS: when glucocorticoids aggravate inflammation. *Neuron*, 64(1), 33-39. doi:10.1016/j.neuron.2009.09.032
- Sorrells, S. F., & Sapolsky, R. M. (2007). An inflammatory review of glucocorticoid actions in the CNS. *Brain Behav Immun*, 21(3), 259-272. doi:10.1016/j.bbi.2006.11.006
- Stahn, C., Lowenberg, M., Hommes, D. W., & Buttgereit, F. (2007). Molecular mechanisms of glucocorticoid action and selective glucocorticoid receptor agonists. *Mol Cell Endocrinol*, 275(1-2), 71-78. doi:10.1016/j.mce.2007.05.019
- Stan, A. D., Ghose, S., Gao, X. M., Roberts, R. C., Lewis-Amezcu, K., Hatanpaa, K. J., & Tamminga, C. A. (2006). Human postmortem tissue: what quality markers matter? *Brain Res*, 1123(1), 1-11. doi:10.1016/j.brainres.2006.09.025
- Stilling, R. M., Benito, E., Gertig, M., Barth, J., Capece, V., Burkhardt, S., . . . Fischer, A. (2014). De-regulation of gene expression and alternative splicing affects distinct cellular pathways in the aging hippocampus. *Front Cell Neurosci*, 8, 373. doi:10.3389/fncel.2014.00373
- Stillman, M. J., Shukitt-Hale, B., Levy, A., & Lieberman, H. R. (1998). Spatial memory under acute cold and restraint stress. *Physiol Behav*, 64(5), 605-609. doi:10.1016/s0031-9384(98)00091-2
- Sugama, S., Takenouchi, T., Fujita, M., Kitani, H., Conti, B., & Hashimoto, M. (2013). Corticosteroids limit microglial activation occurring during acute stress. *Neuroscience*, 232, 13-20. doi:10.1016/j.neuroscience.2012.12.012
- Swanson, K. S., Vester, B. M., Apanavicius, C. J., Kirby, N. A., & Schook, L. B. (2009). Implications of age and diet on canine cerebral cortex transcription. *Neurobiol Aging*, 30(8), 1314-1326. doi:10.1016/j.neurobiolaging.2007.10.017
- Swindell, W. R., Xing, X., Voorhees, J. J., Elder, J. T., Johnston, A., & Gudjonsson, J. E. (2014). Integrative RNA-seq and microarray data analysis reveals GC content and gene length biases in the psoriasis transcriptome. *Physiol Genomics*, 46(15), 533-546. doi:10.1152/physiolgenomics.00022.2014
- Sze, Y., Gill, A. C., & Brunton, P. J. (2018). Sex-dependent changes in neuroactive steroid concentrations in the rat brain following acute swim stress. *J Neuroendocrinol*, 30(11), e12644. doi:10.1111/jne.12644
- Tan, C. L., Plotkin, J. L., Veno, M. T., von Schimmelmann, M., Feinberg, P., Mann, S., . . . Schaefer, A. (2013). MicroRNA-128 governs neuronal excitability and motor behavior in mice. *Science*, 342(6163), 1254-1258. doi:10.1126/science.1244193

- Tanaka, J., Fujita, H., Matsuda, S., Toku, K., Sakanaka, M., & Maeda, N. (1997). Glucocorticoid- and mineralocorticoid receptors in microglial cells: the two receptors mediate differential effects of corticosteroids. *Glia*, *20*(1), 23-37.
- Tasker, J. G. (2006). Rapid glucocorticoid actions in the hypothalamus as a mechanism of homeostatic integration. *Obesity (Silver Spring)*, *14 Suppl 5*, 259S-265S. doi:10.1038/oby.2006.320
- Tasker, J. G., & Herman, J. P. (2011). Mechanisms of rapid glucocorticoid feedback inhibition of the hypothalamic-pituitary-adrenal axis. *Stress*, *14*(4), 398-406. doi:10.3109/10253890.2011.586446
- ter Horst, J. P., Kentrop, J., de Kloet, E. R., & Oitzl, M. S. (2013). Stress and estrous cycle affect strategy but not performance of female C57BL/6J mice. *Behav Brain Res*, *241*, 92-95. doi:10.1016/j.bbr.2012.11.040
- Thapar, R., & Denmon, A. P. (2013). Signaling pathways that control mRNA turnover. *Cell Signal*, *25*(8), 1699-1710. doi:10.1016/j.cellsig.2013.03.026
- Timmermans, S., Souffriau, J., & Libert, C. (2019). A General Introduction to Glucocorticoid Biology. *Front Immunol*, *10*, 1545. doi:10.3389/fimmu.2019.01545
- Tollenaar, M. S., Elzinga, B. M., Spinhoven, P., & Everaerd, W. A. (2008). The effects of cortisol increase on long-term memory retrieval during and after acute psychosocial stress. *Acta Psychol (Amst)*, *127*(3), 542-552. doi:10.1016/j.actpsy.2007.10.007
- Toth, E., Gersner, R., Wilf-Yarkoni, A., Raizel, H., Dar, D. E., Richter-Levin, G., . . . Zangen, A. (2008). Age-dependent effects of chronic stress on brain plasticity and depressive behavior. *J Neurochem*, *107*(2), 522-532. doi:10.1111/j.1471-4159.2008.05642.x
- Trabzuni, D., Ryten, M., Walker, R., Smith, C., Imran, S., Ramasamy, A., . . . Hardy, J. (2011). Quality control parameters on a large dataset of regionally dissected human control brains for whole genome expression studies. *J Neurochem*, *119*(2), 275-282. doi:10.1111/j.1471-4159.2011.07432.x
- Tutucci, E., Livingston, N. M., Singer, R. H., & Wu, B. (2018). Imaging mRNA In Vivo, from Birth to Death. *Annu Rev Biophys*, *47*, 85-106. doi:10.1146/annurev-biophys-070317-033037
- Tynan, R. J., Naicker, S., Hinwood, M., Nalivaiko, E., Buller, K. M., Pow, D. V., . . . Walker, F. R. (2010). Chronic stress alters the density and morphology of microglia in a subset of stress-responsive brain regions. *Brain Behav Immun*, *24*(7), 1058-1068. doi:10.1016/j.bbi.2010.02.001
- Uno, H., Eisele, S., Sakai, A., Shelton, S., Baker, E., DeJesus, O., & Holden, J. (1994). Neurotoxicity of glucocorticoids in the primate brain. *Horm Behav*, *28*(4), 336-348. doi:10.1006/hbeh.1994.1030
- Urban, J. H., Van de Kar, L. D., Lorens, S. A., & Bethea, C. L. (1986). Effect of the anxiolytic drug buspirone on prolactin and corticosterone secretion in stressed and unstressed rats. *Pharmacol Biochem Behav*, *25*(2), 457-462. doi:10.1016/0091-3057(86)90023-7
- van der Kloet, F. M., Buurmans, J., Jonker, M. J., Smilde, A. K., & Westerhuis, J. A. (2020). Increased comparability between RNA-Seq and microarray data by utilization of gene sets. *PLoS Comput Biol*, *16*(9), e1008295. doi:10.1371/journal.pcbi.1008295

- Vandevyver, S., Dejager, L., & Libert, C. (2014). Comprehensive overview of the structure and regulation of the glucocorticoid receptor. *Endocr Rev*, *35*(4), 671-693. doi:10.1210/er.2014-1010
- Vanitallie, T. B. (2002). Stress: a risk factor for serious illness. *Metabolism*, *51*(6 Suppl 1), 40-45. doi:10.1053/meta.2002.33191
- Velculescu, V. E., Zhang, L., Vogelstein, B., & Kinzler, K. W. (1995). Serial analysis of gene expression. *Science*, *270*(5235), 484-487. doi:10.1126/science.270.5235.484
- Verbitsky, M., Yonan, A. L., Malleret, G., Kandel, E. R., Gilliam, T. C., & Pavlidis, P. (2004). Altered hippocampal transcript profile accompanies an age-related spatial memory deficit in mice. *Learn Mem*, *11*(3), 253-260. doi:10.1101/lm.68204
- Viljoen, K. S., & Blackburn, J. M. (2013). Quality assessment and data handling methods for Affymetrix Gene 1.0 ST arrays with variable RNA integrity. *BMC Genomics*, *14*, 14. doi:10.1186/1471-2164-14-14
- Voelker, R. S., Clay; Bassham, Susan; Catchen, Julien; Sydes, Jason; Cresko, William. RNA-seqlopedia. Retrieved from <https://rnaseq.uoregon.edu/>
- von Dawans, B., Strojny, J., & Domes, G. (2021). The effects of acute stress and stress hormones on social cognition and behavior: Current state of research and future directions. *Neurosci Biobehav Rev*, *121*, 75-88. doi:10.1016/j.neubiorev.2020.11.026
- Wagenmaker, E. R., & Moenter, S. M. (2017). Exposure to Acute Psychosocial Stress Disrupts the Luteinizing Hormone Surge Independent of Estrous Cycle Alterations in Female Mice. *Endocrinology*, *158*(8), 2593-2602. doi:10.1210/en.2017-00341
- Walker, D. J., & Spencer, K. A. (2018). Glucocorticoid programming of neuroimmune function. *Gen Comp Endocrinol*, *256*, 80-88. doi:10.1016/j.ygcen.2017.07.016
- Walt, D. R. (2000). Techview: molecular biology. Bead-based fiber-optic arrays. *Science*, *287*(5452), 451-452. doi:10.1126/science.287.5452.451
- Wang, J. M., Johnston, P. B., Ball, B. G., & Brinton, R. D. (2005). The neurosteroid allopregnanolone promotes proliferation of rodent and human neural progenitor cells and regulates cell-cycle gene and protein expression. *J Neurosci*, *25*(19), 4706-4718. doi:10.1523/JNEUROSCI.4520-04.2005
- Wang, J. M., Singh, C., Liu, L., Irwin, R. W., Chen, S., Chung, E. J., . . . Brinton, R. D. (2010). Allopregnanolone reverses neurogenic and cognitive deficits in mouse model of Alzheimer's disease. *Proc Natl Acad Sci U S A*, *107*(14), 6498-6503. doi:10.1073/pnas.1001422107
- Wei, R., Wang, J., Su, M., Jia, E., Chen, S., Chen, T., & Ni, Y. (2018). Missing Value Imputation Approach for Mass Spectrometry-based Metabolomics Data. *Sci Rep*, *8*(1), 663. doi:10.1038/s41598-017-19120-0
- Wen, D. X., Xu, Y. F., Mais, D. E., Goldman, M. E., & McDonnell, D. P. (1994). The A and B isoforms of the human progesterone receptor operate through distinct signaling pathways within target cells. *Mol Cell Biol*, *14*(12), 8356-8364. doi:10.1128/mcb.14.12.8356-8364.1994
- Weskamp, K., & Barmada, S. J. (2018). RNA Degradation in Neurodegenerative Disease. *Adv Neurobiol*, *20*, 103-142. doi:10.1007/978-3-319-89689-2_5
- Whirledge, S., & Cidlowski, J. A. (2010). Glucocorticoids, stress, and fertility. *Minerva Endocrinol*, *35*(2), 109-125.

- White, K., Yang, P., Li, L., Farshori, A., Medina, A. E., & Zielke, H. R. (2018). Effect of Postmortem Interval and Years in Storage on RNA Quality of Tissue at a Repository of the NIH NeuroBioBank. *Biopreserv Biobank*, *16*(2), 148-157. doi:10.1089/bio.2017.0099
- Williams, M. N., Grajales, C. A. G., & Kurkiewicz, D. (2013). Assumptions of multiple regression: Correcting two misconceptions. *Practical Assessment, Research, and Evaluation*, *18*(1), 11.
- Wirth, M. M. (2011). Beyond the HPA Axis: Progesterone-Derived Neuroactive Steroids in Human Stress and Emotion. *Front Endocrinol (Lausanne)*, *2*, 19. doi:10.3389/fendo.2011.00019
- Wohleb, E. S., Hanke, M. L., Corona, A. W., Powell, N. D., Stiner, L. M., Bailey, M. T., . . . Sheridan, J. F. (2011). beta-Adrenergic receptor antagonism prevents anxiety-like behavior and microglial reactivity induced by repeated social defeat. *J Neurosci*, *31*(17), 6277-6288. doi:10.1523/JNEUROSCI.0450-11.2011
- Wong, T. P., Howland, J. G., Robillard, J. M., Ge, Y., Yu, W., Titterness, A. K., . . . Wang, Y. T. (2007). Hippocampal long-term depression mediates acute stress-induced spatial memory retrieval impairment. *Proc Natl Acad Sci U S A*, *104*(27), 11471-11476. doi:10.1073/pnas.0702308104
- Wright, A., & Vissel, B. (2012). The essential role of AMPA receptor GluR2 subunit RNA editing in the normal and diseased brain. *Front Mol Neurosci*, *5*, 34. doi:10.3389/fnmol.2012.00034
- Wu, X., & Brewer, G. (2012). The regulation of mRNA stability in mammalian cells: 2.0. *Gene*, *500*(1), 10-21. doi:10.1016/j.gene.2012.03.021
- Wu, Z., & Irizarry, R. A. (2007). A Statistical Framework for the Analysis of Microarray Probe-Level Data. In (Vol. 1, pp. 333-357). *The Annals of Applied Statistics: Institute of Mathematical Statistics*.
- Yamamoto, M., Wakatsuki, T., Hada, A., & Ryo, A. (2001). Use of serial analysis of gene expression (SAGE) technology. *J Immunol Methods*, *250*(1-2), 45-66. doi:10.1016/s0022-1759(01)00305-2
- Yang, J. A., Song, C. I., Hughes, J. K., Kreisman, M. J., Parra, R. A., Haisenleder, D. J., . . . Breen, K. M. (2017). Acute Psychosocial Stress Inhibits LH Pulsatility and Kiss1 Neuronal Activation in Female Mice. *Endocrinology*, *158*(11), 3716-3723. doi:10.1210/en.2017-00301
- Yuen, E. Y., Liu, W., Karatsoreos, I. N., Feng, J., McEwen, B. S., & Yan, Z. (2009). Acute stress enhances glutamatergic transmission in prefrontal cortex and facilitates working memory. *Proc Natl Acad Sci U S A*, *106*(33), 14075-14079. doi:10.1073/pnas.0906791106
- Zafir, A., & Banu, N. (2007). Antioxidant potential of fluoxetine in comparison to Curcuma longa in restraint-stressed rats. *Eur J Pharmacol*, *572*(1), 23-31. doi:10.1016/j.ejphar.2007.05.062
- Zhang, B., & Herman, P. K. (2020). It is all about the process(ing): P-body granules and the regulation of signal transduction. *Curr Genet*, *66*(1), 73-77. doi:10.1007/s00294-019-01016-3
- Zhu, H., Li, J., Li, Y., Zheng, Z., Guan, H., Wang, H., . . . Hu, D. (2021). Glucocorticoid counteracts cellular mechanoresponses by LINC01569-dependent glucocorticoid receptor-mediated mRNA decay. *Sci Adv*, *7*(9). doi:10.1126/sciadv.abd9923

VITA

Education

University of Kentucky
Ph.D. in Pharmacology and Nutritional Sciences 2021

Wittenberg University
B.S. in Biology 2015
Minor in Neuroscience
Cum laude

Organizational and Professional Positions

Nutritional Sciences and Pharmacology Student Association 2017 - present

- President 2020 - 2021
- Vice-President 2019 – 2020

Society for Neuroscience 2018 - present

Graduate Student Congress 2018 - 2021

- External Affairs Committee 2019-2021
- External Affairs Officer 2020 – 2021
- Communication and Documents Committee 2018-2020
- Director of Recruitment 2018 – 2020

Alzheimer’s State Champion 2018 - 2020

National Association of Graduate and Professional Students 2019 – 2021

- Legislative Concerns Committee 2019 – 2021
- Special Assistant to the Director of Legislative Affairs 2020
- Interim/ Co-Director of Legislative Affair 2020

Kentucky Advocates for Science Policy and Research 2019 - present

- President 2020 - present
- Secretary 2019 - 2020

Framework for Accountability in Academic Research and Mentorship 2019 - present

- Legislative Director 2020 - present

National Science Policy Network	2020 - present
Kentucky Science Debate Coalition	2020
University of Kentucky Vice-President of Research Advisory Committee	2021

Peer Reviewed Publications

Johnson ES, Stenzel KE, Lee S, Blalock EM. (Submitted). Reduced RNA indicates selective mRNA degradation in post-mortem human brain tissue. PlosOne.

Johnson ES, Gant JC, Thibault JR, Naidugari JR, Deng P, Craig DR, Kraner S, Frazier H, Blalock EM. (in prep). Progesterone pretreatment decrease acute stress effect on cognition and impacts downstream expression.

Frazier HN, Ghoweri AO, Sudkamp E, Johnson E, et al. Long-term intranasal insulin aspart: a profile of gene expression, memory, and insulin receptors in aged F344 rats. *Journal of Gerontology: Biological Sciences*; 20(20): 1-10. doi: 10.1093/gerona/glz105 2020

Bahrani AA, Powell DK, Yu G, Johnson ES, et al. White Matter Hyperintensity Associations with Cerebral Blood Flow in Elderly Subjects Stratified by Cerebrovascular Risk. *Journal of Stroke and Cerebrovascular Disease*; 26(4): 779-786. 2017
doi:10.1016/j.jstrokecerebrovasdis.2016.10.017

Smith CD, Johnson ES, Van Eldik LJ, et al. Peripheral (deep) but not periventricular MRI white matter hyperintensities are increased in clinical vascular dementia compared to Alzheimer's disease. *Brain and Behavior*; 6(3):e00438. doi:10.1002/brb3.438. 2016

Non-Peer Reviewed Publications

Potter, T., Johnson, E. Legislative Letter 12-14-2020.
<http://nagps.org/legislative-letters-12-14-2020/>

Johnson, E. Legislative Letter 11-23-2020.

<http://nagps.org/legislative-letters-11-23-2020/>

Johnson, E, Potter, T. Legislative Letter 11-02-2020.

<http://nagps.org/legislative-letters-11-02-2020/>

Johnson, E. Review of 2020 in Higher Education.

<http://nagps.org/newsite/wp-content/uploads/2020/09/Review-Legislative-Letter.pdf>

Johnson, E. Legislative Letters 8-31-20. <http://nagps.org/legislative-letters-8-31-20/>

Johnson, E. Legislative Letters 8-9-20. <http://nagps.org/legislative-letters-8-9-20/>

Johnson, E. Legislative Letters 7-12-20. <http://nagps.org/legislative-letters-7-12-20/>

Johnson, E. Legislative Letters 6-14-20. <http://nagps.org/legislative-letters-6-14-20/>

Johnson, E. Legislative Letters 5-31-20. <http://nagps.org/legislative-letters-5-31-20/>

Johnson, E. Legislative Letters 5-17-20. <http://nagps.org/legislative-letters-5-17-20/>

Johnson, E. Legislative Letters 5-3-20. <http://nagps.org/legislative-letters-5-3-20/>

Johnson, E. Legislative Letters 4-18-20. <http://nagps.org/legislative-letters-4-18-20/>

Johnson, E. Legislative Letters 4-4-20. <http://nagps.org/legislative-letters-4-4-20/>

Johnson, E. Legislative Letters 3-23-20. <http://nagps.org/legislative-letters-3-23-20/>

Ford, M, Johnson, E. Legislative Letters 3-9-20.

<http://nagps.org/legislative-letters-3-9-20/>

Johnson, ES, Police S. Healthy Brain Aging. *Health and Wellness*. 2020; 17(6). <http://healthandwellnessmagazine.net/healthy-brain-aging.html>

Ford, M, Johnson, E. Legislative Letters 2-24-20.
<http://nagps.org/legislative-letters-2-24-20/>

Ford, M, Johnson, E. Legislative Letters 2-10-20.
<http://nagps.org/legislative-letters-2-10-20/>

Ford, M, Johnson, E. Legislative Letters 1-27-20.
<http://nagps.org/legislative-letters-1-27-20/>

Ford, M, Johnson, E. Legislative Letters 1-13-20.
<http://nagps.org/legislative-letters-1-13-20/>

Scholastic and Professional Honors

Graduate Student Congress Travel Awards	2018, 2020
National Association of Graduate and Professional Students' Above and Beyond Award	2020
Graduate School Congress Pillar Award for Academic Success	2021